การบำบัดน้ำเสียปนเปื้อนวัตถุระเบิดด้วยกระบวนการเฟนตันไฟฟ้า

นายปิยวัฒน์ ตัณฑ์วณิช

วิทยานิพนธ์นี้เป็นส่วนหนึ่งของการศึกษาตามหลักสูตรปริญญาวิทยาศาสตรดุษฎีบัณฑิต

สาขาวิชาการจัดการสิ่งแวดล้อม (สหสาขาวิชา)

บัณฑิตวิทยาลัย จุฬาลงกรณ์มหาวิทยาลัย

ปีการศึกษา 2553

TREATMENT OF EXPLOSIVES WASTEWATER BY ELECTRO-FENTON PROCESS

Mr. Piyawat Tanvanit

A Dissertation Submitted in Partial Fulfillment of the Requirements
for the Degree of Doctor of Philosophy Program in Environmental Management
(Interdisciplinary Program)
Graduate School
Chulalongkorn University
Academic Year 2010

Thesis Title	TREATMENT OF EXPLOSIVES WASTEWATER BY ELECTRO-FENTON PROCESS
By	Mr. Piyawat Tanvanit
Field of Study	Environmental Management
Thesis Advisor	Associate Professor Jin Anotai, Ph.D.
Thesis Co-advisor	Professor Ming-Chun Lu, Ph.D.

Accepted by the Graduate School, Chulalongkorn University in Partial Fulfillment of the Requirements for the Doctoral Degree

....Dean of the Graduate School

(Associate Professor Pornpote Piumsomboon, Ph.D.)

THESIS COMMITTEE

....Chairman

(Assistant Professor Manaskorn Rachakornkij, Ph.D.)

....Thesis Advisor

(Associate Professor Jin Anotai, Ph.D.)

....Thesis Co-advisor

(Professor Ming-Chun Lu, Ph.D.)

....Examiner

(Assistant Professor Chantra Tongcumpou, Ph.D.)

....Examiner

(Assistant Professor Pichaya Rachdawong, Ph.D.)

....External Examiner

(Associate Professor Nurak Grisdanurak, Ph.D.)

ปิยวัฒน์ ตัณฑ์วณิช : การบำบัดน้ำเสียปนเปื้อนวัตถุระเบิดด้วยกระบวนการอิเลคโตรเฟนตัน. (TREATMENT OF EXPLOSIVES WASTEWATER BY ELECTRO-FENTON PROCESS). อ. ที่ปรึกษาวิทยานิพนธ์หลัก : รศ.ดร. จินต์ อโณทัย, อ. ที่ปรึกษาวิทยานิพนธ์ร่วม : Prof. Ming-Chun Lu, Ph.D., 115 หน้า

น้ำเสียจากการผลิตวัตถุระเบิดปนเปื้อนด้วยสารเคมีที่ใช้เป็นส่วนผสมของวัตถุระเบิดเข้มข้น เนื่องจากความเป็นกรดที่สูงและประกอบด้วยสารอินทรีย์เข้มข้น น้ำเสียจากการผลิตวัตถุระเบิดจึงไม่เหมาะสมที่จะบำบัดด้วยวิธีการทางชีวภาพโดยตรง งานวิจัยนี้ศึกษาความเป็นไปได้ในการบำบัดน้ำเสียปนเปื้อนวัตถุระเบิดด้วยกระบวนการอิเลคโตรเฟนตัน การย่อยสลาย ไตรไนโตรโทลูอีน (ทีเอ็นที) เฮกซะไฮโดร-,1,3,5-ไตรไนโตร-1,3,5-ไตรเอซีน (อาร์ดีเอ็กซ์) และออกตะไฮโดร-1,3,5,7-เตตระไนโตร-1,3,5,7-เตตระโซซีน (เอ็ชเอ็มเอ็กซ์) ในสารละลายอิเลคโตรไลท์ 10 มิลลิโมลาร์ของโซเดียมซัลเฟตได้ถูกศึกษาในถังปฏิกรณ์อิเลคโตรเฟนตันขนาดโต๊ะทดลอง วิธีการพื้นผิวตอบสนองถูกนำมาใช้ในการออกแบบการทดลองและศึกษาสภาวะที่เหมาะสม ความสอดคล้องของสมการถูกตรวจสอบด้วยการวิเคราะห์ความแปรปรวนและค่าสัมประสิทธิ์การกำหนดพหุ ผลของสัดส่วนของไฮโดรเจนเปอร์ออกไซด์ต่อเฟอรัส ความเข้มข้นของเฟอรัส กระแสไฟฟ้า และพีเอช ที่มีต่อการบำบัด ทีเอ็นที อาร์ดีเอ็กซ์ และเอ็ชเอ็มเอ็กซ์ ด้วยกระบวนการอิเลคโตรเฟนตันถูกศึกษาโดยอาศัยการออกแบบการทดลองด้วยวิธีการทางสถิติชนิด บ็อกซ์-เบหนเคน (Box-Behnken) จลนศาสตร์อันดับหนึ่งแบบเสมือนและประสิทธิภาพการใช้ไฮโดรเจนเปอร์ออกไซด์ได้ถูกศึกษาด้วย สภาวะในการบำบัดที่เหมาะสมของทีเอ็นทีที่ 78 มิลลิกรัมต่อลิตร คือกระแสไฟฟ้า 0.66 แอมแปร์ พีเอช 3.0 เฟอรัส 0.05 มิลลิโมลาร์ และสัดส่วนของไฮโดรเจนเปอร์ออกไซด์ต่อเฟอรัสที่ 1.8 ส่วนสภาวะในการบำบัดที่เหมาะสมของอาร์ดีเอ็กซ์ที่ 40 มิลลิกรัมต่อลิตร หรือ เอ็ชเอ็มเอ็กซ์ที่ 2.2 มิลลิกรัมต่อลิตร คือกระแสไฟฟ้า 0.04 แอมแปร์ พีเอช 2.6 เฟอรัส 0.8 มิลลิโมลาร์ และสัดส่วนของไฮโดรเจนเปอร์ออกไซด์ต่อเฟอรัสเท่ากับ 3 ประสิทธิภาพของการบำบัดและอัตราการออกซิเดชั่นมีความสัมพันธ์กับพีเอชอย่างมีนัยสำคัญ ในขณะที่ประสิทธิภาพการใช้ไฮโดรเจนเปอร์ออกไซด์นั้นลดลงเมื่อความเข้มข้นของไฮโดรเจนเปอร์ออกไซด์สูงขึ้น

สาขาวิชา การจัดการสิ่งแวดล้อม ลายมือชื่อนิสิต ....

ปีการศึกษา 2553 ลายมือชื่อ อ.ที่ปรึกษาวิทยานิพนธ์หลัก ....

ลายมือชื่อ อ.ที่ปรึกษาวิทยานิพนธ์ร่วม ....

4989440120 : MAJOR ENVIRONMENTAL MANAGEMENT
KEYWORDS: ADVANCED OXIDATION PROCESSES / BOX-BEHNKEN / ELECTRO-FENTON / EXPLOSIVE / HMX / RDX / TNT / RSM / WASTEWATER

PIYAWAT TANVANIT: TREATMENT OF EXPLOSIVES WASTEWATER BY ELECTRO-FENTON PROCESS. ADVISOR: ASSOC. PROF. JIN ANOTAI, Ph.D., CO-ADVISOR: PROF. MING-CHUN LU, Ph.D., 115 pp.

Wastewater generated from munitions production facilities contains very concentrated explosive materials. Due to its very acidic and high organic content, this wastewater is not appropriate to be directly treated by a conventional biological process. This research investigated the treatability of explosives wastewater by the electro-Fenton process. Degradations of 2,4,6,-trinitrotoluene (TNT), hexahydro-1,3,5-trinitro-1,3,5-triazine (RDX) and octahydro-1,3,5,7-tetranitro-1,3,5,7-tetrazocine (HMX) in 10 mM Na_2SO_4 electrolytes have been studied in a bench-scale electro-Fenton reactor. The surface methodology was applied for the experimental design and optimization. Goodness of the model was examined by the analysis of variance and the coefficient of determination. Effects of hydrogen peroxide to ferrous ratio, ferrous concentration, current, and pH on the removal of TNT, RDX, and HMX by electro-Fenton method have been investigated by using Box-Behnken statistical experiment design. The pseudo 1^{st}-order rate and hydrogen peroxide efficiency have also been investigated. The optimum current, pH, ferrous, and hydrogen peroxide to ferrous ratio for the removal of 78 mg/L TNT, were 0.66 A, 3.0, 0.05 mM, and 1.8, respectively. For 40 mg/L RDX or 2.2 mg/L HMX, the optimum conditions were 0.04 A, 2.6, 0.8 mM, and 3, respectively. The removal efficiency and oxidation rates were significantly correlated with pH while the H_2O_2 efficiency decreased as H_2O_2 increased.

Field of Study : Environmental Management Student's Signature ....

Academic Year : 2010 .... Advisor's Signature ....

Co-advisor's Signature ....

ACKNOWLEDGEMENTS

I would like to take this opportunity to express sincere gratitude towards my advisors, Assoc. Prof. Dr. Jin Anotai and Prof. Dr. Ming-Chun Lu, who consistently provided valuable suggestion and useful idea to this research. The completion of this research would have not been possible without their invaluable support and assistance. I would also like to thank my thesis committee: Asst. Prof. Dr. Manaskorn Rachakornkij, Asst. Prof. Dr. Chantra Tongcumpou, Asst. Prof. Dr. Pichaya Rachdawong and Assoc. Prof. Dr. Nurak Grisdanurak for their helpful and valuable comments which significantly enhanced the quality of this research. I am also very appreciating all faculty staffs of the Department of Environmental Engineering, King Mongkut's University of Technology Thonburi, including Ms. Phirada Wongkatsada, Mrs. Jongkolnee Praditpong, Mrs. Denjai Phothong, Ms. Nualchan Laohasirichaikul, Mr. Kampol Ananon, the National Center of Excellence for Environmental and Hazardous Waste Management (NCE-EHWM), Chulalongkorn University (Thailand) including Ms. Walanya Kongseng, and Mr. Soontorn Punnok for their valuable assistances. I am also thanks Mr. Chatree Ritthong, Mr. Weerapun Wattanaweeradej, and all other friends at Chulalongkorn University for their mindfulness. Also a good deal of thanks to wonderful friends in Taiwan including Ms. Wan-Ping Ting, Mr. Min-Jie Chao, Mr. Chung-Lin Chaung, Mr. Yu-Lin Liu, Mr. Chien-Wei Chen, Ms. Shyuan Chen, Mr. Yu-Lun Wei, Mr. Jun-Ying Huang, Mr. Chun-Cheng Fan and friends, Thai friends: Ms. Nalinrut Masomboon, Ms. Mullika Teerakun, Mr. Porntawee Kongroy, Ms. Sarunporn Meesee, Ms. Sutthinee Narkwittaya, Ms. Nonglak Boonrattanakij, Ms. Amornrat Jevprasesphant, Ms. Thapanan Putta, Ms. Siriporn Akewaranugulsiri, Ms. Wichidtra Sudjarid, Ms. Ornuma Pisitsak, Mr. Piaw Phatai, Mr. Ronnakorn Wongsansuk, Mr. Pumis Thuptimdang, Mr. Sermpong Sairiam, Ms. Somporn Singhadech, Ms. Warisa Boonmahotti, Ms. Isara Muangthai, Mr. Visanu Tanboonchuy, Ms. Nittaya Puewchote, Mr. Thanakorn Methatham, Philippines friends: Ms. Joanne O. Encarnacion, Ms. Buenda Rogel, Ms. Luzvisminda M. Bellotindos, Mr. Rishi Arjun Nonnatus P. Llamas, Ms. Anna Francia Mariano, Ms. Delia B. Senoro, Mr. Fibor J. Tan, Ms. Sonia Inarra Buscan, Mr. Erickson Cabuhat Roque, Ms. Cybelle Concepcion Morales Futalan and everybody, who took care and helped me while staying at Chia Nan University of Pharmacy and Science, Tainan in Taiwan and my lovely friends at KMUTT. They always gave me a beautiful friendship to me. Moreover, I would like to be grateful to my best assistance, Ms. Malee Tanvanich, my aunt, who assisted and help me. Finally, I would like to thank my family and relatives for their support with great patience and loving care throughout my life.

Finally, I wish to acknowledge gratefully the financial support under a grant given by National Center of Excellence for Environmental and Hazardous Waste Management, Chulalongkorn University, Thailand, and The National Science Council, Taiwan.

CONTENTS

Page

Page

Page

Page

LIST OF TABLES

LIST OF FIGURES

Figure | Page

Figure Page

LIST OF ABBREVIATIONS

A	=	ampere
AOPs	=	Advanced Oxidation Processes
BBD	=	Box-Behnken Design
BOD	=	Biochemical Oxygen Demand
C	=	coulomb
CCD	=	Central Composite Design
COD	=	Chemical Oxygen Demand
DC	=	direct current
DSA	=	dimension stable anode
g	=	gram
HMX	=	octahydro-1,3,5,7-tetranitro-1,3,5,7-tetrazocine
hr	=	hour
L	=	litre
m	=	metre
mg	=	milligram
min	=	minute
mM	=	millimolar
mol	=	mole
M	=	molar
$M^{-1}\cdot s^{-1}$	=	per molar per second
MΩ·cm	=	megohm centimeter
RDX	=	hexahydro-1,3,5-trinitro-1,3,5-trinitramine
RSM	=	Response Surface Methodology
s^{-1}	=	per second
TNT	=	trinitrotoluene
TOC	=	Total Organic Carbon
V	=	volt
W/L·h	=	watt per litre per hour
μ	=	micro
°C	=	degree Celsius

CHAPTER I

INTRODUCTION

1.1 Statement of Problems

Explosive chemicals are highly hazardous to the environment due to their fast reaction leading to explosion. Explosives can be discharged to the environment in various ways. Explosives can accumulate in air, water and groundwater which are toxic when present at high concentrations. Among them, 2,4,6-trinitrotoluene (TNT) is the most serious global pollutant. Many of its derivations are highly toxic and readily released into the environment because of their high mobility. On economic point of view, TNT, hexahydro-1,3,5-trinitro-1,3,5-triazine (RDX) and octahydro-1,3,5,7-tetranitro-1,3,5,7-tetrazocine (HMX) were mostly used during the World War I and II. On molar basis, TNT is far more toxic to human than any explosives. Low level of explosives still has chronic effects on living organisms.

Among various treatment technologies, Fenton process (a kind of advanced oxidation processes) is the efficient and reliable method that can treat many kinds of organic contaminants. The final products of mineralization are carbon dioxide, water, and inorganic anions. However, sludge after pH adjustment and precipitation is the drawback of this method. Electro-Fenton process is the promising technology that helps minimizing sludge.

Traditional approach of changing one variable at a time to study the effects of variables on the response functions is a time and budget consuming. Statistical design of experiments reduces the number of experiments to be performed, considers interactions among the variables and can be used for the optimization of the operating parameters (Ay *et al.*, 2009).

1.2 Objectives

This study aimed to investigate the application of the electro-Fenton method for treatment of wastewater containing explosives. Specific objectives of this study were as follows:

- To determine the feasibility of treating highly acidic and polluted explosive-containing wastewater by electro-Fenton method.

- To increase the H_2O_2 efficiency via electrolysis by electro-Fenton method.

- To determine the optimal operating parameters of the electro-Fenton method.

- To determine the kinetics of explosives wastewater treatment by electro-Fenton method.

- To determine the intermediates of explosives wastewater treatment by electro-Fenton method.

- To compare the costs of electro-Fenton method with conventional Fenton method for treatment of explosive production wastewater.

1.3 Scope of Investigation

- Use synthetic wastewater.
- Use lab-scale batch reactor under room conditions.
- Target compounds are TNT, RDX and HMX.

1.4 Hypotheses

- Hydroxyl radicals can oxidize explosive chemicals.
- Electro-Fenton can treat organic contaminant better than conventional Fenton method.
- The suitable dosage of ferrous, hydrogen peroxide and current can degrade COD and TOC of explosive wastewater to carbon dioxide and water.
- A statistical experimental design is an effective tool used for optimization of the operating parameters in multivariable systems.

1.5 Expected Results

- Mechanism of explosive chemicals oxidation by hydroxyl radical.
- Kinetics information for explosive chemicals oxidation by electro-Fenton process.

CHAPTER II

LITERATURE REVIEWS

2.1 Introduction

Environmental problems are deal with two main kinds of contaminant; organic compounds (e.g. PCBs, PAH, pesticides, etc.) and inorganic compounds for examples: heavy metals (e.g., Pb, Hg, Cd, As, Cr, Cu, Ni, Zn, etc.). They can transport in the air, surface water, ground water, soil or among of them. Nowadays water is the most serious environmental problems. In order to treat these contaminants in the water, there are many kinds of processes which can be divided into three groups:-

a. Physical treatment: sedimentation, adsorption, filtration, floatation, etc.

b. Chemical treatment: coagulation, flocculation, oxidation, reduction, etc.

c. Biological treatment: aerobic treatment, anaerobic treatment, phytoremediation, etc.

Selection of treatment method is the art and science. No absolute answer is suitable for all kind of wastewater.

2.2 Chemical Oxidation

Chemical oxidation is the oxidation of contaminants to products by oxidants or oxidizing agents. There are many chemicals that are used as oxidants such as chlorine and hydrogen peroxide. Some oxidants may react with specific target compounds only. The oxidation potential of oxidants is summarized in Table 2.1. The more positive potential, the stronger oxidants are. The oxidant potential primarily relates with the pH. By-products should be considered when choosing the oxidants.

2.3 Advanced Oxidation Processes

Advanced oxidation processes (AOPs) are processes that produce highly reactive hydroxyl radical (•OH). These radicals are produced by several methods as follows (Cooper *et al.*, 2009):

-ozonation
-hydrogen peroxide/ultraviolet irradiation (H_2O_2/UV)
-hydrogen peroxide/ozone (H_2O_2/O_3)
-ozone/ultraviolet irradiation (O_3/UV)
-hydrogen peroxide/ozone/ultraviolet (H_2O_2/O_3/UV)
-ultrasound irradiation (US) with and without H_2O_2 or O_3
-vacuum ultraviolet irradiation (VUV)
-microwave
-photocatalysis with TiO_2, CdS, ZnO, SnO_2, WO_3
-sonophotocatalysis

-Super Critical Water Oxidation (SCWO)
-Wet Air Oxidation (WAO)
-Ionizing irradiation
-Pulsed plasma
-Electrochemical oxidation
-Fenton's reagent.

The advantages of AOPs are highly oxidizing power, non selective process and completely mineralization. However, the disadvantages of AOPs are scavenging effect with alkalinity, DOM, nitrate, etc. (Brezonik and Fulkerson-Brekken, 1998).

Table 2.1 Oxidation power of selected oxidizing species, adopted from Beltran *et al.*, 1998.

Oxidants	E^0 (V)	Reference
$F_{2(g)}$	2.89	Quantitative chemical analysis 6th ed.
$SO_4^{\bullet -}$	2.6	Killian, *et.,al.* 2007.
$HO^{\bullet}$	2.56	Quantitative chemical analysis 6th ed.
$NO_3^{\bullet}$	2.45	Zuo, *et.,al.* 1997.
$O^{\bullet}_{(g)}$	2.43	Quantitative chemical analysis 6th ed.
$ClO_3^{\bullet}$	2.35	Zuo, *et.,al.* 1997.
$HFeO_4^-$	2.08	Bratsch, 1989.
$O_{3(g)}$	2.075	Quantitative chemical analysis 6th ed.
$S_2O_8^{2-}$	2.01	Quantitative chemical analysis 6th ed.
Ag^{2+}	1.989	Quantitative chemical analysis 6th ed.
Co^{3+}	1.92	Quantitative chemical analysis 6th ed.
HSO_5^-	1.82	Betterton and Hoffmann, 1990.
H_2O_2	1.763	Quantitative chemical analysis 6th ed.
Ce^{4+}	1.72	Quantitative chemical analysis 6th ed.
MnO_4^-	1.692	Quantitative chemical analysis 6th ed.
$HClO_2$	1.674	Quantitative chemical analysis 6th ed
HOCl	1.630	Quantitative chemical analysis 6th ed.
$CO_3^{\bullet -}$	1.59	Huie *et al.*, 1991.
HOBr	1.584	Quantitative chemical analysis 6th ed.
BrO_3^-	1.513	Quantitative chemical analysis 6th ed.
$HO_2^{\bullet}$	1.44	Quantitative chemical analysis 6th ed.
HOI	1.430	Quantitative chemical analysis 6th ed.
$Cl_{2(aq)}$	1.396	Quantitative chemical analysis 6th ed.
$Cr_2O_7^{2-}$	1.36	Quantitative chemical analysis 6th ed.
$O_{2(g)}$	1.229	Quantitative chemical analysis 6th ed.
ClO_4^-	1.226	Quantitative chemical analysis 6th ed.
ClO_3^-	1.157	Quantitative chemical analysis 6th ed.
ClO_2	1.068	Quantitative chemical analysis 6th ed.
$Br_{2(aq)}$	1.098	Quantitative chemical analysis 6th ed.
CH_3CO_3H	1.06	Knutson, 2004.
Fe^{3+}	0.771	Quantitative chemical analysis 6th ed.
$I_{2(aq)}$	0.620	Quantitative chemical analysis 6th ed.
IO_3^-	0.269	Quantitative chemical analysis 6th ed.

2.4 Fenton Process

Fenton was named after Henry John Horstman Fenton whose experiment for the oxidation of tartaric acid by hydrogen peroxide and iron (II) in the journal of chemical society (Koppenol, 1993). A Fenton process consists of completely stirred reactor, acid with pH controller, a ferrous sulfate catalyst solution and hydrogen peroxide. Fenton's chemistry is a complex collection of reaction pathways as follow (Uri, 1952; Walling and Goosen, 1973; Walling, 1975; Farhataziz and Ross, 1977; Buxton *et al.*, 1988; Stumm and Morgan, 1996; Kang *et al.*, 2006; Pignatello *et al.*, 2006):

Reaction	rate constant ($M^{-1}s^{-1}$)	
$Fe^{2+} + H_2O_2 \rightarrow Fe^{3+} + \bullet OH + OH^-$	k=40-80	(2.1)
$Fe^{3+} + H_2O_2 \Leftrightarrow Fe-OOH^{2+} + H^+$	$K_a=10^{-2.44}$	(2.2)
$Fe-OOH^{2+} \rightarrow Fe^{2+} + \bullet OOH$	k=0.002-0.011s^{-1}	(2.3)
$\bullet OH + H_2O_2 \rightarrow \bullet OOH + H_2O$	k=1.2-4.5$\times 10^7$	(2.4)
$\bullet OH + Fe^{2+} \rightarrow Fe^{3+} + OH^-$	k=3.2-3.5$\times 10^8$	(2.5)
$\bullet OH + \bullet OH \rightarrow H_2O_2$	k=5.2-6.2$\times 10^9$	(2.6)
$\bullet OOH \Leftrightarrow O_2^{-\bullet} + H^+$	$K_a=10^{-4.8}$	(2.7)
$\bullet OOH + Fe^{2+} \rightarrow Fe-OOH^{2+}$	k=1.2$\times 10^6$	(2.8)
$\bullet OOH + Fe^{3+} \rightarrow Fe^{2+} + O_2 + H^+$	k<2$\times 10^3$	(2.9)
$\bullet OOH + \bullet OOH \rightarrow H_2O_2 + O_2$	k=8.3$\times 10^5$	(2.10)
$\bullet OH + \bullet OOH \rightarrow H_2O + O_2$	k=6.6$\times 10^9$	(2.11)
$4Fe^{2+} + O_2 + 4H^+ \rightarrow 4Fe^{3+} + 2H_2O$	k=5$\times 10^{-14}$ $M\cdot s^{-1}$	(2.12)
$\bullet OH + Fe^{3+} \rightarrow FeO^{2+} + H^+$		(2.13)
$\bullet OOH + H_2O_2 \rightarrow \bullet OH + H_2O + O_2$	k=3	(2.14)

Fenton-like process is the use of hydrogen peroxide with the other catalysts that is not ferrous. The non-ferrous metal are Fe^{3+}, Ag^+, Co^{2+}, Cr^{2+}, Cu^+, Mn^{2+}, Ni^{2+}, Ti^{3+}, VO^{2+}, Zn^{2+} or iron oxide (Goldstein *et al.*, 1993; Tarr, 2003). The fluidized bed Fenton is the use of Fenton-like process to generate hydroxyl radical with crystallizing of iron on the carriers that help reducing iron sludge. For most applications, it does not matter ferrous (Fe^{2+}) or ferric (Fe^{3+}) ions are used to catalyze the reaction. The catalytic cycle indicated in Figure 2.1 begins quickly if hydrogen peroxide and organic pollutants are abundant (Pera-Titus *et al.*, 2004)

The advantages of Fenton process are fast and reliable, easy and simple for applying this method, and after mineralization will get CO_2, H_2O and inorganic anions only. However, the disadvantages of Fenton process are limited amount of H_2O_2 applied (if H_2O_2 35% = 1130 g/l×0.35= 395.5 g/l and the dilution factor is 10%, then H_2O_2 40 g/l can degrade COD about 18.6 g/l for the maximum treatment capacity), solubility of ferrous ($FeSO_4$ solubility is 328 g/l), heat generation by applying much of Fenton's reagent (especially with high concentration wastewater which enhancing oxidation rate and reducing wastewater volume by evaporation. The suggestion for high concentration wastewater is using wet air oxidation for better performance and reducing chemical cost), scavenging effect, limited range of pH (appropriate for acidic wastewater only), amount of sludge to be disposed off, toxic oxidation by-products and neutralization of wastewater after treatment with Fenton process.

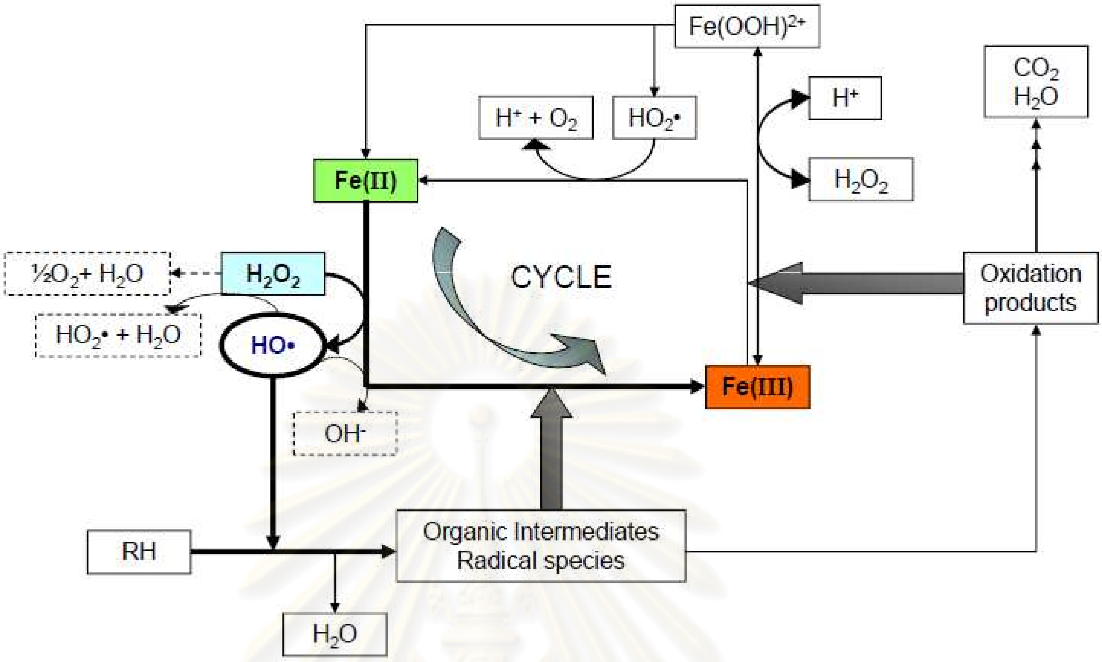

Figure 2.1 Mechanism for degradation of organic pollutants in Fenton and Fenton-like reactions (adapted from Pera-Titus *et al.*, 2004). Scavenging of radicals is not included.

2.5 Electro-Fenton Process (EF)

Electro-Fenton is an indirect oxidation process using electro-assisted generation of hydroxyl radicals. There are many types of electro-Fenton process as follow (Huang *et al.*, 1999):

EF-H_2O_2 – the first type is electrogenerated by hydrogen peroxide with added ferrous ion. In these systems, H_2O_2 can be produced on graphite, reticulated vitreous carbon, or carbon-PTFE cathodes via the two-electron reduction of sparged oxygen. However, a significant drawback is the electrolysis of water often competed with the O_2 reduction and lower the energy efficiency (Do and Chen, 1994).

$$2H^+ + O_2 + 2e^- \rightarrow H_2O_2 \qquad (2.15)$$

EF-FeOx – the second type applied electrogenerated Fe^{2+} by the sacrificial iron anode and additional H_2O_2 (Pratap and Lemley, 1994). However, its disadvantage is the service life of anode.

$$Fe_{(s)} \rightarrow Fe^{2+} + 2e^- \qquad (2.16)$$

EF-FeRe – the last type is electro-regenerated ferrous with addition of H_2O_2. These systems may be defined as Fenton sludge recycling System (FSR).

$$Fe^{3+} + e^- \rightarrow Fe^{2+} \qquad (2.17)$$

The electro-Fenton method has been extensively investigated by many groups of researcher for the individual method or the combination of method above. The mechanistic pathway for electro-Fenton processes is shown in Figure 2.2. The advantages of electro-Fenton process (FeRe) are clean technology by using electron substitutes some of ferrous catalyst which reducing amount of sludge comparing to conventional Fenton process, and effectively apply of H_2O_2. However, the disadvantages of electro-Fenton processes are not suitable for very low concentration of wastewater (low conductivity wastewaters have to add some electrolytes for facilitating electric current in order to reduce electrical cost and increase current efficiency), and not suitable for wastewater with high suspended solids.

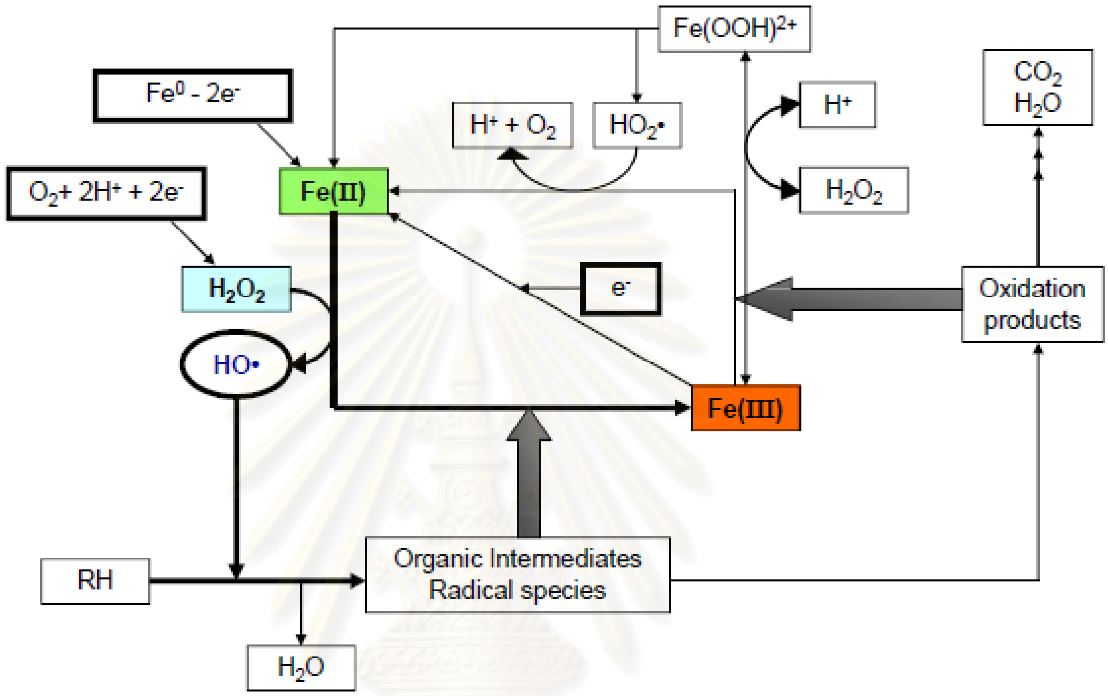

Figure 2.2 General scheme of reactions for electro-Fenton treatment of organic pollutants (adapted from Pera-Titus *et al.*, 2004).

The major parts of electrochemical processes are electrodes which electron transfer occurs. Electrodes can be divided into two types, anode and cathode, depending on their functions. For anode examples are iron, Pt, Ti/SnO_2, Ti/SnO_2-Sb_2O_5, Ti/PdO-Co_3O_4, Ti/RhO_x-TiO_2, Ti/Cr_2O_3-TiO_2, RuO_2-TiO_2 (DSA-Cl_2), IrO_2-Ta_2O_5 (DSA-O_2), Ti/TiO_2-SnO_2, Ti/TiO_2-RuO_2-PbO_2, Pb/PbO_2, Ti/PbO_2, Ti/Pt, Ti/TiO_2, Ti/IrO_2, Ti/RuO_2, Ti/Pt-Ir, Ti/Pt-IrO_2, Ti/MnO_2-RuO_2, Ebonex/PbO_2, Pt/WO_x, *p*-Si/BDD (Boron Doped Diamond), Ti/BDD, Nb/BDD, Ta/BDD, W/BDD, etc. For cathode, they are usually made from stainless steel, graphite, graphite-PTFE, carbon felt, reticulated vitreous carbon (RVC), etc. (Martínez-Huitle and Brillas, 2009). Selection of the electrode depends on electrocatalytic activity and electrochemical stability (Martínez-Huitle and Ferro, 2006). Some electrodes cannot be used due to low reaction rate, low efficiency, or electrode fouling.

The amount of electron transfer can be calculated by Faraday's Law which stated that

$$n = \left(\frac{It}{F}\right) \cdot \left(\frac{1}{z}\right) \qquad (2.18)$$

n is the number of moles (mol)
I is the current applied ($A = C\ s^{-1}$)
t is the time of electrical discharge (s)

F is Faraday constant = 96,485 C mol^{-1}
z is the number of electron transfer (no unit)

Example current 0.80 A applied for 1 L reactor with 1 hour reaction at galvanostatic mode.

$$n = \left(\frac{0.80\frac{C}{s} \times \frac{60s}{1\min} \times \frac{60\min}{1hr}}{96{,}485\frac{C}{mol}} \right) \cdot \left(\frac{1}{1} \right) = 0.0298 mol$$

In 1 L reactor = 0.0298 mol/ 1 L = 0.0298 M or 29.8 mM

2.6 Design of experiments

Currently the optimization of the variables involved in the treatment process is carried out following one of two procedures (Gázquez *et al.*, 1998).

a. traditional univariate method (one at a time). This procedure is valid only when the variables to be optimized do not interact with each other. In addition, it is time-consuming and costly since it requires a large number of experiments.

b. statistical experimentation. The multidimensional optimizations are used because they are very effective, allowing more than one variable to be optimized simultaneously (some of these theniques show whether there is an interaction between them) and providing substantial amounts of information (e.g., interactions) on the studied system. One possible option is based on the response surface methodology (RSM).

2.6.1 Response Surface Methodology (RSM)

This technique includes a group of mathematical statistical methods that is designed to optimize the analytical response by producing a model which a response function corresponds to several variables. Different types of RSM designs are available.

2.6.1.1 Three-level full factorial

Factorial experiments are one of the most efficient designs when multiple parameters interact significantly among themselves and when they have a complementary impact on each other (Kannan *et al.*, 2008). The three-level full factorial design requires three factor levels each, assuming linearity in the factor effects. However, one big drawback with full-factorial design is that the total number of experiments increases sharply as the number of factors increases.

2.6.1.2 Central Composite Design (CCD)

Central composite designs contain imbedded factorial or fractional factorial designs with center points that are augmented with a group of axial (star) points that allow estimation of curvature. The star points represent new extreme values (low and high) for each factor in the design (Hanrahan and Lu, 2006).

2.6.1.3 Box-Behnken Design (BBD)

A modified central composite experimental design known as the Box-Behnken design is an independent, rotatable quadratic design with no embedded factorial or fractional factorial points where the variable combinations are at the midpoint of the edges of the variable space and at the center (Catalkaya and Kargi, 2007). For three factors its graphical representation can be seen in two forms:

a. A cube that consists of the central point and the middle points of the edges, as shown in Figure 2.3 (a).

b. A figure of three interlocking 2^2 factorial designs and a central point, as can be observed in Figure 2.3 (b).

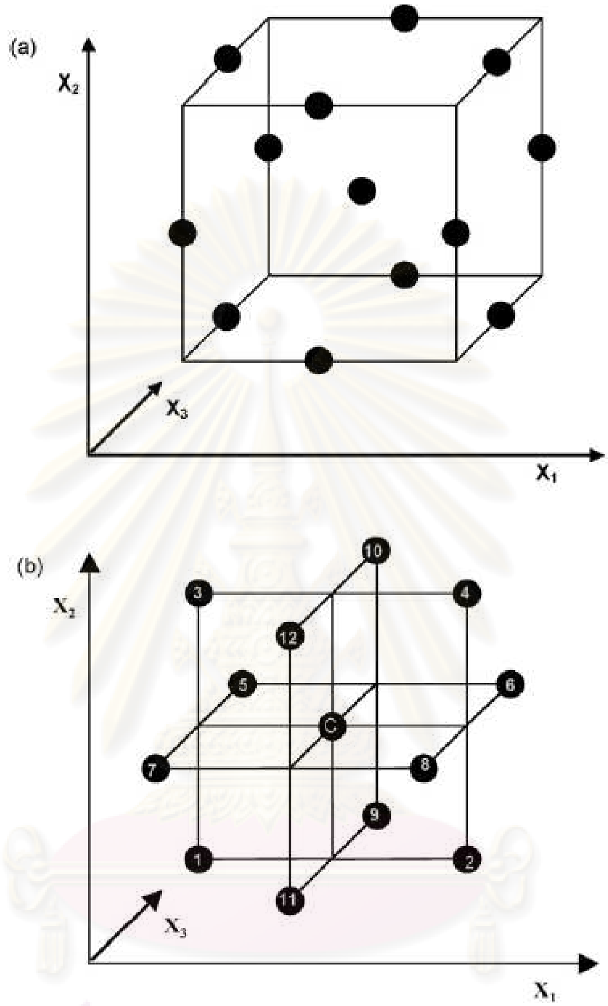

Figure 2.3 (a) the cube for BBD and three interlocking 2^2 factorial design (b) (Ferreira *et al.*, 2007b).

The number of experiments (N) required for the development of BBD is defined as $N = 2k(k-1) + C_0$, (where k is the number of factors and C_0 is the number of central points). For comparison, the number of experiments for CCD is $N = 2^k + 2k + C_0$ (Ferreira *et al.*, 2004) while three-level factorial design is $N = 3^k + C_0$ and for doehlert design is $N = k^2 + k + C_0$ (Sakkas *et al.*, 2010). Table 2.2 establishes a comparison among the number of experiments of the BBD and other response surface designs for the quadratic model. This table demonstrates also that the three-level full factorial designs are costly when the factor number is higher than 2 (Ferreira *et al.*, 2007b). Another advantage of the BDD is that it does not contain combinations for which all factors are simultaneously at their highest or lowest levels. So these designs are useful in avoiding experiments performed under extreme conditions, for which unsatisfactory results might occur. Conversely, they are not indicated for situations in which we would like to know the responses at the extremes, that is, at the vertices of the cube.

Table 2.2 Number of experiments for each RSM technique.

Factors	Centers	Number of experiments (N)				
(k)	(C_0)	3-level factorial	CCD	BBD	D-optimal	Doehlert
2	4	12	12	-	20	10
3	5	31	19	17	25	17
4	5	85	29	29	30	25
5	6	248	48	46	37	36
6	6	734	82	66	44	48
7	6	2,192	148	90	52	62
8	8	6,568	280	120	68	80

2.6.1.4 D-Optimal

The D-optimal criterion, one of several “alphabetic” optimalities, was developed to select design points in a way that minimizes the variance associated with the estimates of specified model coefficients. For details on optimality criteria see *Response Surface Methodology* (Myers and Montgomery, 2002).

2.6.1.5 Doehlert matrices

The Doehlert design describes a spherical experimental domain and it stresses uniformity in space filling. Although this matrix is neither orthogonal nor rotatable, it does not significantly diverge from the required quality for effective use (Massart *et al.*, 2003). In Doehlert designs the number of levels is not the same for all variables (Ferreira *et al.*, 2007a). In a three-variable Doehlert design, for example, one variable is studied at five levels while the others two are studied at seven and three levels respectively.

The applications of RSM for the related Fenton’s treatment and the other treatments of contaminants are summarize in Table 2.3 and Table 2.4 respectively.

Table 2.3 Summary of RSM with Fenton's related process.

No.	contaminant	process	experimental design	factors	responses	software	References
1	*o*-toluidine	photo-Fenton	Box-Behnken	UVA irradiation, [Fe(II)], [H_2O_2]	*o*-T, COD	Design Expert 7.0	Masomboon *et al.*, 2010
2	landfill leachate	electro-Fenton	central composite design	[H_2O_2]:Fe(II), current density, pH, time	COD, Color	Design Expert 6.0.7	Mohajeri *et al.*, 2010
3	acid yellow 36	electro-Fenton	central composite design	current density, [Fe2+], time	Ay 36	Design Expert 6.0.1	Cruz-González *et al.*, 2010
4	simulated industrial wastewaters	Fenton	Box-Behnken	w(HCOONa)%, [Fe(II/III), [H_2O_2], type of Fe	TOC_{120}	Design Expert 6.0.6	Grčić *et al.*, 2009
5	azo dye Procion Red H-EXL	Fenton	central composite design	temp, [H_2O_2], [Fe^{2+}]	TOC	JMP 5.0.1	Rodrigues *et al.*, 2009
6	Simazine	Fenton	Box-Behnken	[simazine], [H_2O_2], [Fe^{2+}]	simazine, TOC	Stat-Ease regression program	Catalkaya and Kargi, 2009
7	formic acid	Fenton, photo-Fenton	D-optimal	temp, [Fe^{3+}], [H_2O_2]:[Formic], irrad.	X_{H2O2}, X_{formic}		Farias *et al.*, 2009
8	Leachate	Fenton	central composite design	pH, [H_2O_2]:[Fe^{2+}], [Fe^{2+}], COD	COD	JMP 3.2	Zhang *et al.*, 2009
9	Alizarin red S	Fenton	central composite design	[H_2O_2]:[Alizarin], [H_2O_2]:[$FeSO_4$], pH	color	MINITAB ® R.14	dos Santos and Masini, 2009

Table 2.3 (continued)

No.	contaminant	process	experimental design	factors	responses	software	References
10	4-chlorophenol	photo-Fenton	central composite design	[Fe(II)], [H_2O_2], [4-CP]	TOC	statistical software	Pérez-Moya *et al.*, 2008
11	Phenol	advanced Fenton processing (Fe^0)	3 level Full-Factorial Design	[Catalyst], [H_2O_2]	TOC, Fe_{total}		Chakinala *et al.*, 2008
12	direct red azo dye (DR 28)	photo-Fenton	Box-Behnken	Dye, [H_2O_2], [Fe(II)]	color, TOC	Stat-Ease Design Expert 7.0	Ay *et al.*, 2009
13	direct red azo dye (DR 28)	Photo-Fenton	Box-Behnken	Dye, [H_2O_2], [Fe(II)]	color, TOC	Stat-Ease regression program	Ay *et al.*, 2008
14	Orange II Dye	clay-based Fenton-like	central composite design	Temp., [H_2O_2], [catalyst]	color, TOC	Labview 5.0	Herney-Ramirez *et al.*, 2008
15	C.I. Acid Red 14	Photo-Fenton	central composite design and artificial neural network	H_2O_2:Dye, pHi, [Catalyst], [Dye]	dye	Matlab V.7	Kasiri *et al.*, 2008
16	chlortoluron	electro-Fenton	two level full factorial design + Doehlert matrix	time, [chlortoluron], current intensity	chlortoluron	NEMROD	Abdessalem *et al.*, 2008
17	Phenol	Peroxidase-Catalyzed Oxidative Coupling Process	Half-Fractional Factorial Designs, Central Composite Designs	pH, [enzyme], Temp., [H_2O_2]	phenol removal efficiency	Design Expert 6.0	Ghasempur *et al.*, 2007
18	Diuron	Fenton	Box-Behnken	[diuron], [H_2O_2], [Fe(II)]	diuron, TOC, AOX	Stat-Ease regression program	Catalkaya and Kargi, 2007
19	4-chlorophenol 200 mgL^{-1}	photo-Fenton	central composite design	[H_2O_2], [Fe^{2+}], [NaCl]	TOC	Statgraphics Plus 4.1	Bacardit *et al.*, 2007

Table 2.3 (continued)

No.	contaminant	process	experimental design	factors	responses	software	References
20	PAHs	Fenton	partial least squares projections to latent structures (PLS)	pH, Conductivity, organic matter content	PAHs	Simca 10.0	Jonsson *et al.*, 2007
21	Basic Red 2 dye	Photolytic degradation	D-optimal	[BR2], [H_2O_2], pH	color	Stat-Ease Design Expert 6.0	Körbahti and Rauf 2007
22	Poly R-478	Chelator-mediated Fenton	two level full factorial design + CCD	pH, [DOPAC], [Fe^{2+}], [H_2O_2]	color	Stat-Ease Design Expert 6.0 + STATISTICA 6.0	Arantes *et al.*, 2006
23	chemical lab WW	Fenton's + precipitation	two level full factorial design + steepest ascent	[COD]:[H_2O_2], [H_2O_2]:[Fe^{2+}], pH	COD	SAS Institute (version 6.12)	Benatti *et al.*, 2006
24	Reactive Blue 4	Photo-Fenton	central composite design + neural networks	[Fe(II)], [H_2O_2], [RB4], pH, Temp.	Color, TOC	in-house Excel spreadsheet	Durán *et al.*, 2006
25	Diuron & Linuron	photo-Fenton+biological	Multivariate experimental design	[Fe(II)], [H_2O_2]	TOC	MODDE 5.0	Farré *et al.*, 2006
26	PCE	Fenton (metal chelating)	Factorial design	soil type, catalyst type, [H_2O_2]	Cl^- release %	Stat-Ease Design Expert 6.0	Kang *et al.*, 2006
27	winery wastewaters	photo-Fenton	2^k factorial design	[H_2O_2], COD, [Clay], Particle size, Time	TOC	MINITAB®	Mosteo *et al.*, 2006
28	2,4-Dichlorophenol	Fenton	Design of experiment	[Fe(II)], [H_2O_2], Temp.	2,4-DCP	JMP 501	Oliveira *et al.*, 2006

Table 2.3 (continued)

No.	contaminant	process	experimental design	factors	responses	software	References
29	winery wastewaters	photo-Fenton	2^k factorial design	COD, [H_2O_2], [Fe(II)], Time	TOC	MINITAB®	Ormad *et al.*, 2006
30	Trifluraline	Coagulation-Fenton	fractional factorial design	pH, Fenton sludge, [Fe(III)], [Fe(II)], [H_2O_2]	color, H_2O_2, COD	-	Martins *et al.*, 2005
31	olive oil processing wastewater	Fenton's peroxidation	central composite design	[H_2O_2]:[Fe^{2+}], pH, [OMW]	COD, Total Phenolics, color, aromatocity	Design Expert 5 + Statistica 5	Ahmadi *et al.*, 2005
32	Orange II Dye	Fenton	central composite design	Temp., [H_2O_2], [Fe^{2+}]	color, TOC	JMP 501	Herney-Ramirez *et al.*, 2005
33	raw gasoline	photo-Fenton	Neural Network Modeling	[Fe(II)], [H_2O_2], [NaCl]	TOC	-	Moraes *et al.*, 2004
34	Atrazine	Fenton	2 level Full-Factorial Design + 3 center points	pH, Temp., [Fe2+], [H2O2]	Abs.	Statistica	López-Cueto *et al.*, 2004
35	Petroleum	Fenton	Factorial design	[H_2O_2], [Fe2+], pH, [Sand], Time,	O&G	-	Millioli *et al.*, 2003
36	cellulose bleaching	Fenton vs photo-Fenton	Factorial design	[Fe(II)], [H_2O_2], Temp.	TOC	FATORIAL	Torrades *et al.*, 2003
37	2,4-xylidine	Photo-Fenton	3D Doehlert uniform array + artificial neural networks	[H_2O_2], [Fe^{2+}], temp.	initial rate	-	Göb *et al.*, 2001
38	3,4-xylidine	light-enhanced Fenton	Doehlert's uniform array + RSM	[H_2O_2], [Fe^{2+}]	xylidine, TOC	NEMROD	Oliveros *et al.*, 1997

Table 2.4 Summary of RSM with the other treatment methods.

No.	contaminant	process	experimental design	factors	responses	software	References
1	Acid green 20 (AG 20)	US/H_2O_2	Box-Behnken	power density, pH, [H_2O_2]	decolorization %	Design Expert 7.1.4 (trial version)	Zhang *et al.*, 2009
2	Phenol	microwave irradiated	central composite design	[phenol], time, microwave power	phenol	MINITAB® R.14	Prasannakumar *et al.*, 2009
3	Rose Bengal	UV/H_2O_2	D-optimal	[Dye], [H_2O_2], pH	color	Stat-Ease Design Expert 7.1	Rauf *et al.*, 2008
4	Carmine	UV/H_2O_2	D-optimal	[Carmine], [H_2O_2], pH, time	color	Stat-Ease Design Expert 7.1	Körbahti and Rauf, 2009
5	Levafix Blue CA reactive dye	electrochemical (iron electrodes)	central composite design	pollution load percent, applied potential, [electrolyte], temp., time	COD, color, turbidity	Design Expert 6.0 (trial version)	Körbahti and Tanyolaç, 2008
6	industrial paint	electrochemical (carbon electrodes)	central composite design	pollution load percent, applied potential, [electrolyte], temp., time	COD, color, turbidity, CODi removal rate	Design Expert 6.0	Körbahti *et al.*, 2007
7	textile dye wastewater	electrochemical (iron electrodes)	central composite design	[dye], current density, [electrolyte], time	dye	Design Expert 6.0 (trial version)	Körbahti 2007
8	Suwannee river dissolved organic matter	Photobleaching	central composite design	[Fe(III)], [NO_3^-], SRDOM, salinity	k_{obs}	Design Expert 5.0.3 Stat-Ease	Hefner *et al.*, 2006

15

Table 2.4 (continued)

No.	contaminant	process	experimental design	factors	responses	software	References
9	Domoic acid	Photodegradation	central composite design	[DOM], [Fe(III)], $[NO_3^-]$, [total-PO_4^{3-}]	k_{obs}	Design Expert 5.0.3 Stat-Ease	Fisher *et al.*, 2006
10	palm oil mill effluent	coagulation-flocculation process supported with membrane separation	central composite design	coagulant dosage, flocculent dosage, pH	turbidity, log turbidity, water recovery	Design Expert 6.0	Ahmad *et al.*, 2005
11	Cr(VI)	reduction and electrocoagulation	central composite design	current, [NaCl], time	Cr(VI)	Design Expert 7.1.3 (trial version)	Ölmez *et al.*, 2009
12	Leachate	coagulation-flocculation using PACl and Alum	central composite design	dosage, pH	COD, Turbidity, Color, TSS	Design Expert 7.0	Ghafari *et al.*, 2008
13	Table olive processing wastewater	electrochemical (BDD electrodes)	2^k factorial design	COD, Current, pH_0, time, $[H_2O_2]$	COD, total phenols	MINITAB® R.14	Deligiorgis *et al.*, 2008
14	Table olive processing wastewater	Wet air oxidation	2^k factorial design	COD, temp., pH_0, time, $[H_2O_2]$	COD, total phenols, Aromatics, Color	MINITAB® R.14	Katsoni *et al.*, 2008
15	reactive black 5	laccase	Box-Behnken	Dye, Enzyme, HBT, time	color	Design Expert 6.0 (trial version)	Murugesan *et al.*, 2007
16	fulvic acid (11.95 mg/L)	photoelectrocatalytic oxidation	Box-Behnken	pH, K2S2O8, Bias potential	FA removal	SAS + Matlab 6.5	Fu *et al.*, 2007
17	reactive red 180	laccase	Box-Behnken	temp., pH, Enzyme	color	Statistica v.5.1 (Statsoft Inc.)	Cristóvão *et al.*, 2008

16

Table 2.4 (continued)

No.	contaminant	process	experimental design	factors	responses	software	references
18	MTBE	biodegradation packed bed	full factorial design + CCD	μ_{max}, K_s, Y, K_x	χ^2_{pred}	Stat-Ease Design Expert 7.1	Waul *et al.*, 2008
19	uniform shell designs		Doehlert design		Y_{MO}	DOEHLOPT	González and González-Arjona 1999
20	analytical chemistry		Doehlert design				Ferreira *et al.*, 2004
21	palm oil mill effluent	UASFF	central composite face-centered design	Q_F, V_{up}	TCOD, SCOD, Eff pH, Eff TVFA, Eff HCO3 Alk , Eff TSS, Methane yield, CH_4 fraction, SMA, Food-to-sludge ratio, sludge height, SRT	Design Expert	Zinatizadeh *et al.*, 2006
22	supported membrane formation		Doehlert design	Percentage of DSPE-PEG-NHS, [Lipid], Contact time between the Vesicles and the Surface, Resting Time after Buffer Rinse	Y_{mass}, Y_D, Y_M	Excel + Maple 9 software	Rossi *et al.*, 2007

Table 2.4 (continued)

No.	contaminant	process	experimental design	factors	responses	software	references
23	terephthalic acid	TiO_2 photocatalyst	central composite design	time, [TiO_2], [terephthalic acid]	fluorescence response	Statistica v.7.1 (Statsoft France)	Eremia *et al.*, 2008
24	review box-behnken	analytical methods	Box-Behnken				Ferreira *et al.*, 2007b
25	landfill leachate	conventional Fenton/ photo-Fenton	turkey's test	temp., pH, [H_2O_2]:[Fe^{2+}]		SigmaStat 2.0 (SPSS Inc.)	Hermosilla *et al.*, 2009
26	Pb in drinking water	Automatic on-line pre-concentration system using a knotted reactor for the FAAS determination	Box-Behnken	pH, [buffer], Sampling Flow Rate	Absorbance	Statistica	Souza *et al.*, 2007
27	Cr(VI)	electrochemical reduction	Box-Behnken	flow velocity, current density, electrode thickness, electrode porosity, [Cr(VI)]	current efficiency, space-time yield, energy consumption	Statistica 5.1	Ruotolo *et al.*, 2005
28	analysis of Castor Oil	Supercritical Fluid Extraction/Reaction Methodology	Box-Behnken	methanol, water, temp., pressure	fatty acid methyl esters (FAMEs) yield	SAS ADX + SAS PROC REG	Turner *et al.*, 2004
29	imipramine	photocatalytic	CCD + ANN	[H_2O_2], [Fe(II)], [TiO_2]	%degradation	Statistica 7.0	Calza *et al.*, 2008

18

2.7 Explosives wastewater

2.7.1 Theoretical Backgrounds

An explosive material is a material that either is chemically or otherwise energetically unstable or produces a sudden expansion of the material usually accompanied by the production of heat and large changes in pressure (and typically also a flash and/or loud noise) upon initiation; this is called the explosion (Wikipedia, 2009). A chemical explosive is a compound or a mixture of compounds which, when subjected to heat, impact, friction, or shock, undergoes very rapid, self-propagating, heat-producing decomposition. This decomposition produces gases that exert tremendous pressures as they expand at the high temperature of the reaction.

2.7.1.1 Low Explosives

A low explosive is usually a mixture of a combustible substance and an oxidant that decomposes rapidly (deflagration), as opposed to most high explosives, which are compounds. Under normal conditions, low explosives undergo deflagration at rates that vary from a few centimeters per second to approximately 400 meters per second. It is possible for them to deflagrate very quickly, producing an effect similar to a detonation. This usually occurs when ignited in a confined space. Low explosives are normally employed as propellants. Included in this group are gun powders, pyrotechnics such as flares and illumination devices.

2.7.1.2 High Explosives

High explosives normally are employed in mining, demolition, and military warheads. High explosive compounds detonate at rates ranging from 3,000 to 9,000 meters per second, and are, conventionally, subdivided into two explosives classes, differentiated by sensitivity:

Primary explosives are extremely sensitive to mechanical shock, friction, and heat, to which they will respond by burning rapidly or detonating. Examples include mercury fulminate, lead styphnate and lead azide.

Secondary explosives, also called *base explosives*, are relatively insensitive to shock, friction, and heat. They may burn when exposed to heat or flame in small, unconfined quantities, but detonation can occur. These are sometimes added in small amounts to blasting caps to boost their power. Dynamite, nitroglycerine (NG), tetryl, TNT, RDX, pentaerythritol tetranitrate (PETN), HMX, hexanitrohexaazaisowurtzitane (HNIW), and others are secondary explosives. PETN is the benchmark compound; compounds more sensitive than PETN are classed as primary explosives.

Some definitions add a third category:

Tertiary explosives or *blasting agents*, are insensitive to shock, they cannot be reliably detonated with practical quantities of primary explosive, and, instead, require an intermediate explosive booster, of secondary explosive, e.g. ammonium nitrate/fuel oil mixture (ANFO) and slurry (wet bag) explosives that are primarily used in large-scale mining and construction.

Noted that many, if not most, explosive chemical compounds may usefully deflagrate and detonate, and are used in high- and low-explosive compounds. Thus, under the correct conditions, a propellant (for example nitrocellulose) might deflagrate if ignited, or may detonate if initiated with a detonator

2.7.2 2,4,6-Trinitrotoluene (TNT)

TNT is a crystalline substance. The importance of TNT as a military explosive is based upon its relative safety in manufacture, loading, transportation, and stowage, and upon its explosive properties. Manufacturing yields are high and production relatively economical. The chemical names for TNT are trinitrotoluene and trinitrotol. Other (commercial) names are Trilite, Tolite, Trinol, Trotyl, Tritolol, Tritone, Trotol, and Triton. TNT is toxic, odorless, comparatively stable, nonhygroscopic, and relatively insensitive. When TNT is pure, it is known as grade A TNT and varies from white to pale yellow. When the proportion of impurities is much greater, the color is darker, often brown, and the chemical is known as grade B TNT. It maybe ignited by impact, friction, spark, shock, or heat. TNT does not form sensitive compounds with most metals. The melting point varies between 80.6 °C for grade A (refined TNT) and 76 °C for grade B (crude TNT). TNT properties are summarized in Table 2.5.

TNT does not appear to be affected by acids but is affected by alkalies (lye, washing soda, and so on), becoming pink, red, or brown, and more sensitive. It is practically insoluble in water, but soluble in alcohol, ether, benzene, carbon disulfide, acetone, and certain other solvents. The velocity of detonation is approximately 22,300 fps.

Exudate has been known to separate from cast TNT. It may appear pale yellow to brown and may vary in consistency from an oily liquid to a sticky substance. The amount and rate of separation depend primarily upon the purity of the TNT and, secondarily, upon the temperature of the stowage place. Grade B (low-melting point) TNT may exude considerable liquid and generate some gas. This exudation is accelerated with an increase in temperature. Pure TNT will not exude since exudate consists of impurities that have not been extracted in the refining process. Exudate is a mixture of lower melting isomers of TNT, nitrocompounds of toluene of lower nitration, and possible nitrocompounds of other aromatic hydrocarbons and alcohols. It is flammable and has high sensitivity to percussion when mixed with absorbents. Its presence does no appreciable harm to the stability but somewhat reduces the explosive force of the main charge (GlobalSecurity.org, 2009b).

TNT is one of the most common bulk explosives. TNT is an explosive used in military munitions and in civilian mining and quarrying activities. TNT was first used on a wide scale during World War I and is still used today. The United States military stopped production of TNT in the mid-1980s.

TNT is classified as a secondary explosive because it is less susceptible to initiation and requires a primary or initiating explosive to ignite it. TNT can be used as a booster or as a bursting charge for high-explosive shells and bombs. Also, TNT may be mixed with other explosives such as Royal Demolition Explosive (RDX) and High Melting Explosive (HMX) and it is a constituent of many explosives, such as amatol, pentolite, tetrytol, torpex, tritonal, picratol, ednatol, and Composition B. It has been used under such names as Triton, Trotyl, Trilite, Trinol, and Tritolo.

The advantages of TNT include low cost, safety in handling, fairly high explosive power, good chemical and thermal stability, compatibility with other explosives, a low melting point favorable for melt casting operations and moderate toxicity.

In some ammunition, an inert wax pad is used in the loading operation, and, in some cases, waxy material may ooze from the case. It should not be confused with the TNT exudate previously described. This material should, however, be tested for

TNT to confirm its actual composition, TNT exudate, when mixed with a combustible material, such as wood chips, sawdust, or cotton waste, will form a low explosive that is highly flammable and ignites easily from a small flame. It can be exploded in a reamer similar to a low grade of dynamite, but the main danger is its fire hazard. Accumulation of exudate is considered a great risk of explosion and fire. Its accumulation should always be avoided by continual removal and disposal as it occurs. While TNT is no longer used in Navy gun ammunition, some 3"/50, 40-mm, and 20-mm stocks loaded with TNT may still be in the inventory. These stocks should be identified and checked periodically for the presence of exudate. The exudate is soluble in acetone or alcohol. One of these solvents (requiring adequate ventilation) or clean, hot water should be used to facilitate removal and disposal of the exudate.

Under no circumstances should soap or other alkaline preparations be used to remove this exudate. The addition of a small amount of hydroxide, caustic soda, or potash will sensitize TNT and cause it to explode if heated to 71 °C.

During production TNT is in the form of a liquid which is then cooled and washed with water to form solid flakes in the form of colorless crystals, though commercial crystals are yellow. The flakes can be remelted at low temperatures (180 degrees Fahrenheit) and poured into munitions shells and casings. TNT was widely used by the military because of its low melting point and its resistance to shock or friction which allows it to be handled, stored, and used with comparative safety.

In order to detonate, TNT must be confined in a casing or shell and subjected to severe pressures and/or temperatures (936 degrees Fahrenheit) such as from a blasting cap or detonator. In fact, U.S. Army tests on pure TNT show that when struck by a rifle bullet TNT failed to detonate 96% of the time and when dropped from an altitude of 4,000 feet onto concrete, a TNT filled bomb failed to explode 92% of the time.

TNT causes liver damage and aplastic anemia. Deaths from aplastic anemia and toxic hepatitis were reported in TNT workers prior to the 1950s. With improved industrial practices, there have been few reports of fatalities or serious health problems related to its use.

Exposures at or below 0.5 mg/m^3 have been reported to cause destruction of red blood cells. Among some groups of workers, there is a reduction in average hemoglobin and hematocrit values. Workers deficient in glucose-6-phosphate dehydrogenase may be particularly at risk of acute hemolytic disease. Three such cases occurred after a latent period of 2 to 4 days and were characterized by weakness, vertigo, headache, nausea, paleness, enlarged liver and spleen, dark urine, decreased hemoglobin levels, and reticulocytosis. Although no simultaneous measurements of atmospheric levels were available, measurement on other occasions showed exposure levels up to 3.0 mg/m^3.

Cataracts are also reportedly produced with chronic exposures for more than 5 years. The opacities did not interfere with visual acuity or visual fields. The induced cataracts may not regress once exposure ceases, although progression is arrested.

The vapor or dust can cause irritation of mucous membranes resulting in sneezing, cough, and sore throat. Although intense or prolonged exposure to TNT may cause some cyanosis, it is not regarded as a strong producer of methemoglobin. Other occasional effects include leukocytosis or leukopenia, peripheral neuritis, muscular pains, cardiac irregularities, and renal irritation.

Table 2.5 Properties of TNT, RDX, and HMX (DuBois and Baytos, 1991; ATSDR, 1996a, 1996b, 1997; Owen Compliance Services Inc., 2006a).

Properties	TNT	RDX	HMX
Formula structures	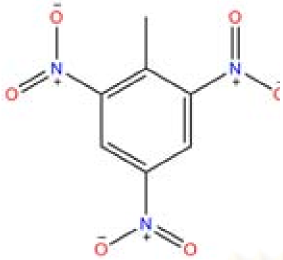	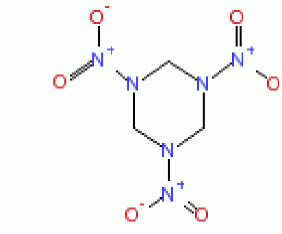	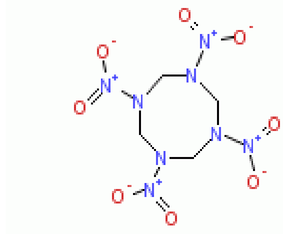
Chemical name	2,4,6-trinitrotoluene, 2-methyl-1,3,5-trinitrobenzene, Tolite, Triton, Trotyl, Trilite	1,3,5-trinitro-1,3,5-triazacyclohexane, cyclotrimethylene trinitramine, hexahydro -1,3,5-trinitro-S-triazine, Hexogen, Cyclonite, T4	cyclo-1,3,5,7-tetramethylene-2,4,6,8-tetranitramine, cyclotetramethylene tetranitramine, Octogen
Chemical formula	$C_7H_5N_3O_6$	$C_3H_6N_6O_6$	$C_4H_8N_8O_8$
CAS NO.	118-96-7	121-82-4	2691-41-0
Molecular weight	227.1	222.117	296.155
Solubility (ppm)	129	34	5
Melting point (˚C)	80	205	276-286
Density (g/cm^3)	1.65	1.82	1.96
Vapor Pressure	0.057 MPa @ 82˚C	4.08×10^{-5} @ 100˚C	N/A
Hazard class	Explosive 1.1D	Explosive 1.1D	Explosive 1.1D
Human carcinogenicity by U.S.EPA	Class C (possible)	Class C (possible)	Not classified
Detonation velocity (m/s)	6,900 m/s	8,750 m/s	9,110 m/s
Log K_{ow}	1.97	0.85	0.15
Estimates of $t_{½}$ from 20 years weathering	1 year	36 years	39 years

TNT is absorbed through skin fairly rapidly, and reference to airborne levels of vapor or dust may underestimate total systemic exposure if skin exposure also occurs. Apparent differences in dose-response relationships based only on airborne levels may be explained by differences in skin contact. TNT causes sensitization dermatitis; the hands, wrist, and forearms most commonly are affected, but skin at friction points such as the collar line, belt line, and ankles also is often involved. Erythema, papules, and an itchy eczema can be severe. The skin, hair, and nails of exposed workers may be stained yellow.

Rats administered 50 mg/kg/day in their diets had anemia, splenic lesions, and liver and kidney damage. Hyperplasia and carcinoma of the urinary bladder also were observed in female rats.

Historically, control of exposure to TNT has been accomplished through general safety and hygiene measures, yet additional, specific measures are necessary. The Hazard Communication Program, for example, should instruct workers about the need for strict personal and shop hygiene, and about the hazards of the particular operations that are conducted in that plant. In addition, soap that contains 5% to 10% potassium sulfite will not only help remove TNT dust from the skin, suds that turn red will also indicate any remaining contamination. Furthermore, respiratory protection equipment should be selected according to NIOSH guidance, and should be worn during operations that release dust, vapor, or fumes.

Before the World War II, research suggested that improving the nutritional status of TNT workers might help improve their resistance to toxic effects. However, in a World War II era cohort study, multivitamin capsules were not shown to be efficacious in preventing TNT toxicity.

TNT interacts with certain medications - including isoniazid, phenylbutazone, phenytoin, and methotrexate. Anyone taking these medications while working with TNT should be closely followed by the occupational physician.

Medical Monitoring. The U.S. Army currently recommends preplacement and periodic (semiannual) examinations of TNT workers. To identify workers with higher-than-normal sensitivity to TNT toxicity during the first three months of exposure, monthly hemoglobin, LDH, and AST should be done.

The ACGIH TLV Committee for Chemical Substances recommended that the 8-hour TLV for TNT be lowered from 0.5 mg/m^3 to 0.1 mg/m^3 on 21 May 1997 after reviewing scientific reports of human and animal exposure. In some studies, evidence of liver toxicity, changes in blood cell production, and cataracts were noted when exposure levels ranged below 0.5 mg/m^3 (the old ACGIH TLV). TNT workers should never be exposed to ambient levels of TNT above 0.1 mg/m^3 for an 8-hour time weighted average (TWA) without appropriate respiratory protection. Based on the evidence reviewed by the ACGIH, the extra margin of safety afforded by this lowered TLV is necessary to protect workers health. Skin absorption has also been noted to be a significant means of exposure in several studies. Dermal exposure over an 8 hour period cannot be readily quantitated at a worksite; however use of protective clothing to include head cover and impermeable gloves is essential to prevent skin absorption of TNT.

The drinking water standards with lifetime exposure assuming the residential exposure of 70 years of TNT is 0.002 mg L^{-1} (US.EPA, 2006).

2.7.3 Hexahydro-1,3,5-trinitro-1,3,5-triazine (RDX)

RDX stands for Royal Demolition eXplosive. It is also known as cyclonite or hexogen. RDX is currently the most important military high explosive in the United States. RDX is an explosive nitramine compound. It is in the form of a white powder with a density of 1.806 g/cm^3 with nitrogen content of 37.84%. The chemical name for RDX is hexahydro-1,3,5-trinitro-1,3,5-triazine. The chemical formula for RDX is $C_3H_6N_6O_6$ and the molecular weight is 222.117. Its melting point is 205 °C. RDX has very low solubility in water and has an extremely low volatility. RDX does not sorb to soil very strongly and can move into the groundwater from soil. It can be broken down in air and water in a few hours, but breaks down more slowly in soil. Physical and chemical properties of RDX are shown in Table 2.5. RDX is second in strength to nitroglycerin among common explosive substances. When compressed to a specific gravity of 1.70, it has a confined detonation velocity of about 27,000 fps. RDX is used as an explosive, usually in mixtures with other explosives, oils, or waxes. It has a high degree of stability in storage and is considered the most powerful and brisant of the military high explosives. RDX is used as a base charge in detonators and in blasting caps. RDX can be used alone or with other explosives, including PETN. RDX can be mixed with plasticizers to make C-4, and the most common explosive combining RDX and PETN is Semtex. RDX forms the base for the following common military explosives: Composition A, Composition B, Composition C, HBX, H-6 and Cyclotol. Composition A consists of RDX melted with wax; in Composition B, RDX is mixed with TNT; and Composition C contains RDX blended with a non-explosive plasticizer. Pure RDX is used in press-loaded projectiles. Cast loading is accomplished by blending RDX with a relatively low melting point substance.

RDX has both military and civilian applications. As a military explosive, RDX can be used alone as a base charge for detonators or mixed with another explosive such as TNT to form cyclotols, which produce a bursting charge for aerial bombs, mines, and torpedoes. Common military uses of RDX have been as an ingredient in plastic bonded explosives, or plastic explosives which have been used as explosive fill in almost all types of munition compounds. Civilian applications of RDX include use in fireworks, in demolition blocks, as a heating fuel for food rations, and as an occasional rodenticide. Combinations of RDX and HMX, another explosive, have been the chief ingredients in approximately 75 products.

Although RDX was first prepared in 1899, its explosive properties were not appreciated until 1920. RDX was used widely during World War II because petroleum was not needed as a raw ingredient. During and since World War II, RDX has become the second-most-widely used high explosive in the military, exceeded only by TNT. As with most military explosives, RDX is rarely used alone; it is widely used as a component of plastic explosives, detonators, high explosives in artillery rounds, Claymore mines, and demolition kits. RDX has limited civilian use as a rat poison.

RDX can cause seizures in humans and animals when large amounts are inhaled or ingested. Nausea and vomiting have also been observed. The effects of long-term (365 days or longer), low-level exposure on the nervous system are not known. No other significant health effects have been reported in humans. Rats and mice that ate RDX for 3 months or more had decreased body weights and slight liver and kidney damage. It is not known whether RDX causes birth defects in humans. It did not cause birth defects in rabbits, but did result in smaller offspring in rats. It is not known whether RDX affects reproduction in humans. The EPA has determined that RDX is a possible human carcinogen (Class C). In one study, RDX caused liver tumors in mice that were exposed to it in the diet. However, carcinogenic effects were not noted in rat studies and no human data are available. RDX does not bioaccumulate in fish or in humans.

RDX has been produced several ways, but the most common method of manufacture used in the United States is the continuous Bachmann process. The Bachmann process involves reacting hexamine with nitric acid, ammonium nitrate, glacial acetic acid, and acetic anhydride. The crude product is filtered and recrystallized to form RDX. The byproducts of RDX manufacture include nitrogen oxides, sulfur oxides, acid mists, and unreacted ingredients. A second process that has been used to manufacture RDX, the direct nitration of octahydro-1,3,5,7-tetranitro-1,3,5,7-tetrazocine (HMX), has not yielded a percentage of RDX as high as the percentage produced in the Bachmann process.

Production of RDX peaked in the 1960s when it was ranked third in explosive production by volume in the United States. The average volume of RDX produced from 1969 to 1971 was 15 million pounds per month. However, production of RDX decreased to a yearly total of 16 million pounds for 1984.

RDX is not produced commercially in the United States. Production in the United States is limited to Army ammunition plants such as Holston Army ammunition plant in Kingsport, Tennessee, which has been operating at 10-20% capacity. Several Army ammunition plants, such as Louisiana (Shreveport, Louisiana), Lone Star (Texarkana, Texas), Iowa (Middletown, Iowa), and Milan (Milan, Tennessee), also handle and package RDX. Since the release of RDX is not required to be reported under SARA Section 313, there are no data on RDX in the Toxics Release Inventory (US.EPA, 1995).

Waste-water treatment sludges resulting from the manufacture of RDX are classified as hazardous wastes and are subject to EPA regulations. Munitions such as RDX have been disposed of in the past by dumping in deep sea water. By-products of military explosives such as RDX have also been openly burned in many Army ammunition plants in the past. There are indications that in recent years as much as 80% of waste munitions and propellants have been disposed of by incineration. Wastes containing RDX have been incinerated by grinding the explosive wastes with a flying knife cutter and spraying the ground material with water to form slurry. The types of incineration used to dispose of waste munitions containing RDX include rotary kiln incineration, fluidized bed incineration, and pyrolitic incineration. The primary disadvantage of open burning or incineration is that explosive contaminants are often released into the air, water, and soils.

Soldiers and other workers have been exposed to RDX during its manufacture, in the field, and through the contamination of the environment. The main occupational exposure to RDX during its manufacture is through the inhalation of fine dust particles. Ingestion may also be a possible route of exposure, but it is poorly absorbed through the dermis.

The greatest potential for occupational exposure to RDX occurs at ammunition plants with load, assemble and pack (LAP) operations, where workers involved with melt-pouring and maintenance operations have the greatest potential for exposures.

In 1962, five cases of convulsions or unconsciousness or both occurred at an RDX manufacturing plant in the United States. All five employees had convulsions during their work shifts or within a few hours after their shifts were over. These patients exhibited little or no prodrome, and the postictal phase lasted up to 24 hours. No abnormal laboratory or physical findings were noted.

Troops have also become intoxicated during field operations from exposure to composition C4 plastic explosive, which contains 91% RDX. These field exposures occurred because C4 was either chewed as an intoxicant or used as a fuel for cooking. Thus, the route of exposure was ingestion or inhalation. At least 40 American soldiers experienced convulsions due to RDX ingestion during the Vietnam War.

After acute exposure by inhalation or ingestion, there is a latent period of a few hours, followed by a general sequence of intoxication that begins with a prodromal period of irritability. Neurological symptoms predominate and include restlessness and hyperirritability; headache; weakness; dizziness; hyperactive reflexes; nausea and vomiting; prolonged and recurrent generalized convulsions; muscle twitching and soreness; and stupor, delirium, and disorientation.

Clinical findings in acute exposures may also include fever, tachycardia, hematuria, proteinuria, azotemia, mild anemia, neutrophilic leukocytosis, elevated AST, and electroencephalogram (EEG) abnormalities. These abnormal effects, transient and unreliable for diagnosis purposes, last at most a few days. In fact, all physical and laboratory tests may remain normal, even in the presence of seizures. EEGs made at the time of convulsions may show bilateral synchronous spike and wave complexes (2-3/sec) in the frontal areas with diffuse slow wave activity; normalization occurs within 1 to 3 months.

RDX in the wastewater from manufacturing and loading operations has also contaminated the environment. Although contamination has appeared in soil and groundwater near some ammunition plants, RDX's low solubility in water has limited its migration in most cases.

Although intensive research with animals has revealed some effects, few effects of chronic human exposure to RDX have been reported. Investigations into the mutagenicity and carcinogenicity of RDX have yielded conflicting results. RDX does not appear to be a mutagen, based on negative results in the Ames tests, the dominant lethal test, and the unscheduled deoxyribonucleic acid synthesis assay. RDX has not been found to be carcinogenic in gavage studies performed on rats, but increased hepatocellular carcinoma and adenoma were noted in females of one strain of mice. Due to this finding, the U.S. Environmental Protection Agency has classified RDX as a possible human carcinogen (GlobalSecurity.org, 2009a).

Reproductive effects have been noted in rabbits and rats. A study performed on rabbits showed teratogenic effects at 2 mg/kg/day (10% of the dose that caused maternal toxicity). Similarly, a teratology study performed on pregnant rats exposed to RDX resulted in offspring with lower body weights and shorter body lengths than were found in the control group. These researchers therefore recommended that human females of childbearing age be protected from exposure to RDX.

Despite the low toxicity of RDX, exposure should be maintained at the lowest levels possible due to its possible carcinogenicity. General medical surveillance examinations can be conducted (such as liver and kidney function tests), but specific testing for the effects of low level occupational exposure does not appear to be warranted, given the absence of abnormal results even in those patients with RDX-induced seizures. Surveillance for both males and females should also include a screening questionnaire for reproductive history. Pregnant women should avoid exposure to RDX.

2.7.4 Octahydro-1,3,5,7-tetranitro-1,3,5,7-tetrazocine (HMX)

HMX is the highest-energy solid explosive produced on a large scale in the United States. HMX is an explosive polynitramine. The chemical formula is $C_4H_8N_8O_8$ and molecular weight is 296.20. It is a colorless solid with a melting point of 276 to 286 °C. HMX is made by the nitration of hexamine with ammonium nitrate and nitric acid in an acetic acid/acetic anhydride solvent. A small amount of HMX is also formed in making RDX, another explosive similar in structure to HMX. Physical and chemical properties of HMX are shown in Table 2.5. It is also known as Octogen and cyclotetramethylene-tetranitramine, as well as other names. HMX explodes violently at high temperatures (278 °C and above). Because of this property, HMX is used exclusively for military purposes to implode fissionable material in nuclear devices, as a component of plastic-bonded explosives, as a component of rocket propellant, and as a high explosive burster charge. The use of HMX as a propellant and in maximum-performance explosives is increasing.

HMX was discovered as a by-product in the production of RDX. Although it is almost as sensitive and powerful as RDX, it is seldom used alone in military applications but is normally mixed with another compound, such as TNT. In the Navy, HMX is used as an ingredient in plastic-bonded explosives.

HMX is produced by the nitration of hexamine with ammonium nitrate and nitric acid in an acetic acid/acetic anhydride solvent at 44 °C. The raw materials are mixed in a two-step process and the product is purified by recrystallization. This is a modification of the Bachmann Process used to produce RDX, another explosive. The yield of HMX is about 55-60%, with RDX as an impurity. RDX produced by the Bachmann Process usually contains about 8-12% HMX as an acceptable byproduct.

HMX is currently produced at only one facility in the United States, the Holston Army Ammunition Plant in Kingsport, Tennessee. The amount of HMX made and used in the United States at present is not known, but it is believed to be greater than 30 million pounds [15,000 tons] per year between 1969 and 1971. No estimates of current production volume were located, but it is estimated that its use is increasing. Processing may occur at load, assemble, and pack (LAP) facilities operated by the military. There were 10 facilities engaged in LAP operations in the United States in 1976.

No information was located regarding import or export of HMX in the United States. Export of this chemical is regulated by the U.S. State Department.

Wastes from explosive manufacturing processes are classified as hazardous wastes by EPA. Generators of these wastes must conform to EPA regulations for treatment, storage, and disposal. The waste water treatment sludges from processing of explosives are listed as hazardous wastes by EPA based only on reactivity. Waste water treatment may involve filtering through activated charcoal, photolytic degradation, and biodegradation. Rotary kiln or fluidized bed incineration methods are acceptable disposal methods for HMX-containing wastes. At the Holston facility, wastewaters are generated from the manufacturing areas and piped to an industrial water treatment plant on site. Following neutralization and nutrient addition, sludge is aerobically digested and dewatered. It was estimated that the facility generates a maximum of 3,800 tons (7.6 million pounds) of treated, dewatered sludge annually. Based on demonstration by Holston that this sludge is nonhazardous, the EPA proposed granting a petition to exclude the sludge from hazardous waste control. HMX is not listed on the Toxics Release Inventory (TRI) database, because it is not a chemical for which companies are required to report discharges to environmental media.

It dissolves slightly in water. Only a very small amount of HMX will evaporate into the air; however, it can occur in air attached to suspended particles or dust. The taste and smell of HMX are not known.

HMX is a manmade chemical and does not occur naturally in the environment. It is made from other chemicals known as hexamine, ammonium nitrate, nitric acid, and acetic acid. A small amount of HMX is also formed in making cyclotrimethylene-trinitramine (RDX), another explosive similar in structure to HMX.

HMX is only slightly soluble in water. It has low volatility and thus only a small amount of HMX will evaporate into the air (Singh, 2007); however, it can occur in air attached to suspended particles or dust. In surface water, HMX does not evaporate or bind to sediments to any large extent (Roh, *et al*., 2009). Sunlight breaks down most of the HMX in surface water into other compounds, usually in a matter of days to weeks. HMX is likely to move from soil into groundwater, particularly in sandy soils (Martel *et al*., 2009).

Exposure to HMX can occur during the manufacture and filling of munitions or through the environmental contamination of groundwater and soil. HMX, like RDX, is manufactured using the continuous Bachman process. Although its solubility in water is very low, HMX can be present in particulate form in water effluent from manufacturing, LAP, and demilitarization operations (Steevens *et al*., 2002).

Information on the adverse health effects of HMX is limited. In one study on humans, no adverse effects were reported in workers exposed to HMX in air. However, the concentrations of HMX in the workplace air were not reported in this study, and only a small number of workers and effects were investigated.

Studies in rats, mice, and rabbits indicate that HMX may be harmful to the liver and central nervous system if it is swallowed or contacts the skin. The lowest dose producing any effects in animals was 100 milligrams per kilogram of body weight per day (mg/kg/day) orally and 165 mg/kg/day on the skin. Limited evidence suggests that even a single exposure to these dose levels harmed rabbits. The mechanism by which HMX causes adverse effects on the liver and nervous system is not understood.

The reproductive and developmental effects of HMX have not been well studied in humans or animals. At present, the information needed to determine if HMX causes cancer is insufficient. Due to the lack of information, EPA has determined that HMX is not classifiable as to its human carcinogenicity (GlobalSecurity.org, 2009a).

The data on the effects on human health of exposure to HMX are very limited. HMX causes CNS effects similar to those of RDX, but at considerably higher doses. In one study, volunteers submitted to patch testing, this produced skin irritation. Another study of a cohort of 93 workers at an ammunition plant found no hematological, hepatic, autoimmune, or renal diseases. However, the study did not quantify the levels of exposure to HMX.

HMX exposure has been investigated in several studies on animals. Overall, the toxicity appears to be quite low. HMX is poorly absorbed by ingestion. When applied to the dermis, it induces mild skin irritation but not delayed contact sensitization. Various acute and subchronic neurobehavioral effects have been reported in rabbits and rodents, including ataxia, sedation, hyperkinesia, and convulsions. The chronic effects of HMX that have been documented through animal studies include decreased hemoglobin, increased serum alkaline phosphatase, and decreased albumin. Pathological changes were also observed in the animals' livers and kidneys. No data are available concerning the possible reproductive, developmental, or carcinogenic effects of HMX.

The EPA recommends a drinking water guideline of 2 and 400 μg/L for RDX and HMX lifetime exposure for adults respectively.

2.7.5 Explosives wastewater

Explosives can enter the environment from sites where they are manufactured, load, assemble and pack (LAP) operated, stored, disposed, used in military training or demilitarization (Best *et al.*, 1999). In the past, their methods of production and storage led to wide dispersion of explosives in the environment (Vila *et al.*, 2007) especially soil and groundwater. Explosives are typically degraded very slow in environmental systems (Pennington and Brannon, 2002). As with most explosives, all were known to be toxic to aquatic and terrestrial organisms (Heilmann *et al.*, 1996; Aken *et al.*, 2004; Liou and Lu, 2008), and causing groundwater contamination.

There are many methods that can treat the explosive compounds such as incineration, adsorption, advanced oxidation processes, alkaline hydrolysis, chemical reduction, and bioremediation (Emmrich, 1999; Hofstetter *et al.*, 1999; Rodgers and Bunce, 2001). Adsorption by granular activated carbon (GAC) is currently the most common treatment because of its simplicity, effectiveness and relatively low price, but the spent GAC is classified as hazardous waste and needs further treatment. Alkaline hydrolysis or chemical reduction by iron metal may promote transformation and detoxification (Agrawal and Tratnyek, 1996; Hundal *et al.*, 1997; Zoh and stenstrom, 2002; Park *et al.*, 2004), but it is not a stand-alone complete remediation method. The potential advantages of bioremediation include low cost, ease of operation and public acceptance. However, long residence time and resistance to complete mineralization have been the major problems for this biological treatment approach (Rodgers and Bunce, 2001; Aken *et al.*, 2004). Advanced oxidation processes are better than the other methods due to complete remediation and fast reaction. Fenton process, one of the advanced oxidation processes, can degrade explosive compounds (Bose *et al.*, 1998; Bier *et al.*, 1999; Liou *et al.*, 2003; Liou *et al.*, 2004; Liou and Lu, 2007; and Pignatello *et al.*, 2006). However the sludge produced after reaction needs further separation and disposal (Chang *et al.*, 2004). There are also other procedures that improve oxidation efficiency like the photo-Fenton process (Liou *et al.*, 2003) or reducing the sludge by electro-Fenton process.

Table 2.6 Various methods of TNT, RDX, and HMX treatment.

Explosive	Methods	Time of removal	References
TNT, RDX, HMX	Biodegradation	TNT 100 µM 4 day RDX 90 µM 18 day HMX 23 µM >28 day	Moshe *et al.*, 2009
TNT, HMX, RDX	In situ redox manipulation ($S_2O_4^{2-}$)	TNT 286 µM >3 day RDX 90 µM 4 hr HMX 10 µM 10 hr	Boparai *et al.*, 2008
TNT, RDX, HMX	Nickel catalysts	TNT 230 µM 55 min RDX 45 µM 30 min HMX 6.5 µM 30 min	Fuller *et al.*, 2007
RDX, HMX	Adsorption (Activated carbon)	RDX 10 µM 4.1 min HMX 3.7 µM 8.2 min	Morley *et al.*, 2005
TNT, RDX, HMX	Biodegradation	TNT 110 µM 9 day RDX 90 µM 33 day HMX 8.4 µM 40 day	Aken *et al.*, 2004
RDX, HMX	Reduction (Zero-Valent Iron)	RDX 864 µM 6 hr HMX 706 µM 12 hr	Park *et al.*, 2004
RDX, HMX, CL-20	Alkaline Hydrolysis	RDX 17 day HMX > 15 day	Balakrishnan *et al.*, 2003
TNT, RDX, HMX	Anaerobic biodegradation	TNT 50 µM 1 day RDX 25 µM 5 day HMX 8 µM > 29 day	Adrian *et al.*, 2003
TNT, HMX, RDX	AOPs (Fenton + photo-Fenton)	TNT 420 µM 50 min RDX 204 µM 90 min HMX 107 µM > 2 hr	Liou *et al.*, 2003
TNT, RDX, HMX	Phytoremediation	TNT 500 µM n.d. RDX 270 µM n.d. HMX 16 µM n.d.	Hannink *et al.*, 2002
RDX, HMX	AOPs (Fenton)	RDX 45 µM 2 hr HMX 15 µM 4 hr	Zoh and Stenstrom, 2002
RDX	White Rot Fungus	RDX 279 µM 25 day	Sheremata and Hawari, 2000
TNT	Alkaline Hydrolysis	TNT 4 day	Emrich, 1999
TNT	Iron-Reducing Subsurface	TNT 13 µM 53 hr	Hofstetter *et al.*, 1999
TNT	Reduction in montmorillonite	TNT 66 µM 1 day	Brannon *et al.*, 1998
TNT, RDX	Reduction (Iron metal)	TNT 2 hr RDX 4 hr	Hundal *et al.*, 1997
RDX, HMX	Alkaline Hydrolysis	RDX 180 µM 20 min HMX 16 µM 100 min	Heilmann *et al.*, 1996
TNT	Reduction by Photocatalysis	TNT 200 µM 45 min	Schmelling *et al.*, 1996

CHAPTER III

MATERIAL AND METHODS

3.1 Chemicals

TNT, RDX and HMX were provided by the Department of Applied Chemistry, Chung Cheng Institute of Technology, ROC. Hydrogen peroxide (H_2O_2, 35%), ferrous sulfate heptahydrate ($FeSO_4 \cdot 7H_2O$), sodium sulfate (Na_2SO_4), and sulfuric acid (H_2SO_4) were purchased from the Merck Company. Sodium phosphate dibasic dihydrate ($Na_2HPO_4 \cdot 2H_2O$) was purchased from Riedel de Haën. All chemicals were reagent grade and used as received without further purification. All aqueous solutions were prepared by purified water from a Millipore Simplicity system (R = 18.2 MΩ cm).

The explosives wastewater was obtained from an explosives production plant in Taiwan.

3.2 Experimental Setup

TNT or RDX and HMX was dissolved with purified water and pH was adjusted with sulfuric acid to the desired pH for 1, 2 and 3 days before use, respectively. A stainless steel cylinder reactor of diameter 12 cm with 12 cm high was used as a cathode while DSA rod diameter of 1.2 cm at the center was used as an anode. Surface area of the cathode and anode were 370 and 37 cm^2, respectively, with the reactor working volume of 1 L. Both electrodes were connected to the DC power supply (TOPWARD 33010D, Taiwan) operated in galvanostatic mode (potential could varied ± 1.5 V). One mixer was installed to provide complete agitation in the reactor.

At the beginning of each experiment (working in a batch mode), TNT 78 mg/L or RDX 40 mg/L and HMX 2.2 mg/L solution was added with sodium sulfate to 10 mM and ferrous sulfate to generate Fe^{2+} as required. Temperature was controlled constantly at 25±1˚C throughout the experiment by refrigerated circulator (TKS model RCB-412, Taiwan). H_2SO_4 or NaOH was added as necessary to control the pH ± 0.10 at the desired level through out the experiment. Predetermined amount of H_2O_2 was added into the reactor to initiate the reaction and the DC power supply was switched on as needed. At selected time intervals, 5 mL of reaction mixture was taken and immediately injected into an amber vial containing 1 mL of 0.01 M Na_2HPO_4 to quench the Fenton reactions (Liou *et al.*, 2003). The pH was measured using a portable pH/mV meter (SUNTEX TS-1, Taiwan). Temperature was measured by a glass thermometer. The setup equipment was shown in Figure 3.1.

3.3 Analytical Methods

3.3.1 COD

COD was determined using a closed-reflux titrimetric method based on Standard Methods 5220 C (APHA, 2005). Withdrawn samples were diluted as desired with deionized water and 1 M NaOH was added to stop the oxidation reaction (pH 12.0).

Figure 3.1 Equipment Setup

3.3.2 Iron

Ferrous was determined using a phenanthroline method based on Standard Methods 3500-Fe B by the Genesis 20UV-VIS spectrophotometer (APHA, 2005).

Total Iron was determined using a PerkinElmer Atomic Absorption Spectrometer (AAs) model AAnalyst 200 with hollow cathode lamps. The operating conditions was 248.33 nm wavelength, 45 mA lamp current, and 1.8/1.35 nm slit width. The flame was air-acetylene.

3.3.3 Hydrogen Peroxide

The sample was added with potassium titanium (IV) oxalate agent following the potassium titanium (IV) oxalate method (Eisenberg, 1943; Sellers, 1980; Liu *et al.*, 2007). Then, the DI water is added to make up the volume before analyzing by the Genesis 20UV-VIS spectrophotometer (Sermpong Sairiam, 2008).

3.3.4 TOC

TOC was determined using a high-temperature combustion method based on Standard Methods 5310 B (APHA, 2005). The platinum catalyst was used in the combustion chamber of elementar liquiTOC analyzer coupled with non-dispersive infrared (NDIR) detector. The carrier gas was air zero with a flow rate of 200 mL/min. Calibration of the analyzer was achieved with potassium hydrogen phthalate (99.5%, Merck) and sodium carbonate (secondary reference material, Merck) standards for total carbon (TC) and inorganic carbon (IC), respectively. The difference between TC and IC analysis gives TOC data of the sample.

3.3.5 Target Compounds

An analytical system complete with column supplies, high-pressure syringes, detectors, and a data system for measuring peak areas and retention times. Use system capable of injecting 20 µL portions and of performing at a constant flow rate. Primary column: 150 mm long × 6 mm ID stainless steel packed with 5 µm Asahipak C18. The column was operated between 22 and 25℃. Detector: Use UV detector capable of excitation at approximately 254 nm (deuterium). The detector was SpectraSYSTEM model UV1000. Filters: For microfiltration of samples before HPLC analysis, use 25-mm filter holder and 25-mm-diam 0.2-µm polyester filters. Mobile phase: 60:40 v/v acetonitrile:water. Flow rate: 1.0 mL/min. The pump was SpectraSYSTEM model SN4000. Injection volume is 500 µL.

3.3.6 Intermediate Compounds

Intermediate anions was determined using an ion chromatography with chemical suppression of eluent conductivity method based on Standard Methods 4410 B (APHA, 2005). Ion Chromatography (IC) Dionex DX-120 Ion Chromatograph with the operating flow rate were 1.0 mL/min, equipped with Reagent-Free^{TM} Controller with RFIC^{TM} EGC II KOH (RFC-30), Autosampler Thermo Finnigan SpectraSYSTEM model AS1000 with 20 µL injection volume, Guard column IonPac® AG-11 (4×50 mm), an anionic exchanger column IonPac® AS-11 (4×250 mm), column temperature stabilizer model CTS-10 control at 30 ˚C with a CDM-3 conductivity detector. The sensitivity of this detector was improved from electrolyte suppression using an ASRS®-ULTRA II 4-mm self regenerating suppressor. with gradient 0.1 mM KOH 0-4 min, 0.1 – 18 mM KOH time 4-22 min, 18 mM KOH 22-26 min, 0.1 mM KOH 26-30 min. Calibration curves were obtained by using the pure standards of the related ions. Data acquisition through a Chromanager software.

3.3.7 Analysis of BOD

BOD was determined using a 5-day BOD test method based on Standard Methods 5210 B (APHA, 2005). DO meter was WTW model Oxi 330i with Cell Ox 325 probe. Withdrawn samples were diluted as desired with deionized water and 1 M NaOH was added to stop the oxidation reaction (pH 12.0). Before incubate the samples for 5 days, the final pH in BOD bottles were adjusted between 6 and 8.

3.4 Strategy of Experiment

In this research, main experimental works can be divided into 4 phases as follows:

Phase 1. Study of TNT removal by electro-Fenton process. Box-Behnken design was also investigated.

Phase 2. Use Box-Behnken design for optimization of RDX removal by electro-Fenton process.

Phase 3. Use Box-Behnken design for optimization of HMX removal by electro-Fenton process.

Phase 4. Comparative study of explosives wastewater treatment by various methods including electrolysis, H_2O_2/UVA, Fenton, electro-Fenton, and photo-Fenton.

Design Expert® Software version 7.0.0 was used for the experimental design and optimization. Table 3.1 shows the levels with coded of three factors tested with Box-Behnken design.

Table 3.1 The levels of variable in Box-Behnken design experiment

Factor	Symbol	Coded variable level		
		Low -1	Center 0	High +1
Fe^{2+} (mM)	X_1	0.0009	0.0455	0.09
H_2O_2 (mM)	X_2	0.29	1.595	2.90
Current (A)	X_3	0.05	0.43	0.80

Table 3.2 shows the design matrix for the TNT removal by electro-Fenton process. The notations of (-1), (0), and (+1) illustrated the low, middle and high level of Box-Behnken design, respectively. The responses were removal efficiency of TNT and 1st order kinetics were evaluated.

Table 3.2 Design matrix for three factors of Box-Behnken design experiment

	Factors			Responses
Run	Fe^{2+} (mM)	H_2O_2 (mM)	Current (A)	(unit)
1	+1	+1	0	
2	+1	-1	0	
3	+1	0	+1	
4	-1	0	-1	
5	0	-1	-1	
6	+1	0	-1	
7	0	-1	+1	
8	-1	-1	0	
9	0	+1	+1	
10	0	+1	-1	
11	-1	0	+1	
12	-1	+1	0	
13	0	0	0	

The Response Surface Methodology (RSM) based on Box-Behnken design was further developed using RDX or HMX removals by electro-Fenton process. The Box-Behnken design experiment with coded of four factors was shown in Table 3.3. The low, center and high levels of each variable are coded as -1, 0, and +1, respectively.

Table 3.3 Levels of factor in Box-Behnken design

Factor	Symbol	Coded variable level		
		Low -1	Center 0	High +1
$H_2O_2 : Fe^{2+}$ (mM/mM)	X_1	3	16.5	30
Fe^{2+} (mM)	X_2	0.1	0.55	1.0
Current (A)	X_3	0.04	0.12	0.20
pH	X_4	2	3	4

The Box-Behnken experimental design was shown in Table 3.4. The responses were removal efficiency of RDX or HMX, 1st-order kinetics, and hydrogen peroxide efficiency were evaluated. The optimum condition obtained from Box-Behnken design was further tested for accuracy of the model.

Table 3.4 Design matrix for four factors of Box-Behnken design experiment

Run	Factors			
	$H_2O_2 : Fe^{2+}$ (mM/mM)	Fe^{2+} (mM)	Current (A)	pH
1	+1	0	0	+1
2	0	0	0	0
3	0	-1	0	-1
4	-1	0	-1	0
5	0	+1	-1	0
6	0	0	-1	-1
7	0	-1	+1	0
8	-1	-1	0	0
9	+1	0	-1	0
10	0	0	-1	+1
11	0	+1	0	+1
12	0	0	0	0
13	+1	0	+1	0
14	+1	+1	0	0

Table 3.4 continued

Run	Factors			
	$H_2O_2 : Fe^{2+}$ (mM/mM)	Fe^{2+} (mM)	Current (A)	pH
15	0	0	0	0
16	0	+1	0	-1
17	+1	0	0	-1
18	0	0	0	0
19	+1	-1	0	0
20	-1	0	+1	0
21	0	+1	+1	0
22	0	-1	-1	0
23	0	0	+1	+1
24	0	0	+1	-1
25	-1	0	0	+1
26	-1	+1	0	0
27	-1	0	0	-1
28	0	-1	0	+1

CHAPTER IV

RESULTS AND DISCUSSION

4.1 TNT Removal

Treatment of 0.34 mM TNT (78 mg/l) by electrochemical process was studied using Box-Behnken experimental design. Fixed concentration of TNT was used due to each concentration of TNT should have its own optimum condition. The experiment scenario was shown in Table 4.1. ANOVA test indicated the fact that the predictability of the model was at 95% confidence level. Response function predictions for TNT was in good agreement with the experimental data (R^2 >0.95). Application of RSM offers an empirical relationship between the response function and the variables. The mathematical relationship between the response function and the variables can be approximated by a quadratic polynomial Eq. 4.1 (Ghasempur *et al.*, 2007).

$$Y = \beta_0 + \sum_{i=1}^{3} \beta_i X_i + \sum_{i=1}^{3} \beta_{ii} X_i^2 + \sum_{i=1}^{3} \sum_{j=i+1}^{3} \beta_{ij} X_i X_j \qquad (4.1)$$

Table 4.1 Experimental scenarios of TNT treatment by electrochemical method.

Run	X_1: Fe^{2+} (mM)	X_2: H_2O_2 (mM)	X_3: current (A)	%removal	1^{st}-order kinetic (min^{-1})
1	0.09	2.9	0.425	85.2	0.0311
2	0.09	0.29	0.425	93.2	0.0441
3	0.09	1.595	0.80	97.3	0.0596
4	0.0009	1.595	0.05	43.8	0.0096
5	0.04545	0.29	0.05	49.2	0.0107
6	0.09	1.595	0.05	46.3	0.0094
7	0.04545	0.29	0.80	98.5	0.0701
8	0.0009	0.29	0.425	95.1	0.0507
9	0.04545	2.9	0.80	95.1	0.0505
10	0.04545	2.9	0.05	37.6	0.0074
11	0.0009	1.595	0.80	97.7	0.0628
12	0.0009	2.9	0.425	93.0	0.0443
13	0.04545	1.595	0.425	92.5	0.0428

The coefficients (β) of the variables/covariables were determined by correlating the experimental results with the response functions predicted from the quadratic equation using a Stat-Ease Design Expert® program version 7.0.0. The corresponding p-value and the coefficient of determination (R^2) implied the significance of the model. The response functions with the determined coefficients for TNT removal efficiency (R) and 1^{st} order degradation rate constant of TNT (k) in term of coded factor are presented in Eqs. 4.2 and 4.3, respectively. Only significant terms were considered in order to improve R^2 value since the insignificant terms cannot predict the responses accurately.

$$R(\%) = 91.80 - 3.14X_2 + 26.46X_3 - 21.11X_3^2 \tag{4.2}$$

$$k(\min^{-1}) = 0.0430 - 0.0029X_1 - 0.0053X_2 + 0.0260X_3 - 0.0041X_2X_3 - 0.0076X_3^2 \tag{4.3}$$

The three influential variables were ferrous (X_1), hydrogen peroxide (X_2), and current (X_3) with constant pH of 3.0 which is the best condition for Fenton process (Pignatello *et al.*, 2006). The X_i values were between -1 and +1. The removal efficiency (Eq. 4.4) and 1st-order kinetic (Eq. 4.5) in terms of actual factors was also illustrated. Ferrous, hydrogen peroxide and current values were between 0.0009 to 0.09 mM, 0.29 to 2.9 mM, and 0.05 to 0.80 A, respectively.

$$R(\%) = 38.53 - 2.40[H_2O_2] + 198.18 \times current - 150.13 \times current^2 \tag{4.4}$$

$$k(\min^{-1}) = 0.0075 - 0.0651[Fe^{2+}] - 0.0005[H_2O_2] + 0.1278 \times current - 0.0083[H_2O_2] \times current - 0.0540 \times current^2 \tag{4.5}$$

4.1.1 Removal Efficiency

The removal efficiencies of TNT with electrochemical method in 60 minutes were found to depend largely on electric current with 95% level of confidence, i.e., β_3X_3 and $\beta_{33}X_3^2$, the linear and quadratic terms of current from Eq. 4.2. The results also indicated the possibility of an interaction of hydrogen peroxide concentration that maybe significant at the 95% level of confidence, although ferrous concentration alone was not statistically significant. The criteria for minor effect are p-value of ANOVA test between 0.0500 – 0.1000 while no significant effect is p-value less than 0.0500. The correlation of TNT removal was -0.032, -0.105, and 0.888 for ferrous, hydrogen peroxide, and current, respectively. The correlation is +1 in the case of a perfect increasing linear relationship, -1 in the case of a perfect decreasing linear relationship, and some value between -1 and +1 indicating the degree of linear dependence between factors and responses. The results of correlation also had the same trend as ANOVA test. This results indicated that optimum electric current should be 0.66 A as demonstrated in Figure 4.1 for the highest removal efficiency of TNT. Ferrous concentration did not have significant effect on the removal of TNT by electrochemical treatment so the minimum amount of ferrous was applied. This is understandable since ferrous can regenerate by electric current as shown in Eq. 4.6 with sufficient amount of electron charge (the molar ratios of [electron charge]:[Fe^{2+}]:[TNT] were 1.9-29.8 mM : 0.0009-0.09 mM : 0.34 mM).

$$Fe^{3+} + e^- \longrightarrow Fe^{2+} \tag{4.6}$$

Comparison of actual results with the model prediction was shown in Figure 4.2. Although ANOVA test gave the model significant with predict-R^2 of the model was 0.98, some results was still outside the prediction line especially the results that did not include in the model. The model usage should be limited within the boundary.

Control experiments were conducted by various methods as shown in Figure 4.3. Hydrogen peroxide and ferrous were not significant parameters as according to Eq. 4.2 which implies that hydrogen peroxide had minor effect and ferrous had no effect with removal efficiency. The results were surprisingly that electricity alone can degrade TNT.

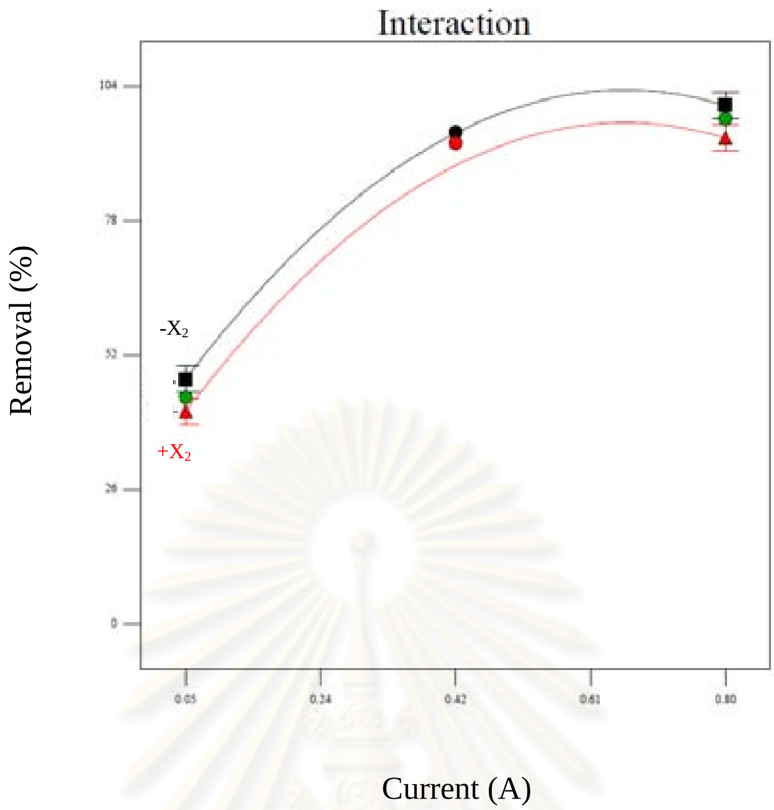

Figure 4.1 Electric current effect on TNT removal by electrochemical treatment at 0.0009 mM Fe^{2+}, ■ 0.29 mM H_2O_2, ▲ 2.9 mM H_2O_2, pH 3.0 and 25 ˚C.

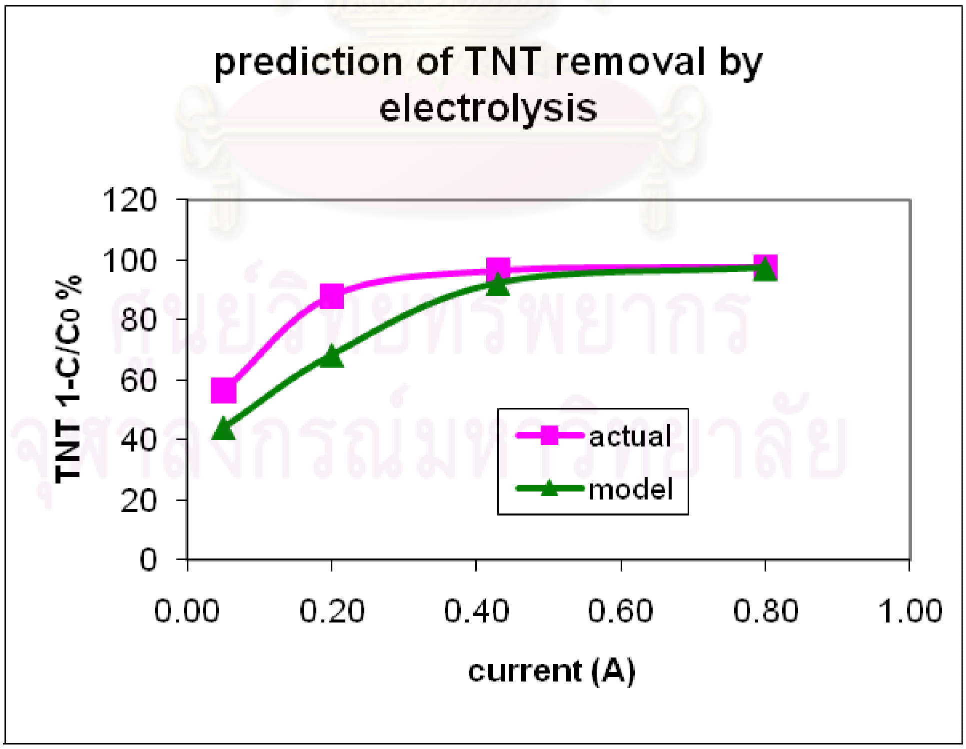

Figure 4.2 Comparison of TNT removal between actual and model prediction with pH 3.0, and 25 ˚C.

This result was coinciding with Palaniswamy *et al*., 2004 and Gilbert and Sale, 2005. Palaniswamy *et al*., 2004 proposed that, at the cathode, the reduction reaction was shown in Eq. 4.7.

$$2H^{+} + 2e^{-} \longrightarrow 2H\bullet \qquad (4.7)$$

Then hydrogen radicals formed at the cathode surface reduced TNT as shown by Eqs. 4.8 to 4.10.

$$C_7H_5(NO_2)_3 + 2H\bullet \longrightarrow C_7H_5(NO_2)_2NO + H_2O \qquad (4.8)$$
$$C_7H_5(NO_2)_2NO + 2H\bullet \longrightarrow C_7H_5(NO_2)_2NHOH \qquad (4.9)$$
$$C_7H_5(NO_2)_2NHOH + 2H\bullet \longrightarrow C_7H_5(NO_2)_2NH_2 + H_2O \qquad (4.10)$$

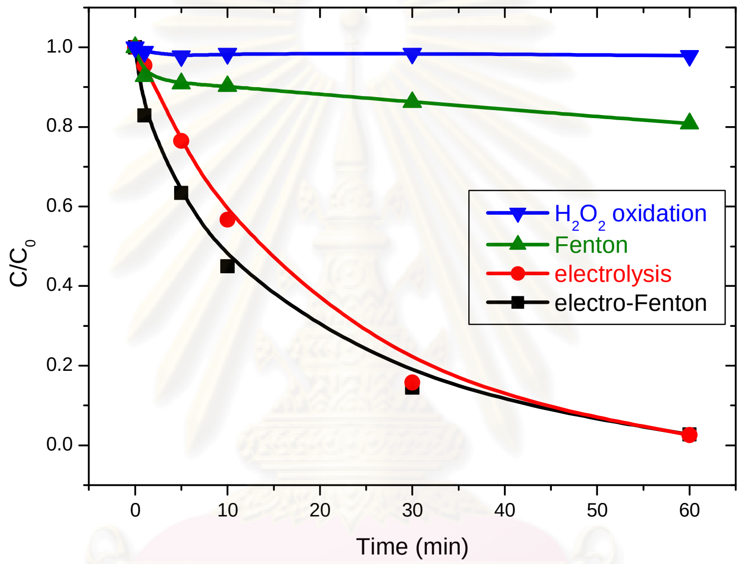

Figure 4.3 Control experiments by various methods with [H_2O_2] 2.9 mM, [Fe^{2+}] 0.09 mM, 0.80 A, pH 3.0, and 25 ˚C.

These reactions occurred competitively with electro-Fenton processes due to the excess amount of electric current applied compared with ferrous concentration or even compared with hydrogen peroxide. The major mechanism among these varied conditions is said to be electro-reduction of TNT. For applying more hydrogen peroxide, the minor reduction of removal efficiency as showed in Figure 4.1 and Eq. 4.2. This is understandable due to competition of hydrogen peroxide as shown in Eq. 4.11 (Agladze *et al*., 2007) with hydrogen ions as shown in Eq. 4.7.

$$H_2O_2 + 2H^{+} + 2e^{-} \longrightarrow 2H_2O \qquad (4.11)$$

Care has to be accounted for the electric current applied only sufficient amount in the utilization of electro-Fenton method.

Background electrolytes were also studied by comparison of type and concentration. Nitrate and sulfate were studied due to naturally occurred with this kind of wastewater. Nitrate retarded the removal efficiency while sulfate enhanced the removal efficiency as shown in Figure 4.4. This should be due to nitrate has the same functional group as nitro-group of TNT which competed with utilization of hydrogen radicals while sulfate did not. The amounts of nitrate anions were ten times higher than TNT which should be considered. Sulfate should be added if the background conductance is low for facilitating electron flow. Comparisons between 1 to 100 mM of sulfate salt were conducted as shown in Figure 4.5 and 4.6. No significant effect on the removal efficiency for 1 to 100 mM sulfates had been observed in both adjustmenting pH with nitric acid or sulfuric acid. This should be due to sulfate did not participate in the electrolysis of TNT. However, if background sulfate is higher, the reactor resistant lower which reducing the electrical cost.

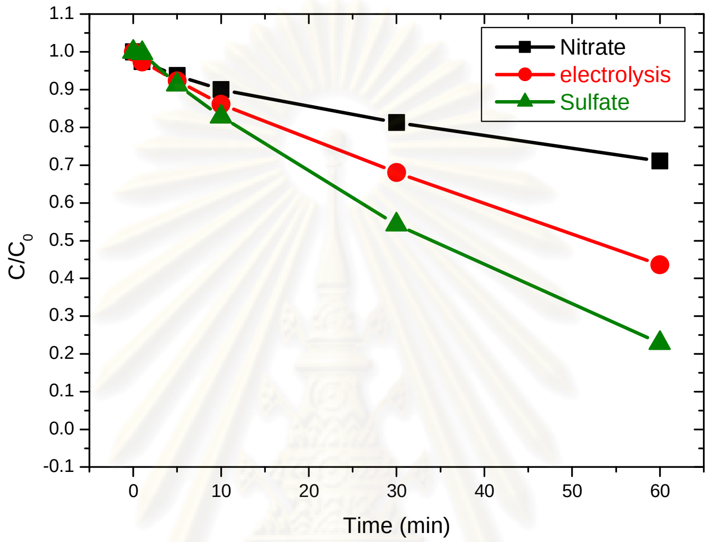

Figure 4.4 Effect of salt for TNT removal by electrolysis with current 0.05 A, pH 3.0, and 25 ˚C.

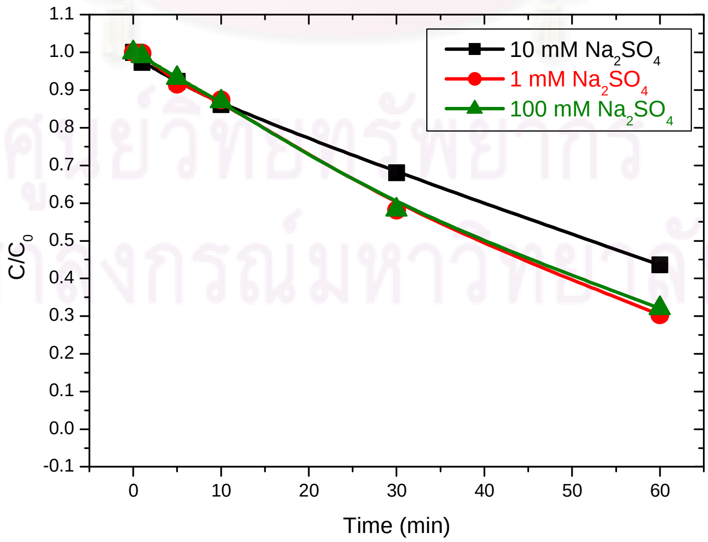

Figure 4.5 Effect of sulfate concentration for TNT removal by electrolysis with current 0.05 A, pH_i 3.0 adjusted by nitric acid, and 25 ˚C.

In Fenton chemistry, pH is a significant factor. Background pH was also studied between 2 to 4 in order to study the effect of pH with removal efficiency. There was no significant effect of pH to the removal efficiency as shown in Figure 4.7. This should be due to amount of hydrogen ions and electric current were higher enough comparing to the TNT concentrations.

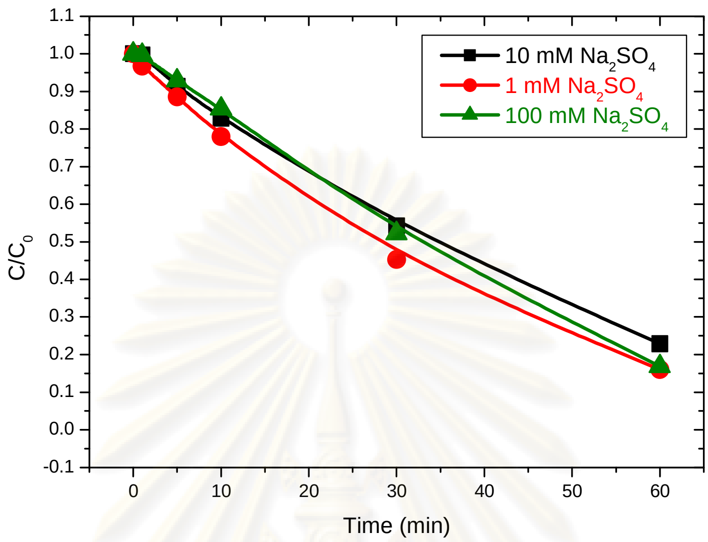

Figure 4.6 Effect of sulfate concentration for TNT removal by electrolysis with current 0.05 A, pH_i 3.0 with sulfuric acid, and 25 ˚C.

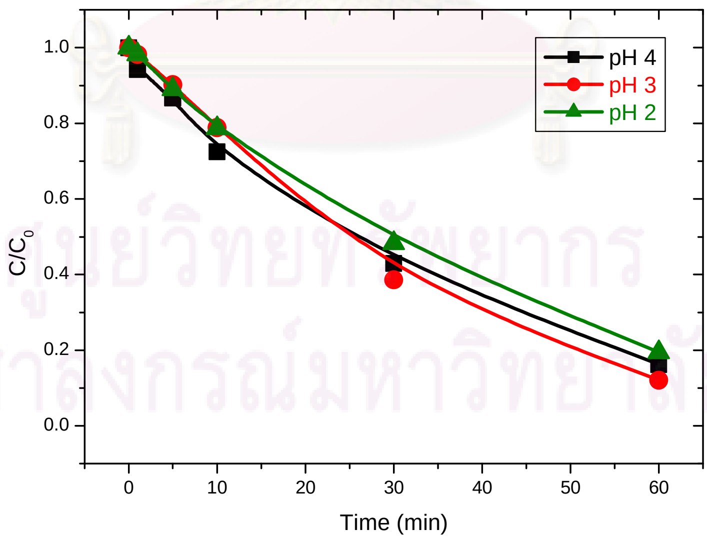

Figure 4.7 Effect of pH for TNT removal by electrolysis with current 0.20 A, pH_i 3.0, and 25 ˚C.

4.1.2 Removal Kinetics

The degradation of TNT with electrochemical method during 60 minutes followed the 1^{st}-order behavior with R^2 higher than 0.93. However, the major mechanism was electrochemical reduction. Therefore, the kinetics determination by initial rate was investigated in order to eliminate any interference from intermediate competition (Anotai *et al.*, 2006). The initial kinetics rate could be obtained from Eq. 4.12. The various TNT concentration treatments by electrochemical process can achieve more than 97.3% and were plotted in Figure 4.8.

$$-\frac{d[TNT]}{dt} = k_{obs,TNT}[TNT]^n \qquad (4.12)$$

The plot between the initial rate and TNT concentration on a log-log scale showed a straight line with the slopes of 1.52 for electrochemical treatment as shown in Figure 4.9; hence, the reaction rate equations became:

$$-\frac{d[TNT]}{dt} = 0.295[TNT]^{1.52} \text{ mM/min} \qquad (4.13)$$

It can be seen that the TNT degradation rate was 1½ order with respect to TNT concentration, which indicates that the decomposition of TNT was controlled by the reaction of TNT. The molar ratio of electron charge was 29.8 mM for degradation 0.34 mM of TNT which indicated that electron charge were in excess. Although most of experiment data were followed the 1st-order reaction kinetic, there were some experiments that more fitted better with the 2nd-order kinetics due to limited amount of reactant (e^-) compared with limited amount of TNT.

The other possibility mechanism that can degrade TNT was alkaline hydrolysis (Heilman *et al.*, 1996). The electrolysis of water at the cathode as the side reaction can be shown in Eq. 4.14.

$$2H_2O + 2e^- \longrightarrow H_2 + 2OH^- \qquad (4.14)$$

Then hydroxide ions will react TNT with the best condition of pH 12 (Emmrich, 1999). These reactions did not occur due to pH controlling at 3.0 with completely stirred tank and the kinetics rate of alkaline hydrolysis is 0.361 hr^{-1} which is very slow.

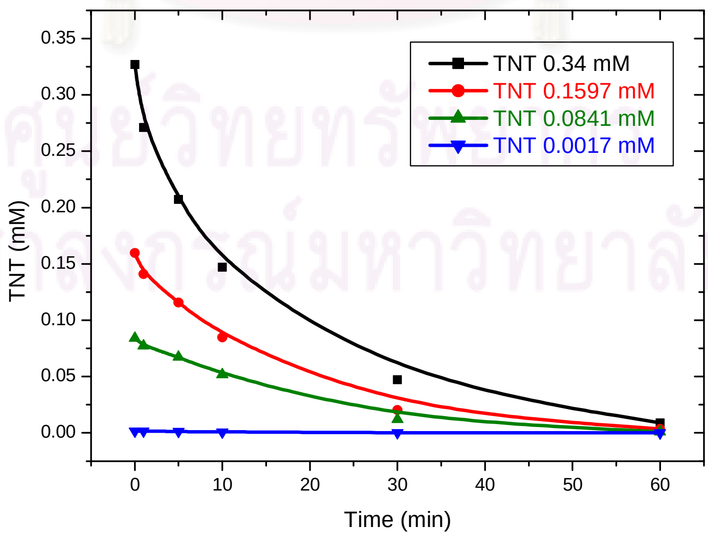

Figure 4.8 Variation TNT concentration by electrochemical method with H_2O_2 2.9 mM, Fe^{2+} 0.09 mM, pH_i 3.0, current 0.80 A, and 25 ˚C.

Due to kinetics rate depending on temperature, the temperature effect of kinetics rate was also studied and was shown in Figure 4.10. The 1st-order kinetics rate at 25, 50, and 75 ˚C were 0.0355, 0.0593, and 0.0717 min^{-1}, respectively. This could be due to increasing temperature should increasing the internal energy which could accelerating the collision of reactants. At high temperature experiment, the evaporation rate was higher and if the reaction time longer, the water will evaporate and volume and concentration should be changes.

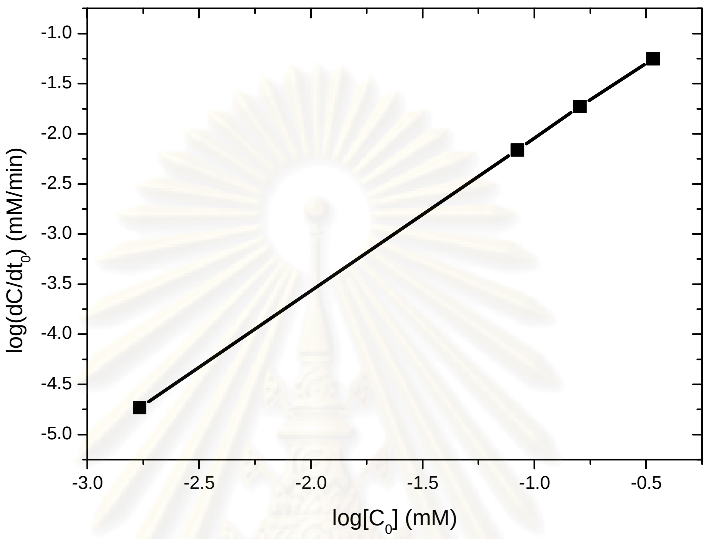

Figure 4.9 Order rate determination of TNT removal by electrochemical method with pH 3.0, current 0.80 A, and 25 ˚C.

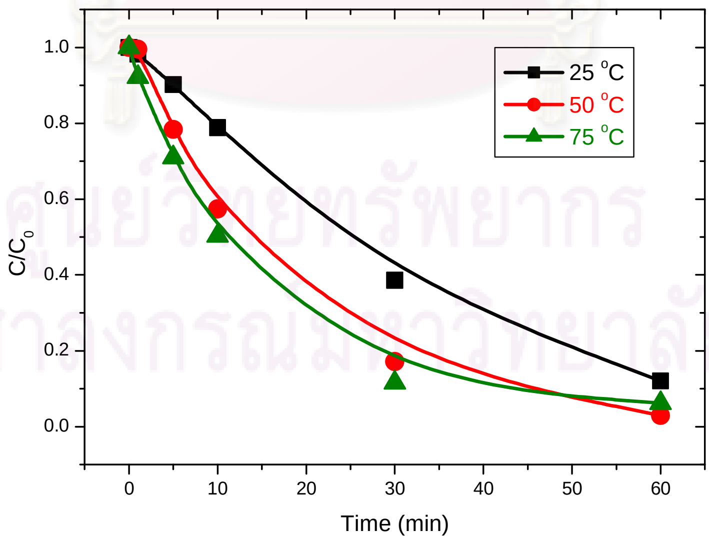

Figure 4.10 Effect of temperature for TNT removal by electrolysis with current 0.20 A, and pH_i 3.0.

4.1.3. Hydrogen Peroxide Efficiency

H_2O_2 in Fenton oxidation is the source of oxidants. Due to major mechanism is electro-transformation of TNT, then the H_2O_2 efficiency cannot be calculated.

4.1.4. Voltage

By Ohm's Law, the voltage drop depend on current which is represented as

$$V = IR \tag{4.15}$$

Where V = potential difference
I = current applied
R = system resistance

The batch resistances depend on temperature and chemical added such as salt, acid, reactant and catalyst. At the beginning, the system resistance is considering the same by controlling temperature, 10 mM Na_2SO_4 with pH of 3.0 and combination of H_2O_2 and Fe^{2+}. Applying more current will cause higher potential drop. The potential drops of electric generator are ranging from 3 to 17 volt. As we know that applying more current will get more electron; however, if we apply much current, the high potential drop will generate side reaction such as electrolysis of water as shown in Eq. 4.15. The water electrolysis causes low current efficiency and high operating cost. Lower potential drop by reducing system resistance can be achieved by adding more electrolytes or reducing distance between electrodes.

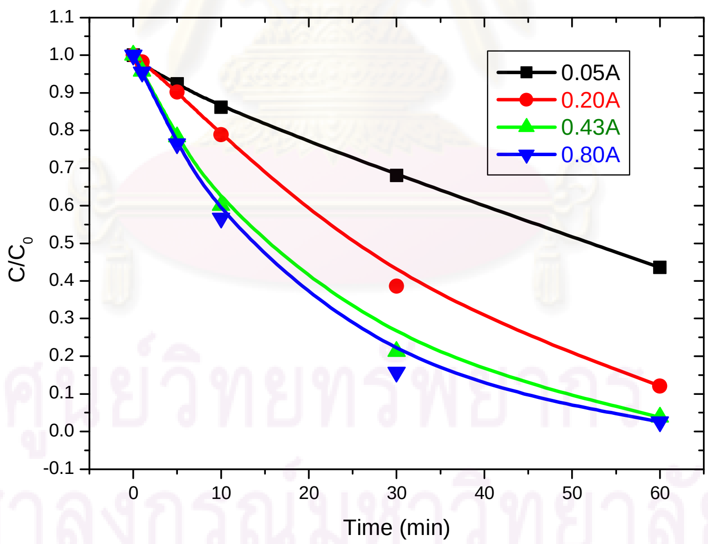

Figure 4.11 Current effect of TNT removal by electrochemical method with pH 3.0, and 25 ˚C.

Current efficiency was compared with removal efficiency and potential applied as shown in Figure 4.12 and 4.13, respectively. The current efficiency was lower than 12% owing to more than one mole of electron requirement per one mole of TNT as shown in Eqs. 4.8 to 4.10. Increasing amount of current while the removal efficiency did not change proportionally will deteriorate the removal efficiency. The potential applied divided by the current applied represented the system resistant as shown by Eq. 4.15. Increasing potential applied can promote side reaction in the water by many reactions such as Eqs. 4.7 and 4.14. Minimizing current applied should cause higher current efficiency and potential applied which lower the electric cost.

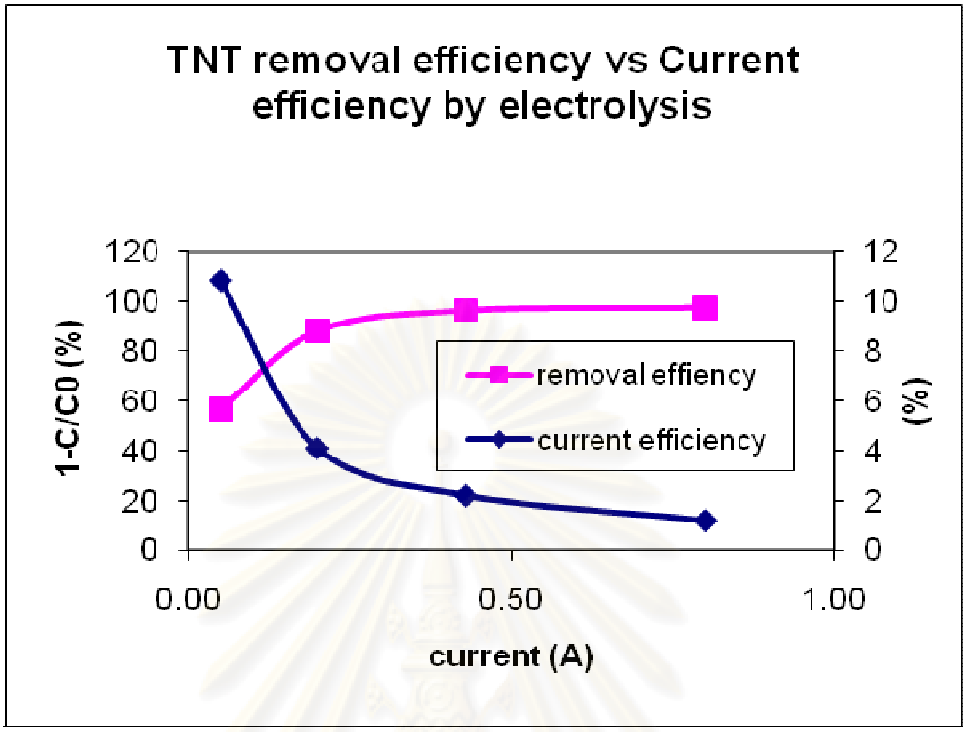

Figure 4.12 Comparison between removal efficiency and current efficiency for TNT removal by electrochemical method with pH 3.0, and 25 ˚C.

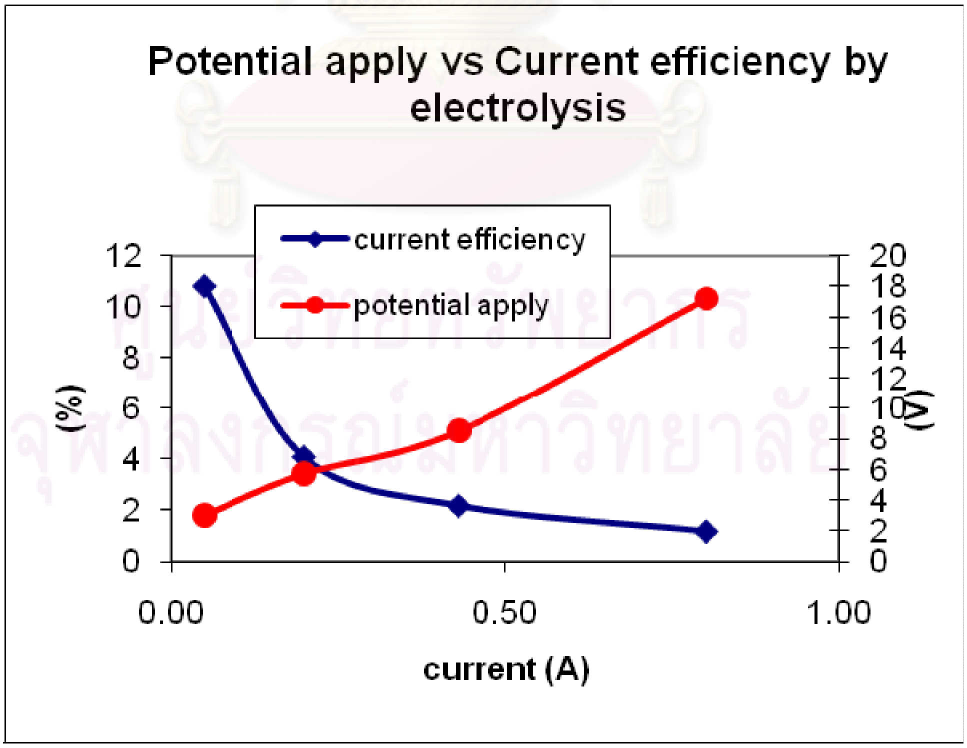

Figure 4.13 Comparison between current efficiency and potential drop for TNT removal by electrochemical method with pH 3.0, and 25 ˚C.

4.1.5. Process Optimization

All parameters have their roles for treatment of explosives. Ferrous is the catalyst of Fenton reaction and controlling removal rate. Applying more ferrous will increase the removal rate, but the chemical and iron sludge disposal costs must be considered as well. H_2O_2 is the oxidant of Fenton reaction which was minor significant in removal efficiency and kinetics rate under the studied conditions. Increase of H_2O_2 will increase the treatment cost. The last factor is the electric current apply which was the most significant factor affecting the removal efficiency but was minor significant for removal kinetics. The optimum current would be applied in order to maximize treatment efficiency. By applying the RSM, the optimum conditions for the highest TNT removal were 0.66 A and pH 3.0 as shown in Figure 4.1. The results showed that Fe^{2+} and H_2O_2 had no effect and minor effect, respectively. This means that Fe^{2+} and H_2O_2 should be minimizing in order to enhance electrochemical removal of TNT.

4.1.6. Pathway of TNT Degradation

Electro-Fenton process is dealt with oxidation of target compounds by hydroxyl radicals. The proposed TNT degradation pathway was shown in Figure 4.14. The intermediates are proposed to be formic acid, nitrate anions, oxalic acid, water, and carbon dioxide. The formic acid and oxalic acid were not detected during one hour of reactions. As the main mechanisms of TNT removal was electrochemical process instead of electro-Fenton process. The possible mechanism for the electro-transformation of TNT was proposed in Figure 4.15. The nitro group, which has electron-withdrawing ability, will transport to cathode and react with electron and hydrogen ion as described by Eqs. 4.8 to 4.10. After one nitro group reduction to amine group, the other nitro group can further reduce to triaminotoluene as shown by Eq. 4.16. This proposed mechanism also coincide with Hofstetter *et al.*(1999) and Palaniswamy *et al.*(2004).

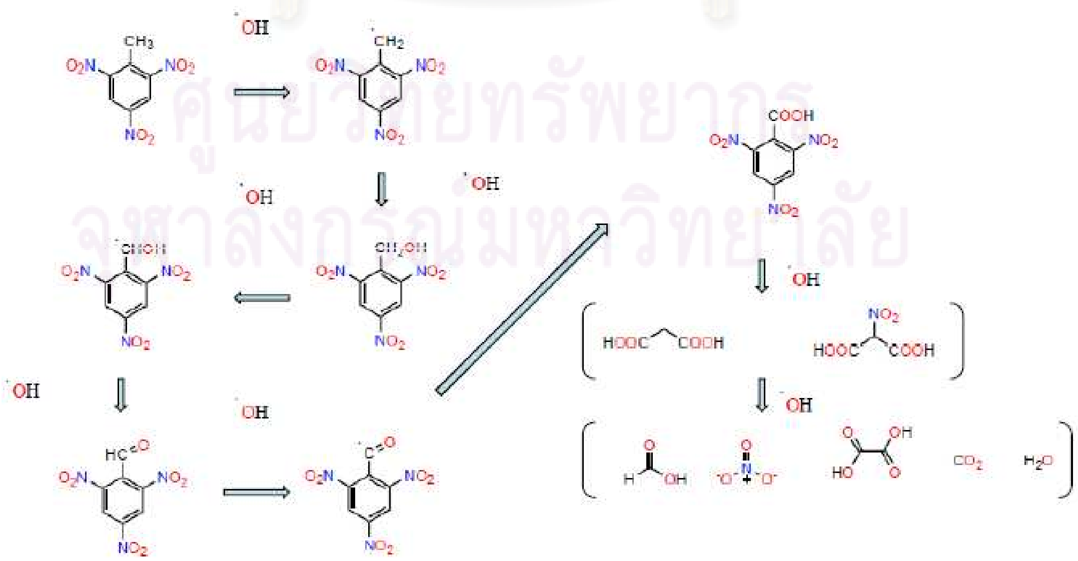

Figure 4.14 Proposed degradation pathway of TNT removal by oxidation.

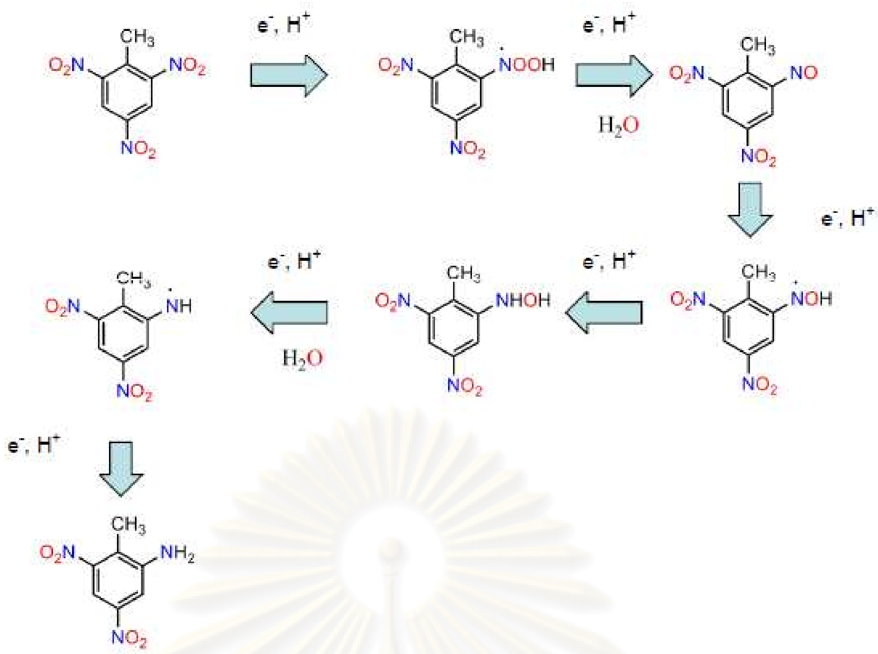

Figure 4.15 Proposed degradation pathway of TNT removal by reduction.

$$C_7H_5(NO_2)_3 \xrightarrow[\text{-2H}_2\text{O}]{\text{6e}^-\text{,6H}^+} C_7H_5(NO_2)_2NH_2 \xrightarrow[\text{-2H}_2\text{O}]{\text{6e}^-\text{,6H}^+} C_7H_5(NH_2)_2NO_2 \xrightarrow[\text{-2H}_2\text{O}]{\text{6e}^-\text{,6H}^+} C_7H_5(NH_2)_3 \quad (4.16)$$

The color of the treated effluents is shown in Figure 4.16. The samples of electrolysis process and Fenton process were collected from time 0 to 60 minutes as shown from left to right. The 30 and 60 minutes sample of electrolysis process gave yellow color intermediates while samples of Fenton process was not changes with time.

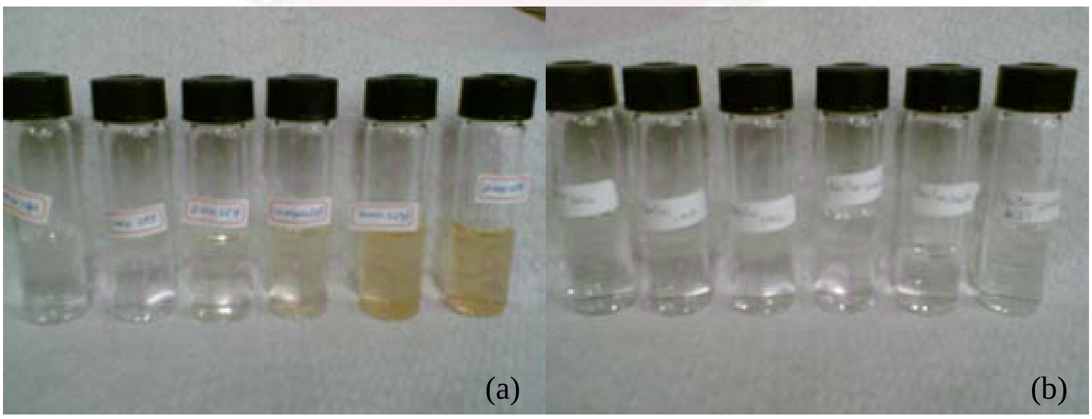

Figure 4.16 Physical appearance of the treated TNT wastewater by electrolysis (a) and Fenton process (b).

This could be Fenton oxidation was not efficient in the studied with 20% removal efficiency only.

4.1.7. Economic Considerations

According to the results, electro-transformation process can remove TNT efficiently compared to electro-Fenton process. This implies that the chemical addition system is not essential. However, electricity cost is the major operating cost.

4.2 RDX and HMX Removal

Control experiments of RDX and HMX removal by various methods are plotted as shown in Figure 4.17. These conditions showed that hydrogen peroxide alone could not degrade RDX and HMX. Electrolysis was not the major mechanism of RDX and HMX removal as compared to TNT. Electric current can enhance Fenton oxidation of RDX and HMX. The TOC removal from RDX wastewater also showed the same trend as RDX removal as shown in Figure 4.18. The center point (0, 0, 0, 0) was repeated 4 times and nearly the same results were obtained indicating the reproducibility of the data. ANOVA test indicated the fact that the predictability of the model was at 95% confidence level. Response function predictions for RDX were in good agreement with the experimental data (R^2 >0.95). Application of RSM offers an empirical relationship between the response function and the variables. The mathematical relationship between the response functions and the variables can be approximated by a quadratic polynomial Eq. 4.17 (Ghasempur *et al.*, 2007).

$$Y = \beta_0 + \sum_{i=1}^{4} \beta_i X_i + \sum_{i=1}^{4} \beta_{ii} X_i^2 + \sum_{i=1}^{4} \sum_{j=i+1}^{4} \beta_{ij} X_i X_j \tag{4.17}$$

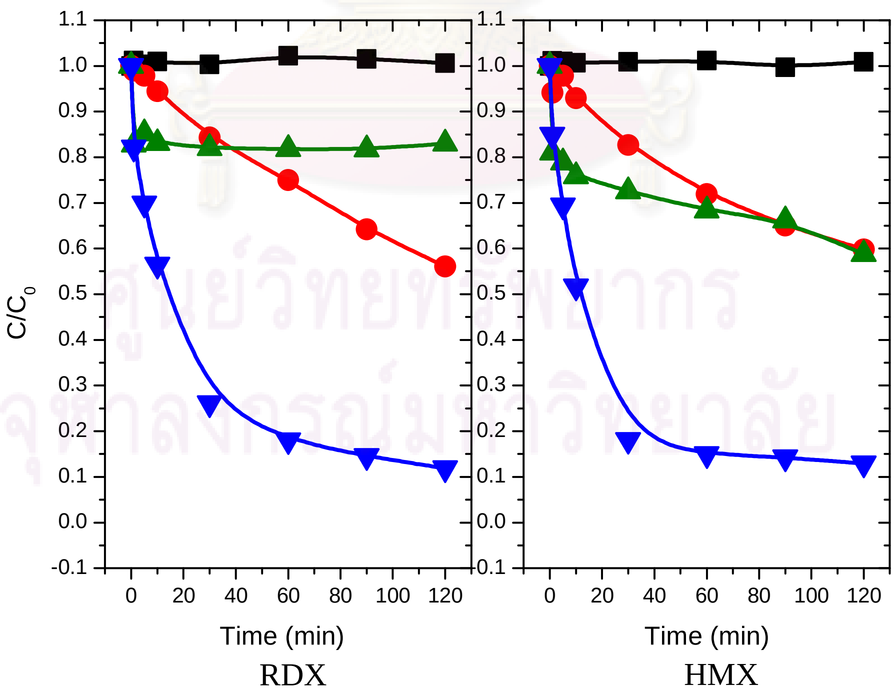

Figure 4.17 RDX (left) and HMX (right) control experiment by various method with $[H_2O_2]$ 2.05 mM, $[Fe^{2+}]$ 0.41 mM, 0.04 A, pH 3.0, and 25 ˚C, ■-H_2O_2 oxidation, ●-electrolysis, ▲-Fenton, ▼-electro-Fenton.

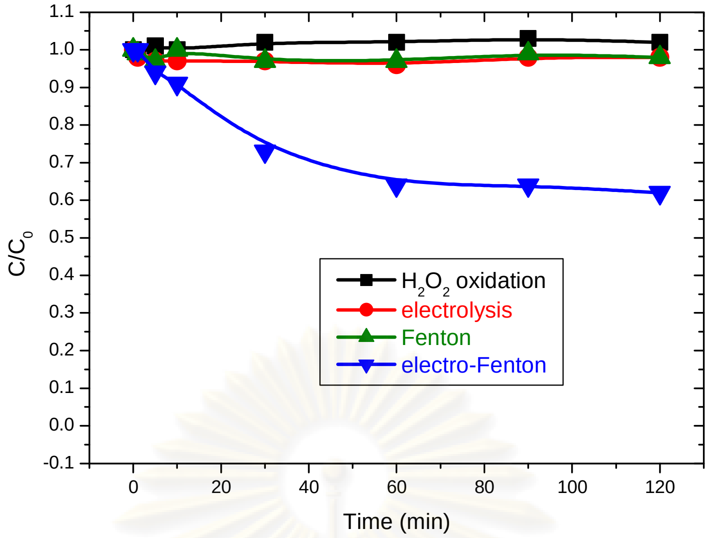

Figure 4.18 RDX control experiment by various method of TOC removal with $[H_2O_2]$ 2.05 mM, $[Fe^{2+}]$ 0.41 mM, 0.04 A, pH 3.0, and 25 °C.

The coefficients (β) of the variables/covariables were determined by correlating the experimental results with the response functions predicted from the quadratic equation using a Stat-Ease Design Expert program. The corresponding *p*-value and the coefficient of determination (R^2) implied the significance of the model. The response functions with the determined coefficients for RDX removal efficiency (R_1), HMX removal efficiency (H_1), 1st-order degradation rate constant of RDX (R_2), the 1st-order degradation rate constant of HMX (H_2), H_2O_2 efficiency for RDX (R_3) and H_2O_2 efficiency for HMX degradation (H_3) in term of coded factor are presented in Eqs 4.18 to 4.23, respectively. Only significant terms were considered in order to improve adj-R^2 value since the insignificant terms cannot predict the responses accurately.

$$R_1 = 97.84 - 0.47X_1 + 3.52X_2 - 36.57X_4 - 6.86X_1X_4 - 5.26X_2X_4 - 3.83X_2^2 - 36.83X_4^2 \tag{4.18}$$

$$H_1 = 102.8 - 3.64X_1 + 3.06X_2 - 18.84X_4 - 18.93X_1X_4 - 14.03X_2^2 - 23.61X_4^2 - 23.61X_4^2 \tag{4.19}$$

$$R_2 = 0.043 + 0.0058X_1 + 0.011X_2 + 0.0025X_3 - 0.016X_4 + 0.0074X_1X_2 - 0.0084X_2X_4 - 0.0076X_1^2 - 0.0058X_2^2 - 0.0035X_3^2 - 0.020X_4^2 \tag{4.20}$$

$$H_2 = 0.030 + 0.0020X_1 + 0.0042X_2 - 0.0068X_4 - 0.011X_1X_4 - 0.010X_4^2 \tag{4.21}$$

$$R_3 = 1.14 - 3.82X_1 - 3.43X_2 - 1.32X_4 + 11.32X_1X_2 + 6.33X_1^2 + 5.92X_2^2 - 2.45X_4^2 - 10.08X_1^2X_2 - 9.97X_1X_2^2 \tag{4.22}$$

$$H_3 = 0.056 - 0.20X_1 - 0.12X_2 - 0.043X_4 + 0.47X_1X_2 + 0.30X_1^2 + 0.22X_2^2 - 0.10X_4^2 - 0.46X_1^2X_2 - 0.39X_1X_2^2 \quad (4.23)$$

The four influential variables were the hydrogen peroxide to ferrous ratio (X_1), ferrous concentration (X_2), current (X_3), and pH (X_4). The X_i values were between -1 and +1. The removal efficiency (Eqs. 4.24 and 4.25), the 1st-order kinetics (Eqs. 4.26 and 4.27), and the hydrogen peroxide efficiency (Eqs. 4.28 and 4.29) in terms of actual factors were also illustrated. Hydrogen peroxide to ferrous ratio, ferrous, current, and pH values were between 3 to 30, 0.1 to 1.0 mM, 0.04 to 0.20 mM, and 2.0 to 4.0, respectively.

$$R_1(\%) = -177.82 + 1.49[H_2O_2]:[Fe(II)] + 63.72[Fe(II)] + 199.23pH - 0.51[H_2O_2]:[Fe(II)]\times pH - 11.69[Fe(II)]\times pH - 18.93[Fe(II)]^2 - 36.83pH^2 \quad (4.24)$$

$$H_1(\%) = -142.83 + 3.94[H_2O_2]:[Fe(II)] + 83.03[Fe(II)] + 145.94pH - 1.40[H_2O_2]:[Fe(II)]\times pH - 18.93[Fe(II)]^2 - 23.61pH^2 \quad (4.25)$$

$$R_2(\min^{-1}) = -0.1587 + 0.0011[H_2O_2]:[Fe(II)] + 0.0915[Fe(II)] + 0.1629current + 0.1123pH + 0.0012[H_2O_2] - 0.0187[Fe(II)]\times pH - 0.00004[H_2O_2]:[Fe(II)]^2 - 0.0285[Fe(II)]^2 - 0.5475current^2 - 0.0196pH^2 \quad (4.26)$$

$$H_2(\min^{-1}) = -0.0889 + 0.0026[H_2O_2]:[Fe(II)] + 0.0092[Fe(II)] + 0.0673pH - 0.0008[H_2O_2]:[Fe(II)]\times pH - 0.0101pH^2 \quad (4.27)$$

$$R_3(\%) = +1.14 - 3.82[H_2O_2]:[Fe(II)] - 3.43[Fe(II)] - 1.32pH + 11.32[H_2O_2] + 6.33[H_2O_2]:[Fe(II)]^2 + 5.92[Fe(II)]^2 - 2.45pH^2 - 10.08[H_2O_2]^2:[Fe(II)] - 9.97[H_2O_2]\times[Fe(II)] \quad (4.28)$$

$$H_3(\%) = +0.056 - 0.20[H_2O_2]:[Fe(II)] - 0.12[Fe(II)] - 0.043pH + 0.47[H_2O_2] + 0.30[H_2O_2]:[Fe(II)]^2 + 0.22[Fe(II)]^2 - 0.10pH^2 - 0.46[H_2O_2]^2:[Fe(II)] - 0.39[H_2O_2]\times[Fe(II)] \quad (4.29)$$

4.2.1 Removal Efficiency

The removal efficiencies of RDX and HMX with electro-Fenton method in 120 minutes were found to depend largely on pH with 95% level of confidence, i.e., β_4X_4 and $\beta_{44}X_4^2$, the linear and quadratic terms of pH (Eqs. 4.18 and 4.19). The result also indicated the possibility of an interaction of H_2O_2:Fe^{2+} ratio and pH that maybe significant at the 95% level of confidence, although the H_2O_2:Fe^{2+} ratio alone was not statistically significant. This result indicated that pH optimum should be within the range of 2.3-2.8 as demonstrated in Figure 4.19. Electric current did not have significant effect on the removal of RDX and HMX by electro-Fenton treatment so the minimum current intensity was applied. This is understandable since the molar ratios of [electron charge]:[Fe^{2+}]:[explosive] were 1.5-7.5 mM : 0.1-1.0 mM : 0.180 mM for RDX or 0.007 mM for HMX.

The degradation of organic contaminants by Fenton reactions usually yields optimal results at a pH slightly below 3 by the speciation of Fe(III) (Qiang *et al.*, 2003 and Pignatello *et al.*, 2006). The results revealed that electro-Fenton could be used effectively to treat RDX and HMX with the efficiency of 80% or higher at the pH lower than 3.

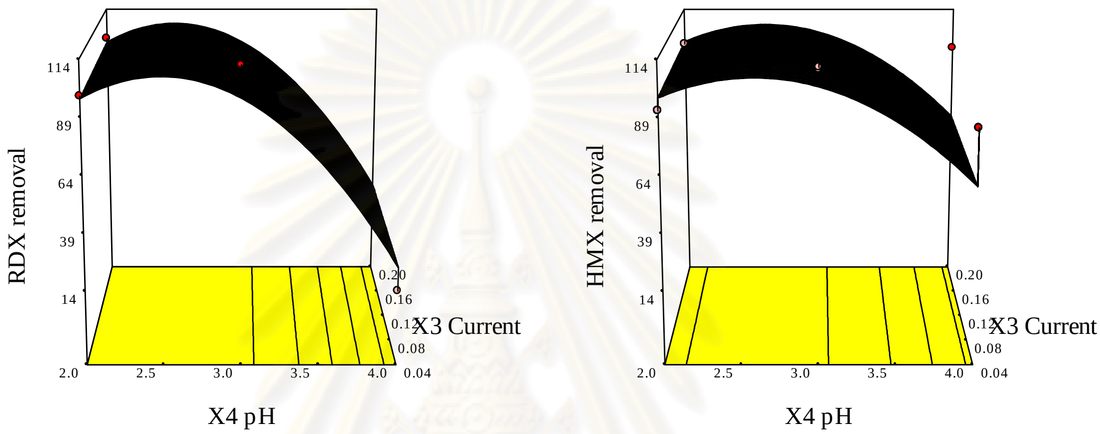

RDX HMX

Figure 4.19 pH effect on explosive removal by electro-Fenton treatment at H_2O_2:Fe^{2+} of 16.5, 0.55 mM Fe^{2+} and 25 ˚C: RDX (left) and HMX (right).

4.2.2 Removal Kinetics

The oxidation of RDX and HMX with electro-Fenton method during 120 minutes followed the 1st-order behavior. Therefore, the 1st-order rates in terms of the initial RDX and HMX concentrations are obtained as shown in Eqs. 4.30 and 4.31.

$$-\frac{d[RDX]}{dt} = k_{obs,RDX}[RDX] \qquad (4.30)$$

$$-\frac{d[HMX]}{dt} = k_{obs,HMX}[HMX] \qquad (4.31)$$

Comparing the efficiencies between Eqs 4.18 and 4.19, it can be seen that the principle system factors affecting the response function were quite similar. Solution pH and ferrous were found to be significant at the confidence level of 95% and 90% as shown in Figures 4.20 and 4.21, respectively, whereas other parameters did not have any significant effect.

Increase in the degradation rate constants of RDX and HMX with respect to ferrous concentration in the electro-Fenton process as shown in Figure 4.21 was due to the electrical enhancement on Fe^{2+}-regeneration. Similar trend was also observed by other researches (Anotai *et al.*, 2006).

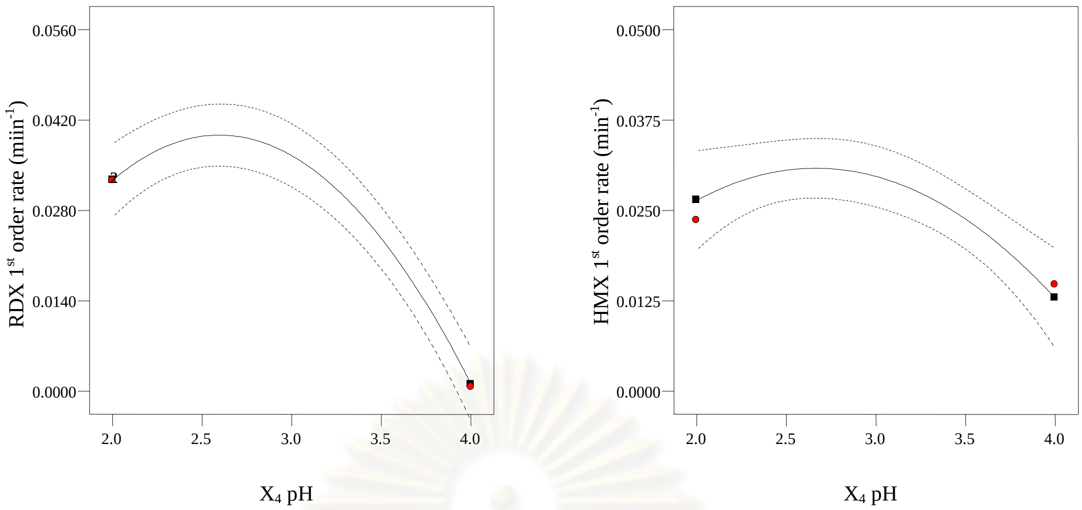

Figure 4.20 Variation of 1st-order rate constant with pH by electro-Fenton method with H_2O_2:Fe^{2+} ratio of 16.5, 0.55 mM Fe^{2+}, 0.04 A current and 25 ˚C. Lines represent the simulations from quadratic equations with ■ are the design points and ● are the experimental data.

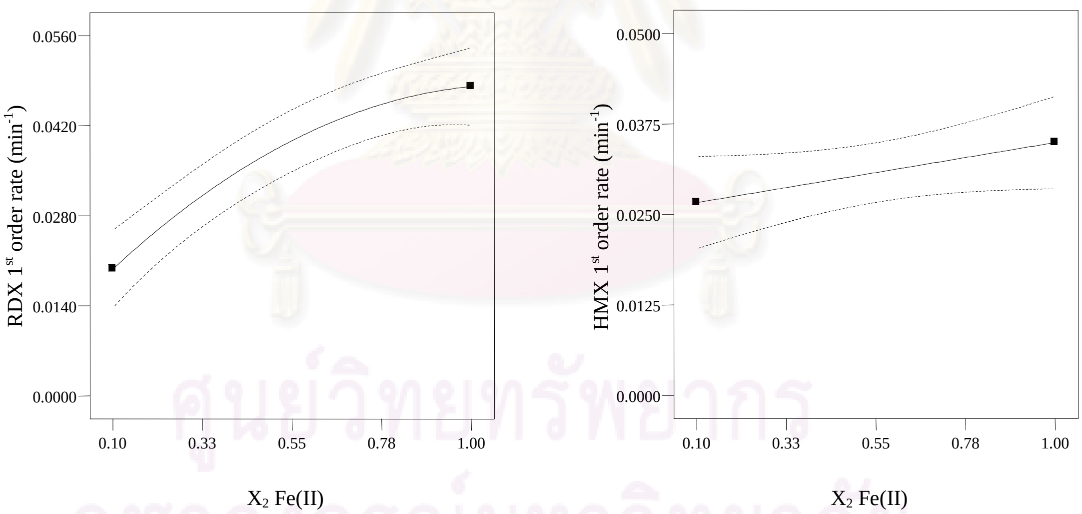

Figure 4.21 variation of 1st order rate with ferrous concentration by electro-Fenton method with H_2O_2:Fe^{2+} ratio of 16.5, 0.04 A current, pH 3 and 25 ˚C. Lines represent simulations from quadratic equations with ■ are the design points.

4.2.3 Hydrogen Peroxide Efficiency

H_2O_2 plays an important role in Fenton oxidation by acting as the source of oxidizing agent. The effectiveness of H_2O_2 usage should be considered and can be calculated by dividing the amount of removed chemical by H_2O_2 that utilized. The equations for calculating H_2O_2 efficiency are shown in Eq. 4.32 (Bishop *et al.*, 1968; Kang and Hwang, 2000; Zhang *et al.*, 2006; and Zhang *et al.*, 2007).

$$H_2O_2\ efficiency = \frac{\Delta COD(mg/L)}{available\ O_2(mg/L)} \quad (4.32)$$

However, solubility of RDX and HMX in this experiment were 29 and 3 mg/L, respectively. COD calculation could perform by reactions 4.33 and 4.34 which 1 mg/L of RDX or HMX equal to 0.432 mg/L COD. The COD calculation of RDX and HMX are 13 and 1.3 mg/L, respectively, which are very low and could not be accurately measured.

$$C_3H_6N_6O_6 + 2Cr_2O_7^{2-} + 16H^+ \rightarrow 4Cr^{3+} + 11H_2O + 3CO_2 + 3N_2O \quad (4.33)$$

$$3C_4H_8N_8O_8 + 8Cr_2O_7^{2-} + 64H^+ \rightarrow 16Cr^{3+} + 44H_2O + 12CO_2 + 12N_2O \quad (4.34)$$

The modified hydrogen peroxide efficiency for comparative study are shown in Eqs. 4.35 and 4.36 for RDX and HMX, respectively.

$$H_2O_2\ efficiency = \frac{\Delta RDX\,(mM)}{\Delta H_2O_2\,(mM)} \quad (4.35)$$

$$H_2O_2\ efficiency = \frac{\Delta HMX\,(mM)}{\Delta H_2O_2\,(mM)} \quad (4.36)$$

The H_2O_2 efficiency of RDX and HMX treatment with electro-Fenton method in 120 minutes were found to primarily relate to H_2O_2 at 95% level of confidence. The test also indicated a possibility of an interaction among H_2O_2:Fe^{2+} ratio, (H_2O_2:Fe^{2+} ratio)^2, $[Fe^{2+}]^2$, (H_2O_2:Fe^{2+} ratio)$\cdot$[H_2O_2] and [H_2O_2]$\cdot$[Fe^{2+}] that maybe significant at the 95% level of confidence. H_2O_2 efficiencies for RDX degradation were in between 0.25 and 55% while were between 0.009 and 2.4% for HMX degradation. The result indicated that as H_2O_2 decreased, the H_2O_2 efficiency increased as shown in Figure 4.22. The reason for this can be described by the ratios between H_2O_2 and explosive which were 0.3-30 mM to 0.180 mM of RDX or 0.007 mM of HMX. This indicated that H_2O_2 was in excess comparing to the explosives. The H_2O_2 efficiency was low due to the amount of explosives is low, electro-Fenton process can mostly degrade RDX and HMX over 82% and also the H_2O_2:RDX molar ratio and H_2O_2:HMX molar ratio are over 1.7 and 43, respectively.

4.2.4 Process Optimization

All parameters have their roles for treatment of explosives. pH is the significant factor controlling the electro-Fenton process. For maximizing removal efficiency, pH must be controlled between 2.3 to 2.8. Either increase or decrease of pH out of this range will decrease the removal efficiency and rate constant. Fe^{2+} is the catalyst of Fenton reaction and controlling removal rate. Applying more ferrous will increase the removal rate, but the chemical and iron sludge disposal costs must be considered. H_2O_2 is the oxidant of Fenton reaction which was not significant in removal efficiency and rate under the studied conditions but played the key role for H_2O_2 efficiency. Increase of H_2O_2 will increase the treatment cost. The last factor is electric current apply which is not a significant factor to all of the responses.

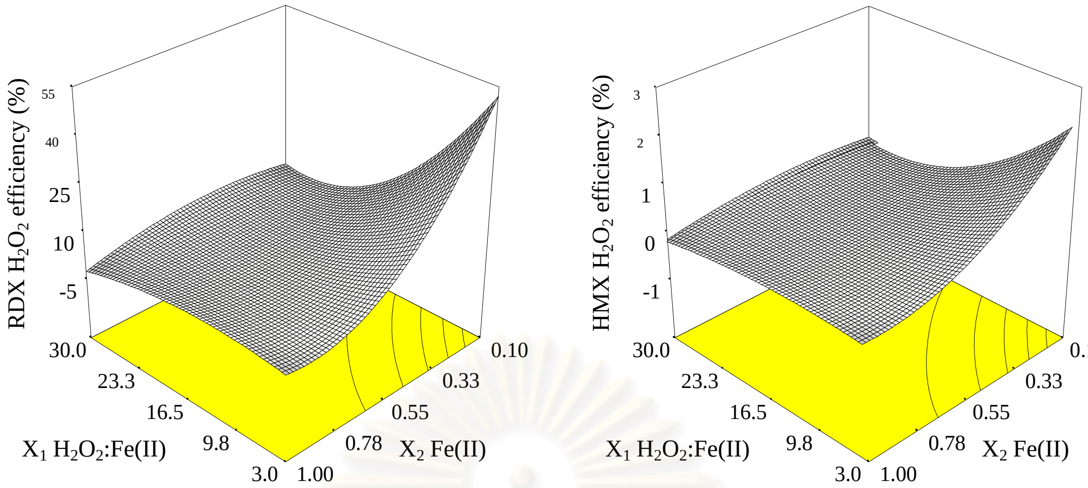

Figure 4.22 Variation of H_2O_2 efficiency with electro-Fenton method. RDX (left) and HMX (right) with H_2O_2:Fe^{2+} ratio of 16.5, 0.55 mM Fe^{2+}, 0.04 A current and 25 ˚C.

The lowest current would be applied in order to reduce the treatment cost. By applying the RSM, the optimum dosages of H_2O_2 and Fe^{2+} at 0.04 A and pH 2.6 were calculated and plotted in an overlay graph as shown in Figure 4.23. The results showed that Fe^{2+} and H_2O_2:Fe^{2+} ratio should be in between 0.4 and 0.8 mM and 3 and 30, respectively. From this research, the amount of H_2O_2 and Fe^{2+} required for the degradtion of RDX and HMX were lower than previous researches (Zoh and Stenstrom, 2002; Liou *et al*., 2003).

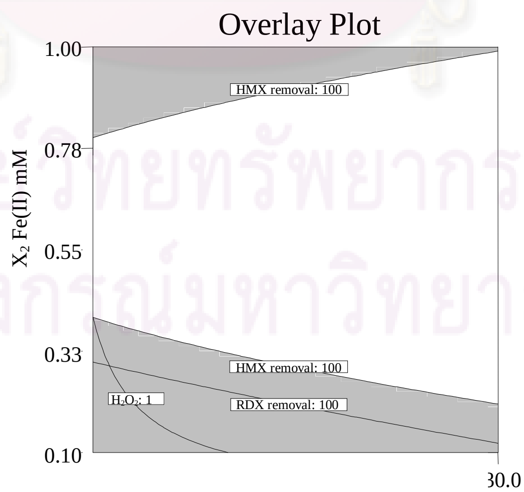

Figure 4.23 Optimum condition for electro-Fenton treatment of RDX and HMX with 0.04 A current, pH 2.6 and 25 ˚C.

4.2.5 Pathway of RDX and HMX Degradation

Figure 4.24 shows possible degradation pathway of HMX by electro-Fenton process. RDX degradation intermediates should be similar to those of HMX since both of them have the same structure of heterocyclic nitramines. The hydroxyl radical (•OH) would abstract H-atom very fast. Sequential reaction with $^{\bullet}$OH after initial ring-opening will generate formic acid. The products of mineralization are nitrate, carbon dioxide, and water with few nitrogen gas and formic acid as the intermediates (Zoh and Stenstrom, 2002). Bier *et al.*, (1999) and Liou *et al.*, (2003) also reported that products of the Fenton reaction of RDX included methylene dinitramine. The degradation of formic acid to carbon dioxide and water by UV/H_2O_2 process was reported by Stefan and Bolton (1998). The detailed mechanisms of formic acid oxidation and pKa of formic acid and carboxyl radical (•COO^-) were reported by Cooper *et al.*, (2009).

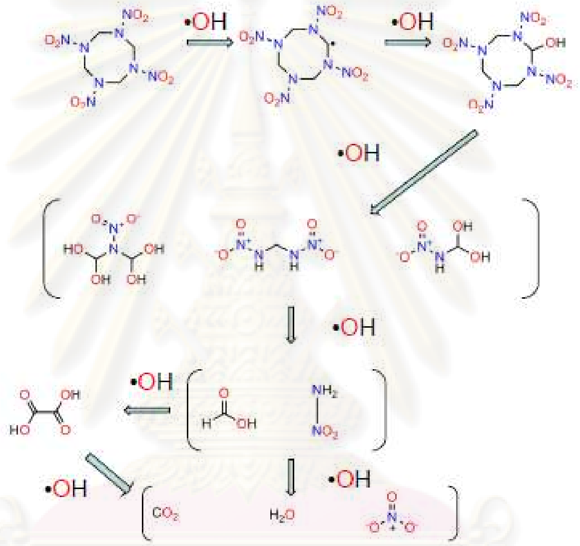

Figure 4.24 Possible degradation pathway of HMX by electro-Fenton method.

4.2.6 Economic Considerations

Traditionally, overall cost comprises of capital cost and O&M cost. Capital cost includes engineering design, site work, equipment, electrical system, piping work, contractor, and contingency, which is directly proportional to the degradation kinetics (Gogate and Pandit, 2004b). For O&M cost, chemical consumption, analytical sampling, electrical consumption, labor expenses, and system O&M are considered. Hydrogen peroxide consumption is directly related to the concentration and type of pollutants (Comninellis *et al.*, 2008). In general, the higher system capacity, the lower overall cost per volume of wastewater or mass of pollutant (usually referring to COD). According to the experimental results, hydrogen peroxide 30%, ferrous sulfate heptahydrate 99%, sulfuric acid 95%, sodium sulfate 99%, and electrical cost (using power generation efficiency of 50%) required are 1.3 g/L, 0.28 g/L, 0.2 g/L, 1.4 g/L, and 2 W/L·h respectively. The chemical and electrical unit prices are varied slightly by the purchased amount and location of usage. The unit prices are time and exchange rate dependently as well. Additional information for cost estimation can be found in Kavanaugh *et al.*, (2004).

4.3 Real Wastewater Oxidation

HMX wastewater from a munitions plant was collected for the study of various treatment methods. The characteristics of this explosive wastewater were shown in Table 4.2. Wastewater was acidic and saturated with RDX and HMX, but without TNT. Higher concentrations of COD, BOD, and TOC imply that a biological treatment is possible; nonetheless, long hydraulic retention time is needed. Advanced oxidation processes generally require smaller treatment plant footprint due to faster reaction. Fenton, electrolysis, H_2O_2-UVA, electro-Fenton, and photo-Fenton were selected for comparative study of munitions production wastewater treatment. Hydrogen peroxide usage was calculated according to the amount of COD with 20% in excess to ensure the sufficiency of H_2O_2. Continuous feeding mode of hydrogen peroxide was selected in order to prevent extremely heat release from the reactions and scavenging effect of hydrogen peroxide with hydroxyl radical according to Eq. 2.4 (Zhang *et al.*, 2005). Feeding was finished in 110 min, and total reaction time was 120 min. Salt was not added due to adequate conductivity. Ferrous addition was maintained at 1:100 by molar of hydrogen peroxide. Temperature was controlled at 60 °C due to exothermic reaction of Fenton's reagent and prevention of significant water evaporation (Huang *et al.*, 2001; Kang *et al.*, 2006). Current applied was maintained at 140 A/m^2.

Table 4.2 Munitions production wastewater characteristics.

Parameters	Characteristics
pH	2.07
Color	white and clear
Conductivity	6.3 mS/cm
COD	30,747 mg/L
BOD	9,958 mg/L
RDX	175 mg/L
HMX	5.8 mg/L
TNT	not detected
TOC	12,585 mg/L
Acetate	25,064 mg/L
Formate	277 mg/L
Chloride	not detected
Nitrite	20 mg/L
Nitrate	27,163 mg/L
Sulfate	620 mg/L

4.3.1 Removal Efficiency

The RDX and HMX degradations were shown in Figure 4.25. RDX was removed at 99% efficiency in 120 minutes by various methods except H_2O_2/UVA process. HMX was removed with 96% efficiency in 120 minutes similar to those of RDX. H_2O_2/UVA could not effectively treat this munitions production wastewater according to UVA could not directly dissociate hydrogen peroxide to hydroxyl radicals. RDX and HMX were degraded by oxidation with hydroxyl radicals or reduction with hydrated electron with the same efficiency. The results indicated that oxidation by H-abstraction are easily. The electron association of RDX and HMX are easily also.

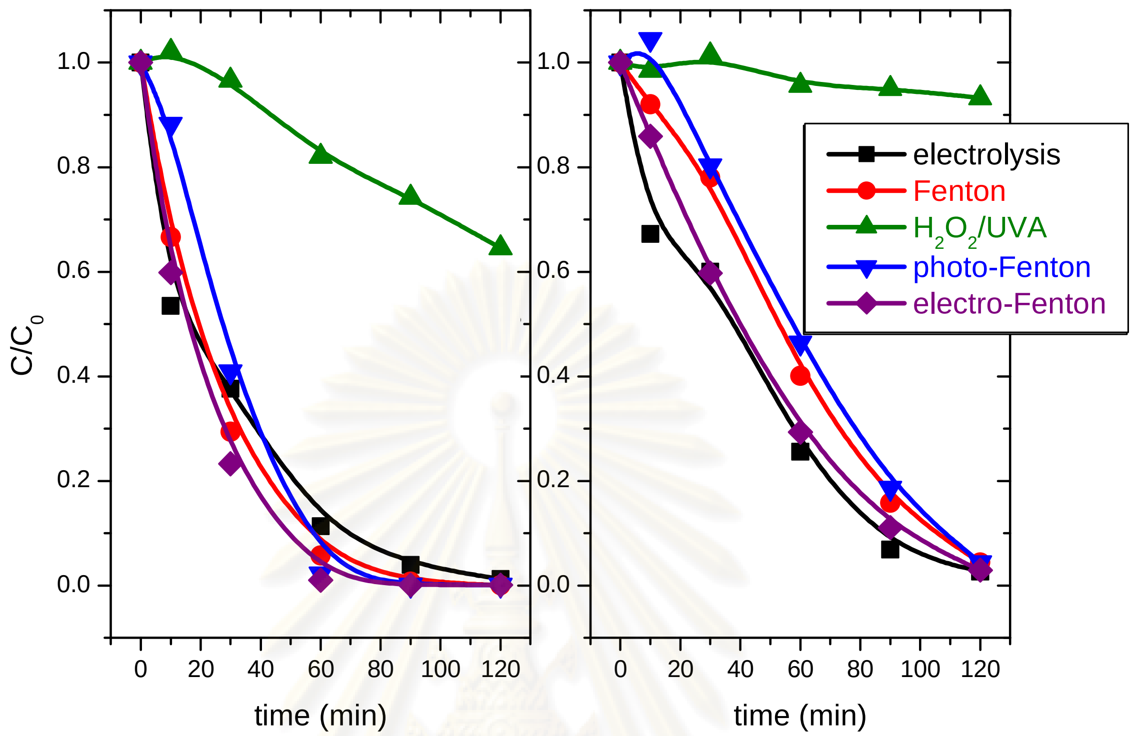

Figure 4.25 RDX (left) and HMX (right) degradation by various methods. (conditions: H_2O_2 2.36 M, Fe^{2+} 25 mM, $pH_{initial}$ 2.9, current 4.27 A/L, 12 of 3-W UVA lamp, and 60 ˚C).

For COD and TOC, the removal efficiencies were 70% in 120 minutes by various Fenton processes while H_2O_2/UVA had slightly efficiency and electrolysis had none. This could be indicated that mechanisms between electrolysis and various Fenton methods are different.

4.3.2 Removal Kinetics

RDX could be removed effectively in 60 minutes with electrolysis, Fenton, photo-Fenton and electro-Fenton process while HMX was removed effectively in 120 minutes. Removal in the first 40 min for RDX and the first 90 min for HMX indicated that reactants were limited as shown by a linear decreasing trend of explosive. At the end, according to higher amount of reactants comparing with explosives, the removal rate is slow down. COD and TOC also had the same kinetic trend as explosive chemicals. According to the results, Fenton, electro-Fenton, and photo-Fenton had nearly the same kinetics rate while electrolysis and H_2O_2/UVA had no efficiency for COD and TOC removal. For RDX and HMX removal, the kinetic rates are in the following order: Fenton = electro-Fenton = photo-Fenton > electrolysis > H_2O_2/UVA. The electro-Fenton processes in this study had faster RDX and HMX removal kinetics than those obtained by previous researcher (Liou *et al.*, 2003).

4.3.3 Hydrogen Peroxide Efficiency

Hydrogen peroxide efficiency for H_2O_2/UVA, Fenton, photo-Fenton, and electro-Fenton process are 6%, 40%, 61%, and 43%, respectively. Providing too much hydrogen peroxide led to lower usage efficiency. According to the excess amount of hydrogen peroxide during continuous addition of hydrogen peroxide, extending the reaction period or increasing catalyst could help usage of hydrogen peroxide effectively. However, this could increase the construction cost and chemical cost which then increasing the disposal of sludge cost also. Hydrogen peroxide can also degrade at cathode as shown by Eq. 4.11, then direct addition to the cathode was prohibited. The optimum conditions such as pH and temperature should be maintained in order to maximize removal efficiency. For better improvement, different method can also applied such as UVC for enhancing utilization of hydrogen peroxide by provided more hydroxyl radicals.

4.3.4 Voltage

Voltage drop at the beginning of the electro-Fenton process is 7.7 Volt and electrolysis was 10.1 Volt. The difference between these two systems was the ferrous which was added in the electro-Fenton experiment and could increase the conductivity of the wastewater. Figures 4.25 and 4.26 imply that the amount of electricity supply was sufficient due to no difference between RDX and HMX removal. After 120 minutes, the voltage for electro-Fenton was increasing to 8.1 Volt while electrolysis was decreasing further to 9.5. This implied that the electro-Fenton method could degrade ionic compounds to non-ionic compounds such as water or gas, whereas the electrolysis could not.

4.3.5 Process Optimization

By comparison of various methods, the treatment effectiveness can be arranged as photo-Fenton = electro-Fenton > Fenton for COD, TOC and BOD removal. H_2O_2/UVA and electrolysis could not effectively remove COD, TOC, and BOD. If considered only RDX and HMX removal, the electrolysis, Fenton, photo-Fenton, and electro-Fenton all had similar effectiveness whereas the H_2O_2/UVA could not remove RDX nor HMX. Among various Fenton processes, photo-Fenton and electro-Fenton are the promising methods in the treatment of high-concentrated wastewater.

4.3.6 Intermediates

HMX-RDX containing wastewater was treated by electrolysis for intermediate determination. The HMX and RDX can degrade simultaneously with two intermediates peak which can detected by HPLC as shown in Figure 4.27. The intermediates peak happened at 4.0 and 4.5 min were not acetone peak as happened at 3.2 min. These intermediates could clarify by HPLC-MS or GC-MS for further studied.

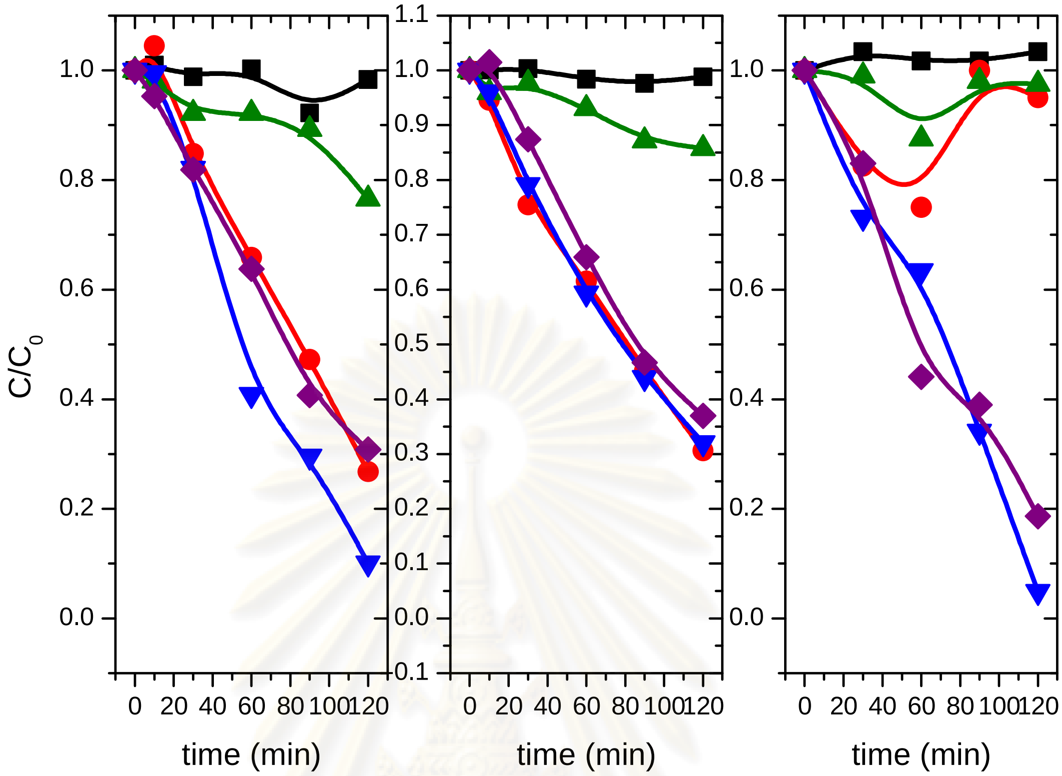

Figure 4.26 COD (left) , TOC (middle), and BOD (right) degradation by various methods (conditions: H_2O_2 2.36 M, Fe^{2+} 25 mM, $pH_{initial}$ 2.9, current 4.27 A/L, 12 of 3-W UVA lamp, and 60 ˚C), ■-electrolysis, ●-Fenton, ▲-H_2O_2/UVA, ▼-photo-Fenton, and ◆-electro-Fenton.

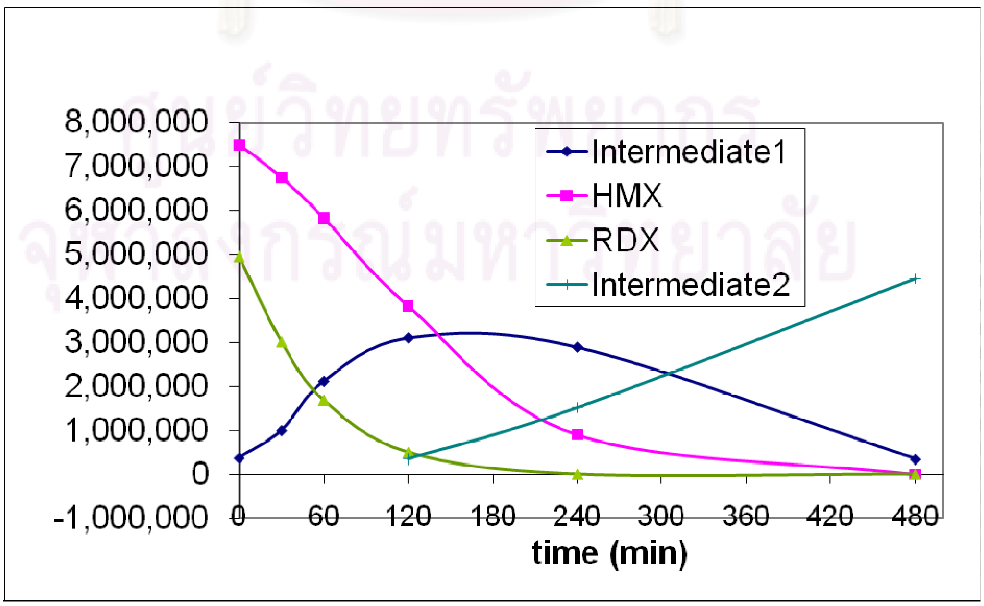

Figure 4.27 HMX-RDX wastewater treatment by electrolysis.

4.3.7 Economic Considerations

In term of removal efficiency, it was found that the treatment processes being tested are capable of treating real munitions production wastewater; however, the chemical cost was very high. Addition of other physico-chemical processes as pretreatment is necessary and maybe the promising method for very high concentrated wastewater.

CHAPTER V

CONCLUSIONS

5.1 Conclusions

The following conclusions were obtained from this study:

- Application of electro-Fenton process successfully treated the explosive TNT, RDX and HMX. Under similar chemical dosages, electro-Fenton process could significantly enhance the decomposition of explosives due to acceleration of ferrous regeneration at the cathode which promoted the hydroxyl radicals production rate.

- The Box-Behnken experimental design was proven to yield a reliable statistically results for the removal of TNT, RDX and HMX and maximize the process performance. The RSM also provided a better understanding for the roles of hydrogen peroxide to ferrous ratio, ferrous, current and pH.

- The optimum current, pH, ferrous, and hydrogen peroxide for the removal of 78 mg/L TNT by electrochemical process was 0.66 A, 3.0, 0.05 mM, and 0.09 mM, respectively. The removal efficiency and removal rates were significantly correlated with electric current. The explosives removal efficiency at this condition was 100%.

- The optimum current, pH, ferrous, and hydrogen peroxide to ferrous ratio for the removal of 40 mg/L RDX or 2.2 mg/L HMX were 0.04 A, 2.6, 0.8 mM, and 3, respectively. The removal efficiency and oxidation rates were significantly correlated with pH while the H_2O_2 efficiency decreased as the H_2O_2 concentration increased. The explosives removal efficiency at this condition was 100%. The empirical relationships between TNT, RDX, or HMX removals and the independent variables were also illustrated in this study.

- Kinetics rate of explosives removal in this study were best fit with 1^{st}-order kinetics with the rate constants of 0.066 and 0.029 min^{-1} for RDX and HMX, respectively.

- Hydrogen peroxide efficiency of electro-Fenton method was found to primarily relate to hydrogen peroxide concentration. The Hydrogen peroxide efficiency increasing while hydrogen peroxide and ferrous usage decreasing. The highest hydrogen peroxide efficiency in this study could be achieved by using 0.3 mM H_2O_2 and 0.1 mM Fe^{2+}. Electric current have no effect with hydrogen peroxide efficiency, then electric current can reducing more. The optimal pH of 2.6 could maximize the hydrogen peroxide efficiency. Higher hydrogen peroxide efficiency can be achieved by adding the appropriate amount of hydrogen peroxide at the appropriate time. Minimizing chemical usages is the major concern for very concentrated wastewater.

- Proposed intermediates of TNT, RDX, and HMX degradation were also illustrated. Water, nitrate, and carbon dioxide should be the product of explosives mineralization.

5.2 Recommendations

Further studies with various types of electrode and surface area are of interest in order to increase the current discharge efficiency of the electro-Fenton process. The artificial neural network for statistical design is also another interesting topic. Finally, in depth of oxidation mechanism of explosive chemicals by hydroxyl radicals may also be challenging and deserved to be investigated.

REFERENCES

Abdessalem, A.K., Oturan, N., Bellakhal, N., Dachraoui, M., and Oturan, M.A. 2008. Experimental dsign methodology applied to electro-Fenton treatment for degradation of herbicide chlortoluron. Applied Catalysis B: Environmental 78: 334-341.

Adrian, N.R., Arnett, C.M., and Hickey, R.F. 2003. Stimulating the anaerobic biodegradation of explosives by the addition of hydrogen or electron donors that produce hydrogen. Water Research 37: 3499-3507.

Adrian, N.R., and Arnett, C.M. 2007. Anaerobic biotransformation of explosives in aquifer slurries amended with ethanol and propylene glycol. Chemosphere 66: 1849-1856.

Agladze, G.R., Tsurtsumia, G.S., Jung, B.-I., Kim, J.-S., and Gorelishvili G. 2007. Comparative study of hydrogen peroxide electro-generation on gas-diffusion electrodes in undivided and membrane cells. Journal of Applied Electrochemistry 37: 375-383.

Agrawal, A., and Tratnyek, P.G. 1996. Reduction of nitro aromatic compounds by zero-valent iron metal. Environmental Science and Technology 30: 153-160.

Ahmad, A.L., Ismail, S., and Bhatia, S. 2005. Optimization of coagulation-flucculation process for palm oil mill effluent using response surface methodology. Environmental Science and Technology 39: 2828-2834.

Ahmadi, M., Vahabzadeh, F., Banakdarpour, B., Mofarrah, E., and Mehranian, M. 2005. Application of the central composite design and response surface methodology to the advanced treatment of olive oil processing wastewater using Fenton's peroxidation. Journal of Hazardous Materials B123: 187-195.

Aken, B.V., Yoon, J.M., and Schnoor, J.L. 2004. Biodegradation of nitro-substituted explosives 2,4,6-trinitrotoluene, hexahydro-1,3,5-trinitro-1,3,5-triazine, and octahydro-1,3,5,7-tetranitro-1,3,5-tetrazocine by a phytosymbiotic *Methylobacterium* sp. associated with poplar tissues (*Populus deltoids* × *nigra* DN34). Applied and Environmental Microbiology 70: 508-517.

Anotai, J., Lu, M.C., and Chewpreecha, P. 2006. Kinetics of aniline degradation by Fenton and electro-Fenton processes. Water Research 40: 1841-1847.

APHA, AWWA, WEF. 2005. Standard methods for the examination of water and wastewater. 21st Edition, Washington DC.

Arantes, V., Baldocchi, C. and Milagres, A. M.F. 2006. Degradation and decolorization of a biodegradable-resistant polymeric dye by chelator-mediated Fenton reactions. Chemosphere 63: 1764-1772.

ATSDR 1996a. ToxFAQs: 2,4,6-trinitrotoluene (TNT) [Online]. Available from http://www.atsdr.cdc.gov/toxfaqs/tfacts81.pdf [2011, 3 May]

ATSDR 1996b. ToxFAQs: RDX (Cyclonite) [Online]. Available from http://www.atsdr.cdc.gov/toxfaqs/tfacts78.pdf [2011, 3 May]

ATSDR 1997. ToxFAQs: HMX (Octogen) [Online]. Available from http://www.atsdr.cdc.gov/toxfaqs/tfacts98.pdf [2011, 3 May]

Ay, F., Catalkaya, E.C., and Kargi, F. 2008. Advanced oxidation of direct red (DR 28) by Fenton treatment. Environmental Engineering Science 25(10): 1455-1462.

Ay, F., Catalkaya, E.C., and Kargi, F. 2009. A statistical experiment design approach for advanced oxidation of direct red azo-dye by photo-Fenton treatment. Journal of Hazardous Materials 162: 230-236.

Balakrishnan, V.K., Halasz, A., and Hawari, J. 2003. Alkaline hydrolysis of the cyclic nitramine explosives RDX, HMX, and CL-20: new insights into degradation pathways obtained by the observation of novel intermediates. Environmental Science and Technology 37: 1838-1843.

Bacardit, J., Stötzner, J., Chamarro, E., and Esplugas, S. 2007. Effect of salinity on the photo-Fenton process. Industrial and Engineering Chemistry Research 46: 7615-7619.

Beltran, F.J., Encinar, J.M., and Alonso, M.A. 1998. Nitroaromatic hydrocarbon ozonation in water. 2. Combined ozonation with hydrogen peroxide or UV radiation. Industrial and Engineering Chemistry Research 37: 32-40.

Benatti, C.T., Tavares, C.R.G. and Guedes, T.A. 2006. Optimization of Fenton’s oxidation of chemical laboratory wastewaters using the response surface methodology. Journal of Environmental Management 80: 66-74.

Best, E. P.H., Sprecher, S.L., Larson, S.L., Fredrickson, H.L., and Bader, D.F. 1999. Environmental behavior of explosives in groundwater from the milan army ammunition plant in aquatic and wetland plant treatments. Removal, mass balances and fate in groundwater of TNT and RDX. Chemosphere 38: 3383-3396.

Betterton, E.A. and Hoffmann, M.R. 1990. Kinetics and mechanism of the oxidation of aqueous hydrogen sulfide by peroxymonosulfate. Environmental Science and Technology 24: 1819-1824.

Bezerra, M.A., Santelli, R.E., Oliveira, E.P., Villar, L.S., and Escaleira, L.A. 2008. Response surface methodology (RSM) as a tool for optimization in analytical chemistry. Talanta 76: 965-977.

Bier, E.L., Singh, J., Li, Z.-M., Comfort, S.D., and Shea, P.J. 1999. Remediating hexahydro-1,3,5-trinitro-1,3,5-triazine contaminated water and soil by Fenton oxidation. Environmental Toxicology and Chemistry 18: 1078-1084.

Bishop, D.F., Stern, G., Fleischman, M., and Marshall, L.S. 1968. Hydrogen peroxide catalytic oxidation of refractory organics in municipal waste waters. Industrial and Engineering Chemistry: Process Design and Development 7(1): 110-117.

Bonin, P.M.L., Bejan, D., Schutt, L., Hawari, J., and Bunce, N.J. 2004. Electrochemical reduction of hexahydro-1,3,5-trinitro-1,3,5-triazine in aqueous solutions. Environmental Science and Technology 38: 1595-1599.

Boparai, H.K., Comfort, S.D., Shea, P.J., and Szecsody, J.E. 2008. Remediating explosive-contaminated groundwater by in situ redox manipulation (ISRM) of aquifer sediments. Chemosphere 71: 933-941.

Bose, P., Glaze, W.H., and Maddox, D.S. 1998. Degradation of RDX by various advanced oxidation processes: I. Reaction rates. Water Researh 32: 997-1004.

Brannon, J.M., Price, C.B., and Hayes, C. 1998. Abiotic transformation of TNT in montmorillonite and soil suspensions under reducing conditions. Chemosphere 36: 1453-1462.

Bratsch, S.G. 1989. Standard electrode potentials and temperature coefficients in water at 298.15K. Journal of Physical and Chemical Reference Data 18: 1-21.

Brezonik, P.L. and Fulkerson-Brekken, J. 1998. Nitrate-induced photolysis in natural waters: controls on concentrations of hydroxyl radical photo-intermediates by natural scavenging agents. Environmental Science and Technology 32: 3004-3010.

Buxton, G.V., Greenstock, C.L., Helman, W.P., and Ross, A.B. 1988. Critical review of Rate constants for reactions of hydrated electrons, hydrogen atoms and hydroxyl radicals (•OH/•O$^-$) in aqueous solution. Journal of Physical and Chemical Reference Data 17: 513-886.

Calza, P., *et al.* 2008. Multivariate experimental design for the photocatalytic degradation of imipramine: Determination of the reaction pathway and identification of intermediate products. Applied Catalysis B: Environmental 84: 379-388.

Catalkaya, E.C., and Kargi, F. 2007. Effects of operating parameters on advanced oxidation of diuron by the Fenton's reagent: A statistical design approach. Chemosphere 69: 485-492.

Chang, P.H., Huang, Y.-H., Hsueh, C.-L., Lu, M.-C., and Huang, G.-H. 2004. Treatment of non-biodegradable wastewater by electro-Fenton method. Water Science and Technology 49(4): 213-218.

Chen, W.R., Wu, C., Elovitz, M.S., Linden, K.G., and Suffet. I.H. 2008. Reactions of thiocarbamate, triazine and urea herbicides, RDX and benzenes on EPA Contaminant Candidate List with ozone and with hydroxyl radicals. Water Research 42: 137-144.

Comninellis, C., Kapalka, A., Malato, S., Parsons, S.A., Poulios, I. and Mantzavinos, D. 2008. Advanced oxidation processes for water treatment: advances and trends for R&D. Journal of Chemical Technology and Biotechnology 83: 769-776.

Cooper, W.J., Cramer, C.J., Martin, N.H., Mezyk, S.P., O'Shea, K.E., and von Sonntag C. 2009. Free radical mechanisms for the treatment of Methyl *tert*-butyl ether (MTBE) via advanced oxidation/reductive processes in aqueous solutions. Chemical Reviews 109: 1302-1345.

Cristóvão, R.O., Tavares, A.P.M., Loureiro, J.M., Boaventura, R.A.R., and Macedo, E.A. 2008. Optimisation of reactive dye degradation by Laccase using Box-Behnken design. Environmental Technology 29(12): 1357-1364.

Cruz-González, K. *et al.*, 2010. Determination of optimum operating parameters for acid yellow 36 decolorization by electro-Fenton process using BDD cathode. Chemical Engineering Journal 160: 199-206.

Deligiorgis, A., Xekoukoulotakis, N.P., Diamadopoulos, E., and Mantzavinos, D. 2008. Electrochemical oxidation of table olive processing wastewater over boron-doped diamond electrodes: Treatment optimization by factorial design. Water Research 42: 1229-1237.

Do, J.-S., and Chen, C.-P. 1994. Kinetics of *in Situ* degradation of formaldehyde with electrogenerated hydrogen peroxide. Industrial and Engineering Chemistry Research 33: 387-394.

dos Santos, A. C.V., and Masini, J.C. 2009. Applying sequential injection analysis (SIA) and response surface methodology for optimization of Fenton-based processes. Talanta 77: 1081-1086.

DuBois, F.W., and Baytos, J.F. 1991. Weathering of explosives for twenty years. Los Alamos National Laboratory report LA-11931. New Mexico.

Durán, A., Monteagudo, J.M. and Mohedano, M. 2006. Neural networks simulation of photo-Fenton degradation of reactive blue 4. Applied Catalysis B: Environmental 65: 127-134.

Eisenberg, G. 1943. Colorimetric determination of hydrogen peroxide. Industrial and Engineering Chemistry: Analytical Edition 15(5): 327-328.

Emmrich, M. 1999. Kinetics of the alkaline hydrolysis of 2,4,6-trinitrotoluene in aqueous solution and highly contaminated soils. Environmental Science and Technology 33: 3802-3805.

Eremia, S.A.V., Chevalier-Lucia, D., Radu, G.-L., and Marty, J.-L. 2008. Optimization of hydroxyl radical formation using TiO_2 as photocatalyst by response surface methodology. Talanta 77: 858-862.

Farhataziz and Ross, A.B. 1977. Selected specific rates of reactions of transients from water in aqueous solution. National Standard Reference Data Series; U.S. National Bureau of Standards Washington, D.C.: NBS-NSRDS, No. 59.

Farias, J., Albizzati, E.D. and Alfano, O.M. 2009. Kinetic study of the photo-Fenton degradation of formic acid. Combined effects of temperature and iron concentration. Catalysis Today 144:117-123.

Farré, M.J., Doménech, X. and Peral, J. 2006. Assessment of photo-Fenton and biological treatment coupling for diuron and linuron removal from water. Water Research 40: 2533-2540.

Ferreira, S.L.C., dos Santos, W.N.L., Bruns, R.E., Quintella, C.M., Neto, B.B., and Bosque-Sendra, J.M. 2007a. Doehlert matrix: a chemometric tool for analytical chemistry-review. Talanta 63: 1061-1067.

Ferreira, S.L.C., *et al.* 2007b. Review Box-Behnken design: An alternative for the optimization of analytical methods. Analytica Chimica Acta 597: 179-186.

Ferreira, S.L.C., dos Santos, W.N.L., Bruns, R.E., Quintella, C.M., Neto, B.B., and Bosque-Sendra, J.M. 2004. Review of Doehlert matrix: a chemometric tool for analytical chemistry. Talanta 63: 1061-1067.

Fisher, J.M., Reese, J.G., Pellechia, P.J., Moeller, P.L., and Ferry, J.L. 2006. Role of Fe(III), phosphate, dissolved organic matter, and nitrate during the photodegradation of domoic acid in the marine environment. Environmental Science and Technology 40: 2200-2205.

Fu, J., Zhao, Y., and Wu, Q. 2007. Optimising photoelectrocatalytic oxidation of fulvic acid using response surface methodology. Journal of Hazardous Materials 144: 499-505.

Fuller, M.E., Schaefer, C.E., and Lowey, J.M. 2007. Degradation of explosives-related compounds using nickel catalysts. Chemosphere 67: 419-427.

Gázquez, D., Sánchez-Viñas, M., Bagur, M.G., and Darcía G. 1998. Application of Doehlert designs in the optimization of experimental variables associated with the simultaneous solvent extraction of several metals. Journal of Analytical Atomic Spectrometry 13: 105-108.

Ghafari, S., Aziz, H.A., Isa, M.H., and Zinatizadeh, A.A. 2008. Application of response surface methodology (RSM) to optimize coagulation-flocculation treatment of leachate using poly-aluminium chloride (PAC) and alum. Journal of Hazardous Materials 163(2-3): 650-656.

Ghasempur, S., Torabi, S.F., Ranaei-Siadat, S.O., Jalali-Heravi, M., Ghaemi, N., and Khajeh, K. 2007. Optimization of peroxidase-catalyzed oxidative coupling process for phenol removal from wastewater using response surface methodology. Environmental Science and Technology 41: 7073-7079.

Gilbert, D.M., and Sale, T.C. 2005. Sequential electrolytic oxidation and reduction of aqueous phase energetic compounds. Environmental Science and Technology 39: 9270-9277.

GlobalSecurity.org 2009a. Explosives – Nitramines [Online]. Available from : http://www.globalsecurity.org/military/systems/munitions/explosives-nitramines.htm [2011, 3 March].

GlobalSecurity.org 2009b. Explosives – Nitroaromatics [Online]. Available from : http://www.globalsecurity.org/military/systems/munitions/explosives-nitroaromatics.htm [2011, 3 March].

Göb, S., Oliveros, E., Bossmann, S.H., Braun, A.M., Nascimento, C.A.O., and Guardani, R. 2001. Optimal experimental design and artificial neural networks applied to the photochemically enhanced Fenton reaction. Water Science and Technology 44(5): 339-345.

Gogate, P.R., and Pandit, A.B. 2004a. A review of imperative technologies for wastewater treatment I: oxidation technologies at ambient conditions. Advances in Environmental Research 8: 501-551.

Gogate, P.R., and Pandit, A.B. 2004b. A review of imperative technologies for wastewater treatment II: hybrid methods. Advances in Environmental Research 8: 553-597.

Goldstein, S., Meyerstein, D., and Czapski, G. 1993. The Fenton reagents. Free Radical Biology & Medicine 15: 435-445.

González, A.G., and González-Arjona, D. 1999. Computational program for evaluating and optimizing response-surface curves based on uniform shell designs. Talanta 49: 433-439.

Hannink, N.K., Rosser, S.J., and Bruce, N.C. 2002. Phytoremediation of explosives. Critical Reviews in Plant Science 21(5): 511-538.

Hanrahan, G. and Lu, K. 2006. Application of factorial and response surface methodology in modern experimental design and optimization. Critical Reviews in Analytical Chemistry 36: 141-151.

Hermosilla, D., Cortijo, M., and Huang, C.P. 2009. Optimizing the treatment of landfill leachate by conventional Fenton and photo-Fenton processes. Science of the Total Environment 407: 3473-3481.

Herney-Ramirez, J., Costa, C.A., and Madeira, L.M. 2005. Experimental design to optimize the degradation of the synthetic dye orange II using Fenton's reagent. Catalysis Today 107-108: 68-76.

Herney-Ramirez, J., Lampinen, M., Vicente, M.A., Costa, C.A. and Madeira, L.M. 2008. Experimental design to optimize the oxidation of orange II dye solution using a clay-based Fenton-like catalyst. Industrial and Engineering Chemistry Research 47: 284-294.

Harris, D.C. 2003. Quantitative chemical analysis. 6th Edition. W. H. Freeman and Company, New York.

Hawthorne, S.B., Lagadec, A.J.M., Karderis, D., Lilke, A.V., and Miller, D.J. 2000. Pilot-scale destruction of TNT, RDX, and HMX on contaminated soils using subcritical water. Environmental Science and Technology 34: 3224-3228.

Hefner, K.H., Fisher, J.M., and Ferry, J.L. 2006. A multifactor exploration of the photobleaching of Suwannee river dissolved organic matter across the freshwater/saltwater interface. Environmental Science and Technology 40: 3717-3722.

Heilmann, H.M., Wiesmann, U., and Stenstrom, M.K. 1996. Kinetic of the alkaline hydrolysis of high explosives RDX and HMX in aqueous solution and adsorbed to activated carbon. Environmental Science and Technology 30: 1485-1492.

Hofstetter, T.B., Heijman, C.G., Haderlein, S.B., Holliger C., and Schwarzenbach, R.P. 1999. Complete reduction of TNT and other (poly)nitroaromatic compounds under iron-reducing subsurface conditions. Environmental Science and Technology 33: 1479-1487.

Hundal, L.S., Singh, J., Bier, E.L., Shea, P.J., Comfort, S.D., and Powers, W.L. 1997. Removal of TNT and RDX from water and soil using iron metal. Environmental Pollution 97(1-2): 55-64.

Huang, Y.-H., Chou, S., Perng, M.-G., Huang, G.-H., and Cheng, S.-S. 1999. Case study on the bioeffluent of petrochemical wastewater by electro-Fenton method. Water Science and Technology 39(10-11): 145-149.

Huang, Y.-H., Chen, C.C., Huang, G.-H., and Chou, S.S. 2001. Comparison of a novel electro-Fenton method with Fenton's reagent in treating a highly contaminated wastewater. Water Science and Technology 43(2): 17-24.

Huie, R.E., Clifton, C.L., and Neta, P. 1991. Electron transfer reaction rates and equilibria of the carbonate and sulfate radical anions. International Journal of Radiation Applications and Instrumentation. Part C. Radiation Physics and Chemistry 38(5): 477-481.

Jonsson, S., *et al*. 2007. Degradation of polycyclic aromatic hydrocarbons (PAHs) in contaminated soils by Fenton's reagent: a multivariate evaluation of the importance of soil characteristics and PAH Properties. Journal of Hazardous Materials 149: 86-96.

Kang, N., Hua, I., and Rao, P.S.C. 2006. Enhanced Fenton's destruction of non-aqueous phase perchloroethylene in soil systems. Chemosphere 63: 1685-1698.

Kang, Y.W., and Hwang, K.-Y. 2000. Effects of reaction conditions on the oxidation efficiency in the Fenton process. Water Research 34: 2786-2790

Kannan, R. *et al*., 2008. A 2^{7-3} fractional factorial optimization of polybenzimidazole based membrane electrode assemblies for H_2/O_2 fuel cells. Journal of Applied Electrochemistry 38: 583-590.

Kasiri, M.B., Aleboyeh, H., and Aleboyeh, A. 2008. Modeling and optimization of heterogeneous photo-Fenton process with response surface methodology and artificial neural networks. Environmental Science and Technology 42: 7970-7975.

Katsoni, A., Frontistis, Z., Xekoukoulotakis, N.P., Diamadopoulos, E., and Mantzavinos, D. 2008. Wet air oxidation of table olive processing wastewater: Determination of key operating parameters by factorial design. Water Research 42: 3591-3600.

Kavanaugh, M., *et al.* 2004. 3.0 Advanced oxidation processes. Removal of MTBE with advanced oxidation processes, pp.109-208. IWA Publishing (Intl Water Assoc).

Killian, P.F., and Bruell, C.J. 2007. Iron(II) activated persulfate oxidation of MGP contaminated soil. Soil & Sediment Contamination 16: 523-537.

Knutson, K.P. 2004. Enzymatic biobleaching of recalcitrant paper dyes. Doctoral dissertation, Institute of Paper Science and Technology, Georgia Institute of Technology.

Koppenol, W.H. 1993. The centennial of the Fenton reaction. Free Radical Biology & Medicine 15: 645-651.

Körbahti, B.K., and Rauf, M.A. 2009. Determination of optimum operating conditions of carmine decoloration by UV/H_2O_2 using response surface methodology. Journal of Hazardous Materials 161: 281-286.

Körbahti, B.K., and Tanyolaç, A. 2008. Electrochemical treatment of simulated textile wastewater with industrial components and Levafix Blue CA reactive dye: Optimization through response surface methodology. Journal of Hazardous Materials 151: 422-431.

Körbahti, B.K., and Rauf, M.A. 2007. Application of response surface analysis to the photolytic degradation of basic red 2 dye. Chemical Engineering Journal 138: 166-171.

Körbahti, B.K., Aktaş, N., and Tanyolaç, A. 2007. Optimization of electrochemical treatment of industrial paint wastewater with response surface methodology. Journal of Hazardous Materials 148: 83-90.

Körbahti, B.K. 2007. Response surface optimization of electrochemical treatment of textile dye wastewater. Journal of Hazardous Materials 145: 277-286.

Lee, S.-J., Son, H.-S., Lee, H.-K., and Zoh, K.-D. 2002. Photocatalytic degradation of explosives contaminated water. Water Science and Technology 46(11-12): 139-145.

Legrini, O., Oliveros, E. and Braun, A.M. 1993. Photochemical processes for water treatment. Chemical Reviews 93: 671-698.

Liou, M.J., Lu, M.C., and Chen, J.N. 2003. Oxidation of explosives by Fenton and photo-Fenton processes. Water Research 37: 3172-3179.

Liou, M.J. and Lu, M.C. 2007. Catalytic degradation of nitroaromatic explosives with Fenton's reagent. Journal of Molecular Catalysis A: Chemical 277: 155-163.

Liou, M.J. and Lu, M.C. 2008. Catalytic degradation of explosives with goethite and hydrogen peroxide. Journal of Hazardous Materials 151: 540-546.

Liu, H. *et al.* 2007. A novel electro-Fenton process for water treatment: Reaction-controlled pH adjustment and performance assessment. Environmental Science and Technology 41: 2937-2942.

López-Cueto, G., Ostra, M., Ubide, C., and Zuriarrain, J. 2004. Fenton's reagent for kinetic determinations. Analytica Chimica Acta 515: 109-116.

Martel, R., Mailloux, M., Gabriel, U., Lefebvre, R., Thiboutot, S., and Ampleman, G. 2009. Behavior of energetic materials in ground water at an anti-tank range. Journal of Environmental Quality 38: 75-92.

Martínez-Huitle, C.A., and Brillas, E. 2009. Decontamination of wastewaters containing synthetic organic dyes by electrochemical methods: A general review. Applied Catalysis B: Environmental 87: 105-145.

Martínez-Huitle, C.A., and Ferro, S. 2006. Electrochemical oxidation of organic pollutants for the wastewater treatment: direct and indirect processes. Chemical Society Reviews 35: 1324-1340.

Martins, A.F., Vasconcelos, T.B. and Wilde M.L. 2005. Influence of variables of the combined coagulation-Fenton-sedimentation process in the treatment of trifluraline effluent. Journal of Hazardous Materials B127: 111-119.

Masomboon, N., Chen, C.-W., Anotai, J. and Lu, M.C. 2010. A statistical experimental design to determine o-toluidine degradation by the photo-Fenton process. Chemical Engineering Journal 159: 116-122.

Massart, D.L., Vandeginste, B.G.M., Buydens, L.M.C., de Jong, S., Lewi, P.J., and Smeyers-Verbeke, J. 2003. Handbook of Chemometrics and Qualimetrics, Part A, Elsevier, Amsterdam.

Meyers, S.K., Deng, S., Basta, N.T., Clarkson, W.W., and Wilber, G.G. 2007. Long-term explosive contamination in soil: Effects on soil microbial community and bioremediation. Soil and Sediment Contamination 16: 61-77.

Millioli, V.S., Freire, D.D.C., and Cammarota, M.C. 2003. Petroleum oxidation using Fenton's reagent over beach sand following a spill. Journal of Hazardous Materials B103: 79-91.

Mohajeri, S., Aziz, H.A., Isa, M.H., Zahed, M.A., and Adlan, M.N. 2010. Statistical optimization of process parameters for landfill leachate treatment using electro-Fenton technique. Journal of Hazardous Materials 176: 749-758.

Moraes, J.E.F., Quina, F.H., Nascimento, C.A.O., Silva, D.N., and Chiavone-Filho, O. 2004. Treatment of saline wastewater contaminated with hydrocarbons by the photo-Fenton process. Environmental Science and Technology 38: 1183-1187.

Morley, M.C., Henke, J.L., and Speitel, G.E. 2005. Adsorption of RDX and HMX in rapid small-scale column tests: Implications for full-scale adsorbers. Journal of Environmental Engineering 131(1): 29-37.

Moshe, S.S., Ronen, Z., Dahan, O., Weisbrod, N., Groisman, L., Adar, E., and Nativ, R. 2009. Sequential biodegradation of TNT, RDX and HMX in a mixture. Environmental Pollution 157: 2231-2238.

Mosteo, R., Ormad, P., Mozas, E., Sarasa, J. and Ovelleiro, J.L. 2006. Factorial experimental design of winery wastewaters treatment by heterogeneous photo-Fenton process. Water Research 40: 1561-1568.

Murugesan, K., Dhamija, A., Nam, I.-H., Kim, Y.-M., and Chang, Y.-S. 2007. Decolourization of reactive black 5 by laccase: Optimization by response surface methodology. Dyes and Pigments 75: 176-184.

Myers, R.H. and Montgomery, D.C. 2002. Response surface methodology: Process and product optimization using designed experiments, 2nd Edition, John Wiley & Sons, USA.

Naja, G., Halasz, A., Thiboutot, S., Ampleman, G., and Hawari, J. 2008. Degradation of hexahydro-1,3,5-trinitro-1,3,5-triazine (RDX) using zerovalent iron nanoparticles. Environmental Science and Technology 42: 4364-4370.

Oliveira, R., Almeida, M.F., Santos, L. and Madiera, L.M. 2006. Experimental design of 2,4-dichlorophenol oxidation by Fenton's reaction. Industrial and Engineering Chemistry Research 45: 1266-1276.

Oliveros, E., Legrini, O., Hohl, M.,, Müller, T., and Braun, A.M. 1997. Large scale development of a light-enhanced fenton reaction by optimal experimental design. Water Science and Technology 35(4): 223-230.

Ölmez, T. 2009. The optimization of Cr(VI) reduction and removal by electrocoagulation using response surface methodology. Journal of Hazardous Materials 162: 1371-1378.

Ormad, M.P., Mosteo, R. Ibarz, C. and Ovelleiro, J.L. 2006. Multivariate approach to the photo-Fenton process applied to the degradation of winery wastewaters. Applied Catalysis B: Environmental 66: 58-63.

Owen Compliance Services, Inc. 2006a. Material Safety Data Sheet (MSDS-TNT) [Online]. Available from : http://www.ocsresponds.com/ref/msds-tnt.pdf [2011, 3 May]

Owen Compliance Services, Inc. 2006b. Material Safety Data Sheet (MSDS-RDX) [Online]. Available from : http://www.ocsresponds.com/ref/msds-rdx.pdf [2011, 3 May]

Owen Compliance Services, Inc. 2006c. Material Safety Data Sheet (MSDS-HMX) [Online]. Available from : http://www.ocsresponds.com/ref/msds-hmx.pdf [2011, 3 May]

Palaniswamy, D.K., Sorial, G.A. and Maloney, S.W. 2004. Electrochemical reduction of 2,4,6-trinitrotoluene. Environmental Engineering Science 21(2): 203-218.

Park, J., Comfort, S.D., Shea, P.J., and Machacek, T.A. 2004. Organic compounds in the environment. Remediating munitions-contaminated soil with zerovalent iron and cationic surfactants. Journal of Environmental Quality 33: 1305-1313.

Pennington, J.C., and Brannon, J.M. 2002. Environmental fate of explosives. Thermochimica Acta 384: 163-172.

Pera-Titus, M., García-Molina, V., Baños, M.A., Giménez, J., and Esplugas, S. 2004. Degradation of chlorophenols by means of advanced oxidation processes: a general review. Applied Catalysis B: Environmental 47: 219-256.

Pérez-Moya, M., Graells, M., Buenestado, P., and Mansilla, H.D. 2008. A comparative study on the empirical modeling of photo-Fenton treatment process performance. Applied Catalysis B: Environmental 84: 313-323.

Pignatello, J.J., Oliveros, E., and Mackay, A. 2006. Advanced oxidation processes for organic contaminant destruction based on the Fenton reaction and related chemistry. Critical Reviews in Environmental Science and Technology 36: 1-84.

Pimentel, M., Oturan, N., Dezotti, M., and Oturan, M.A. 2008. Phenol degradation by advanced electrochemical oxidation process electro-Fenton using a carbon felt cathode. Applied Catalysis B: Environmental 83, 140-149.

Prasannakumar, B.R., Regupathi, I., and Murugesan, T. 2009. An optimization study on microwave irradiated decomposition of phenol in the presence of H_2O_2. Journal of Chemical Technology and Biotechnology 84: 83-91.

Pratap, K. and Lemley, A.T. 1994. Electrochemical peroxide treatment of aqueous herbicide solutions. Journal of Agricultural and Food Chemistry 42: 209-215.

Qiang, Z., Chang, J.H., and Huang, C.P. 2003. Electrochemical regeneration of Fe^{2+} in Fenton oxidation processes. Water Research 37: 1308-1319.

Rauf, M.A., Marzouki, N., and Körbahti, B.K. 2008. Photolytic decolorization of Rose Bengal by UV/H_2O_2 and data optimization using response surface method. Journal of Hazardous Materials 159: 602-609.

Rodgers, J.D. and Bunce, N.J. 2001. Treatment methods for the remediation of nitroaromatic explosives. Water Research 35: 2101-2111.

Rodrigues, C.-S.D., Madeira, L.M., and Boaventura, R.-A.R. 2009. Optimization of the azo dye PROCION red H-EXL degradation by Fenton's reagent using experimental design. Journal of Hazardous Materials 164: 987-994.

Roh, H., Yu, C.P., Fuller, M.E., Chu, K.H. 2009. Identification of hexahydro-1,3,5-trinitro-1,3,5-triazine-degrading microorganisms via ^{15}N-stable isotope probing. Environmental Science and Technology 43: 2505-2511.

Rossi, C., Briand, E., Parot, P., Odorico, M., and Chopineau, J. 2007. Surface response methodology for the study of supported membrane formation. The Journal of Physical Chemistry B 111: 7567-7576.

Ruotolo, L.A.M., and Gubulin, J.C. 2005. A factorial-design study of the variable affecting the electrochemical reduction of Cr(VI) at polyaniline-modified electrodes. Chemical Engineering Journal 110: 113-121.

Sakkas, V.A., Islam, Md.A., Stalikas, C., and Albanis, T.A. 2010. Review of photocatalytic degradation using design of experiments: A review and example of the Congo red degradation. Journal of Hazardous Materials 175: 33-44.

Schmelling, D.C., Gray, K.A., and Kamat, P.V. 1996. Role of reduction in the photocatalytic degradation of TNT. Environmental Science and Technology 30: 2547-2555.

Sellers, R.M. 1980. Spectrophotometric Determination of hydrogen peroxide using potassium titanium (IV) oxalate. Analyst 105: 950-954.

Sermpong Sairiam. 2008. Enhancing treatment efficiency of wastewater containing aniline by electro-Fenton process. Master's Thesis, Environmental Management (Interdisciplinary Program), Chulalongkorn University.

Sheremata, T.W. and Hawari, J. 2000. Mineralization of RDX by the white rot fungus *Phanerochaete chrysosporium* to carbon dioxide and nitrous oxide. Environmental Science and Technology 34: 3384-3388.

Singh, S. 2007. Review in sensors-An effective approach for the detection of explosives. Journal of Hazardous Materials 144: 15-28.

Souza, A.S., *et al.* 2007. Automatic on-line pre-concentration system using a knotted reactor for the FAAS determination of lead in drinking water. Journal of Hazardous Materials 141: 540-545.

Steevens, J.A., Duke, B.A., Lotufo, G.R., and Bridges, T.S. 2002. Toxicity of the explosives 2,4,6-trinitrotoluene, hexahydro-1,3,5-trintiro-1,3,5-triazine, and octahydro-1,3,5,7-tetranitro-1,3,5,7-tetrazocine in sediments to *Chironomus Tentans* and *Hyalella Azteca*: low-dose hormesis and high-dose mortality. Environmental Toxicology and Chemistry 21(7): 1475-1482.

Stefan, M.I. and Bolton, J.R. 1998. Mechanism of the degradation of 1,4-dioxane in dilute aqueous solution using the UV/hydrogen peroxide process. Environmental Science and Technology 32: 1588-1595.

Steffan, R.J., Hatzinger, P.B., and Fuller, M.E. 2007. Treatment options for emerging contaminants. Shaw Environmental, Inc. Lawrenceville, New Jersey.

Stumm W. and Morgan J.J. 1996. Aquatic chemistry; chemical equilibria and rates in natural waters, 3rd Edition, John Wiley & Sons, New York.

Tarr, M.A. 2003. Chemical degradation methods for wastes and pollutants. Marcel Dekker, Inc., New York.

Torrades, F., Pérez, M., Mansilla, H.D., and Peral, J. 2003. Experimental design of Fenton and photo-Fenton reactions for the treatment of cellulose bleaching effluents. Chemosphere 53: 1211-1220.

Turner, C., Whitehand, L.C., Nguyen, T., and McKeon, T. 2004. Optimization of a supercritical fluid extraction/reaction methodology for the analysis of castor oil using experimental design. Journal of Agricultural and Food Chemistry 52: 26-32.

Uri N. 1952. Inorganic free radicals in solution. Chemical Reviews 50(3): 375-454.

U.S. Environmental Protection Agency. 1995. 1993 Toxics Release Inventory: Public Data Release EPA 745-R-95-010, Office of Pollution Prevention and Toxics: Washington DC.

U.S. Environmental Protection Agency. 2006. 2006 edition of the drinking water standards and health advisories EPA 822-R-06-013, Office of Water: Washington DC.

Vila, M., Lorber-Pascal, S., and Laurent F. 2007. Fate of RDX and TNT in agronomic plants. Environmental Pollution 148: 148-154.

Walling, C. 1975. Fenton's reagent revisited. Accounts of Chemical Research 8: 125-131.

Walling, C., and Goosen, A. 1973. Mechanism of the ferric ion catalyzed decomposition of hydrogen peroxide. Effect of organic substrates. Journal of the American Chemical Society 95: 2987-2991.

Waul, C., Arvin, E., and Schmidt, J.E. 2008. Model description and kinetic parameter analysis of MTBE biodegradation in a packed bed reactor. Water Research 42: 3122-3134.

Wikipedia 2009. Explosive Material [Online]. Available from : http://en.wikipedia.org/wiki/Explosive [2011, 3 March].

Wujcik, W.J., Lowe, W.L., and Marks, P.J. 1992. Granular activated carbon pilot treatment studies for explosives removal from contaminated groundwater. Environmental Progress & Sustainable Energy 11: 178.

Zhang, G., Yang, F., Gao, M., Fang, X., and Liu, L. 2008. Electro-Fenton degradation of azo dye using polypyrrole/anthraquinonedisulphonate composite film modified graphite cathode in acidic aqueous solutions. Electrochimica Acta 53: 5155-5161.

Zhang, H., Choi, H.J., Canazo, P. and Huang, C.-P. 2009. Multivariate approach to the Fenton process for the treatment of landfill leachate. Journal of Hazardous Materials 161: 1306-1312.

Zhang, H., Choi, H.J., Huang, C.-P. 2005. Optimization of Fenton process for the treatment of landfill leachate. Journal of Hazardous Materials B125: 166-174.

Zhang, H., Zhang, D., and Zhou, J. 2006. Removal of COD from landfill leachate by electro-Fenton method. Journal of Hazardous Materials B135: 106-111.

Zhang, H., Fei, C., Zhang, D., and Tang, F. 2007. Degradation of 4-nitrophenol in aqueous medium by electro-Fenton method. Journal of Hazardous Materials 145: 227-232.

Zinatizadeh, A.A.L., Mohamed, A.R., Abdullah, A.Z., Mashitah, M.D., Hasnain Isa, M., and Najafpour, G.D. 2006. Process modeling and analysis of palm oil mill effluent treatment in an up-flow anaerobic sludge fixed film bioreactor using response surface methodology (RSM). Water Research 40: 3193-3208.

Zoh, K.D., and Stenstrom, M.K. 2002. Fenton oxidation of hexahydro-1,3,5-trinitro-1,3,5-triazine (RDX) and octahydro-1,3,5,7-tetranitro-1,3,5,7-tetrazocine (HMX). Water Research 36: 1331-1341.

Zuo, Z., Katsumura, Y., Ueda, K., and Ishigure, K. 1997. Laser photolysis study on reactions of sulfate radical and nitrate radical with chlorate ion in aqueous solutions Formation and reduction potential of ClO_3 radical. Journal of the Chemical Society, Faraday Transactions 93(4): 533-536.

APPENDICES

APPENDIX A

Experimental Figures

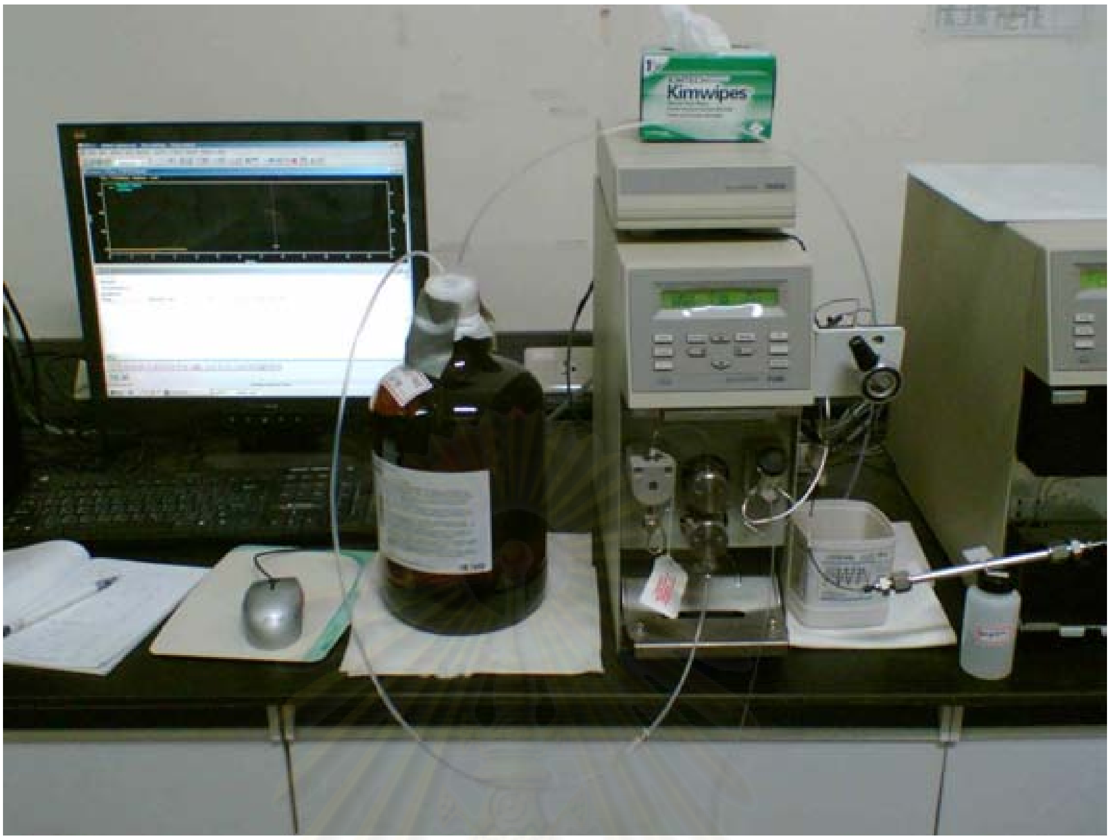

Figure A.1 HPLC for determination of TNT, RDX, and HMX.

Figure A.2 electro-Fenton reactor setup for TNT, RDX, and HMX oxidation.

Figure A.3 photo-Fenton reactor setup for explosive wastewater degradation.

Figure A.4 electro-Fenton reactor setup for explosive wastewater degradation.

APPENDIX B

Experimental Data

B.1 Experimental data of TNT treatment experiments

Table B.1.1 Box-Behnken run no.1 (19 Oct)

Time (min)	Area	TNT (ppm)	conc/conc	area/area	TNT (mM)
0	4983115	75.69	1.0000	1.0000	0.3332
1	4487424	68.15	0.9004	0.9005	0.3000
5	4038690	61.33	0.8103	0.8105	0.2700
10	3543783	53.81	0.7109	0.7112	0.2369
30	1946971	29.54	0.3902	0.3907	0.1300
60	738630	11.17	0.1476	0.1482	0.0492

Table B.1.2 Box-Behnken run no.2 (21 Oct)

Time (min)	Area	TNT (ppm)	conc/conc	area/area	TNT (mM)
0	4988163	75.76	1.0000	1.0000	0.3336
1	4478225	68.01	0.8977	0.8978	0.2994
5	3777923	57.37	0.7572	0.7574	0.2526
10	3088252	46.88	0.6188	0.6191	0.2064
30	1305504	19.78	0.2611	0.2617	0.0871
60	343142	5.16	0.0681	0.0688	0.0227

Table B.1.3 Box-Behnken run no.3 (30 Sep)

Time (min)	Area	TNT (ppm)	conc/conc	area/area	TNT (mM)
0	5319954	80.81	1.0000	1.0000	0.3558
1	4709958	71.53	0.8853	0.8853	0.3149
5	3787297	57.51	0.7117	0.7119	0.2532
10	2791130	42.37	0.5243	0.5247	0.1865
30	883396	13.37	0.1654	0.1661	0.0589
60	146388	2.17	0.0268	0.0275	0.0095

Table B.1.4 Box-Behnken run no.4 (22 Oct)

Time (min)	Area	TNT (ppm)	conc/conc	area/area	TNT (mM)
0	5037524	76.51	1.0000	1.0000	0.3369
1	4983748	75.69	0.9893	0.9893	0.3333
5	4823860	73.26	0.9576	0.9576	0.3226
10	4503604	68.40	0.8939	0.8940	0.3011
30	3792257	57.58	0.7526	0.7528	0.2535
60	2833942	43.02	0.5622	0.5626	0.1894

Table B.1.5 Box-Behnken run no.5 (24 Oct)

Time (min)	Area	TNT (ppm)	conc/conc	area/area	TNT (mM)
0	5031616	76.42	1.0000	1.0000	0.3365
1	4671933	70.96	0.9285	0.9285	0.3124
5	4485026	68.11	0.8913	0.8914	0.2999
10	4219539	64.08	0.8385	0.8386	0.2821
30	3419738	51.92	0.6794	0.6797	0.2286
60	2560258	38.86	0.5085	0.5088	0.1711

Table B.1.6 Box-Behnken run no.6 (22 Oct)

Time (min)	Area	TNT (ppm)	conc/conc	area/area	TNT (mM)
0	5092137	77.34	1.0000	1.0000	0.3405
1	4584559	69.63	0.9002	0.9003	0.3066
5	4277340	64.96	0.8399	0.8400	0.2860
10	4034538	61.27	0.7921	0.7923	0.2697
30	3292173	49.98	0.6463	0.6465	0.2201
60	2736516	41.54	0.5370	0.5374	0.1829

Table B.1.7 Box-Behnken run no.7 (24 Oct)

Time (min)	Area	TNT (ppm)	conc/conc	area/area	TNT (mM)
0	4994016	75.85	1.0000	1.0000	0.3340
1	4461537	67.76	0.8933	0.8934	0.2983
5	3477993	52.81	0.6962	0.6964	0.2325
10	2416737	36.68	0.4835	0.4839	0.1615
30	546681	8.25	0.1088	0.1095	0.0363
60	78766	1.14	0.0150	0.0158	0.0050

Table B.1.8 Box-Behnken run no.8 (21 Oct)

Time (min)	Area	TNT (ppm)	conc/conc	area/area	TNT (mM)
0	4989693	75.79	1.0000	1.0000	0.3337
1	4801844	72.93	0.9623	0.9624	0.3211
5	4244773	64.46	0.8506	0.8507	0.2838
10	3312876	50.30	0.6637	0.6639	0.2214
30	1217003	18.44	0.2433	0.2439	0.0812
60	246429	3.69	0.0486	0.0494	0.0162

Table B.1.9 Box-Behnken run no.9 (28 Sep)

Time (min)	Area	TNT (ppm)	conc/conc	area/area	TNT (mM)
0	5331804	80.99	1.0000	1.0000	0.3566
1	5005316	76.02	0.9387	0.9388	0.3347
5	4392465	66.71	0.8237	0.8238	0.2937
10	3470041	52.69	0.6506	0.6508	0.2320
30	1196696	18.13	0.2239	0.2244	0.0798
60	267551	4.01	0.0495	0.0502	0.0176

Table B.1.10 Box-Behnken run no.10 (21 Oct)

Time (min)	Area	TNT (ppm)	conc/conc	area/area	TNT (mM)
0	5000189	75.94	1.0000	1.0000	0.3344
1	4763572	72.35	0.9526	0.9527	0.3185
5	4549722	69.10	0.9098	0.9099	0.3042
10	4279111	64.98	0.8557	0.8558	0.2861
30	3728274	56.61	0.7454	0.7456	0.2492
60	3122028	47.40	0.6241	0.6244	0.2087

Table B.1.11 Box-Behnken run no.11 (16 Oct)

Time (min)	Area	TNT (ppm)	conc/conc	area/area	TNT (mM)
0	4965372	75.42	1.0000	1.0000	0.3320
1	4668566	70.90	0.9402	0.9402	0.3122
5	3929864	59.68	0.7913	0.7915	0.2627
10	2960774	44.95	0.5960	0.5963	0.1979
30	858571	12.99	0.1723	0.1729	0.0572
60	119432	1.76	0.0233	0.0241	0.0077

Table B.1.12 Box-Behnken run no.12 (19 Oct)

Time (min)	Area	TNT (ppm)	conc/conc	area/area	TNT (mM)
0	4967926	75.45	1.0000	1.0000	0.3322
1	4887933	74.24	0.9839	0.9839	0.3269
5	4384048	66.58	0.8824	0.8825	0.2931
10	3787634	57.51	0.7622	0.7624	0.2532
30	1700700	25.79	0.3418	0.3423	0.1136
60	350280	5.27	0.0698	0.0705	0.0232

Table B.1.13 Box-Behnken run no.13 (25 Oct)

Time (min)	Area	TNT (ppm)	conc/conc	area/area	TNT (mM)
0	5178123	78.65	1.0000	1.0000	0.3463
1	4635001	70.39	0.8950	0.8951	0.3099
5	3948997	59.97	0.7625	0.7626	0.2640
10	3025048	45.92	0.5839	0.5842	0.2022
30	1247170	18.90	0.2403	0.2409	0.0832
60	391796	5.90	0.0750	0.0757	0.0260

Table B.1.14 H_2O_2 Oxidation: H_2O_2 2.9 mM, pH_i 3.0, and Na_2SO_4 10 mM

Time (min)	Area	TNT (ppm)	conc/conc	area/area	TNT (mM)
0	5167770	78.49	1.0000	1.0000	0.3456
1	5110369	77.62	0.9889	0.9889	0.3417
5	5054367	76.77	0.9780	0.9781	0.3380
10	5083444	77.21	0.9837	0.9837	0.3399
30	5088781	77.29	0.9847	0.9847	0.3403
60	5059178	76.84	0.9790	0.9790	0.3383

Table B.1.15 Fenton oxidation: H_2O_2 2.9 mM, Fe^{2+} 0.09 mM, pH_i 3.0, and Na_2SO_4 10 mM

Time (min)	Area	TNT (ppm)	conc/conc	area/area	TNT (mM)
0	5146314	78.17	1.0000	1.0000	0.3441
1	4774733	72.52	0.9277	0.9278	0.3193
5	4678690	71.06	0.9091	0.9091	0.3128
10	4642982	70.52	0.9021	0.9022	0.3105
30	4437292	67.39	0.8621	0.8622	0.2967
60	4160898	63.19	0.8084	0.8085	0.2782

Table B.1.16 electrolysis: current 0.80 A, pH_i 3.0, and Na_2SO_4 10 mM

Time (min)	Area	TNT (ppm)	conc/conc	area/area	TNT (mM)
0	4375689	66.45	1.0000	1.0000	0.2926
1	4179078	63.46	0.9550	0.9551	0.2794
5	3347329	50.82	0.7648	0.7650	0.2238
10	2481422	37.66	0.5667	0.5671	0.1658
30	692371	10.47	0.1575	0.1582	0.0461
60	115389	1.70	0.0255	0.0264	0.0075

Table B.1.17 electro-Fenton oxidation: H_2O_2 2.9 mM, Fe^{2+} 0.09 mM, current 0.80 A, pH_i 3.0, and Na_2SO_4 10 mM

Time (min)	Area	TNT (ppm)	conc/conc	area/area	TNT (mM)
0	4886695	74.22	1.0000	1.0000	0.3268
1	4051946	61.53	0.8290	0.8292	0.2709
5	3100252	47.07	0.6341	0.6344	0.2072
10	2200078	33.38	0.4498	0.4502	0.1470
30	709447	10.72	0.1445	0.1452	0.0472
60	136753	2.02	0.0272	0.0280	0.0089

Table B.1.18 electro-Fenton oxidation: H_2O_2 2.9 mM, Fe^{2+} 0.09 mM, current 0.80 A, pH_i 3.0, and Na_2SO_4 10 mM

Time (min)	Area	TNT (ppm)	conc/conc	area/area	TNT (mM)
0	2390607	36.28	1.0000	1.0000	0.1597
1	2110434	32.02	0.8826	0.8828	0.1410
5	1734238	26.30	0.7250	0.7254	0.1158
10	1270896	19.26	0.5309	0.5316	0.0848
30	307921	4.62	0.1274	0.1288	0.0203
60	56089	0.79	0.0219	0.0235	0.0035

Table B.1.19 electro-Fenton oxidation: H_2O_2 2.9 mM, Fe^{2+} 0.09 mM, current 0.80 A, pH_i 3.0, and Na_2SO_4 10 mM

Time (min)	Area	TNT (ppm)	conc/conc	area/area	TNT (mM)
0	1260844	19.11	1.0000	1.0000	0.0841
1	1157549	17.54	0.9178	0.9181	0.0772
5	1010646	15.30	0.8010	0.8016	0.0674
10	775659	11.73	0.6140	0.6152	0.0516
30	185215	2.76	0.1443	0.1469	0.0121
60	20404	0.25	0.0131	0.0162	0.0011

Table B.1.20 electro-Fenton oxidation: H_2O_2 2.9 mM, Fe^{2+} 0.09 mM, current 0.80 A, pH_i 3.0, and Na_2SO_4 10 mM

Time (min)	Area	TNT (ppm)	conc/conc	area/area	TNT (mM)
0	29478	0.3892	1.0000	1.0000	0.001713
1	29202	0.3850	0.9892	0.9906	0.0017
5	21781	0.27	0.6994	0.7389	0.0012
10	15946	0.18	0.4715	0.5409	0.0008
30	5576	0.03	0.0664	0.1892	0.0001
60	1641	(0.03)	(0.0873)	0.0557	(0.0001)

Table B.1.21 electrolysis: current 0.05 A, pH_i 3.0, and Na_2SO_4 10 mM

Time (min)	Area	TNT (ppm)	conc/conc	area/area	TNT (mM)
0	5353479	81.31	1.0000	1.0000	0.3580
1	5211726	79.16	0.9735	0.9735	0.3485
5	4943720	75.09	0.9234	0.9235	0.3306
10	4612948	70.06	0.8616	0.8617	0.3084
30	3644632	55.34	0.6806	0.6808	0.2436
60	2336734	35.46	0.4361	0.4365	0.1561

Table B.1.22 electrolysis: current 0.20 A, pH_i 3.0, and Na_2SO_4 10 mM

Time (min)	Area	TNT (ppm)	conc/conc	area/area	TNT (mM)
0	5029689	79.87	1.0000	1.0000	0.3516
1	4939367	78.43	0.9820	0.9820	0.3453
5	4537657	72.05	0.9021	0.9022	0.3172
10	3967766	62.99	0.7887	0.7889	0.2773
30	1945061	30.85	0.3862	0.3867	0.1358
60	610276	9.64	0.1207	0.1213	0.0424

Table B.1.23 electrolysis: current 0.43 A, pH_i 3.0, and Na_2SO_4 10 mM

Time (min)	Area	TNT (ppm)	conc/conc	area/area	TNT (mM)
0	5918103	81.72	1.0000	1.0000	0.3598
1	5665907	78.24	0.9574	0.9574	0.3445
5	4633632	63.98	0.7828	0.7830	0.2817
10	3556427	49.09	0.6007	0.6009	0.2161
30	1258665	17.34	0.2122	0.2127	0.0763
60	228513	3.10	0.0380	0.0386	0.0137

Table B.1.24 ANOVA test for TNT removal by Box-Behnken (model reduction).

Source	Sum of squares	df	Mean square	F-value	p-value Prob > F	
Model	7052.36	3	2350.79	358.19	<0.0001	significant
X_2-H_2O_2	78.75	1	78.75	12.00	0.0071	
X_3-current	5602.11	1	5602.11	853.60	<0.0001	
X_3^2	1371.50	1	1371.50	208.98	<0.0001	
Residual	59.07	9	6.56			
Cor Total	7111.43	12				
Std. Dev.	2.56		**R^2**	0.9917		
Mean	78.81		**Adj R^2**	0.9889		
C.V.%	3.25		**Pred R^2**	0.9811		
PRESS	134.60		**Adeq Precision**	41.660		

Table B.1.25 ANOVA test for 1st order kinetics by Box-Behnken (model reduction).

Source	Sum of squares	df	Mean square	F-value	p-value Prob > F	
Model	5.834E-3	5	1.167E-3	165.49	<0.0001	significant
X_1-Fe^{2+}	6.728E-5	1	6.728E-5	9.54	0.0176	
X_2-H_2O_2	2.237E-4	1	2.237E-4	31.72	0.0008	
X_3-current	5.299E-3	1	5.299E-3	751.62	<0.0001	
X_2 X_3	6.642E-5	1	6.642E-5	9.42	0.0181	
X_3^2	1.771E-4	1	1.771E-4	25.12	0.0015	
Residual	4.935E-5	7	7.051E-6			
Cor Total	5.883E-3	12				
Std. Dev.	2.655E-3		**R^2**	0.9916		
Mean	0.038		**Adj R^2**	0.9856		
C.V.%	7.00		**Pred R^2**	0.9739		
PRESS	1.533E-4		**Adeq Precision**	35.333		

Table B.1.26 TNT removal efficiency by experiment and model prediction.

	removal efficiency (%)	
Current (A)	Actual experiment	Model prediction
0.05	56.4	44.2
0.20	87.9	68.3
0.43	96.2	92.1
0.80	97.4	97.1

Table B.1.27 current efficiency of TNT removal by electrochemical process.

Current (A)	removal efficiency (%)	TNT removal (mmol)	Electron applied (mmol)	current efficiency (%)	Potential applied (V)
0.05	56.4	0.202	1.87	10.8	3.0
0.20	87.9	0.309	7.46	4.1	5.7
0.43	96.2	0.346	16.04	2.2	8.5
0.80	97.4	0.346	29.85	1.2	17.2

Table B.1.28 electrolysis: current 0.05 A, pH_i 3.0, and Na_2NO_3 10 mM.

Time (min)	Area	TNT (ppm)	conc/conc	area/area	TNT (mM)
0	5094800	77.38	1.0000	1.0000	0.3407
1	4961831	75.36	0.9739	0.9739	0.3318
5	4776399	72.54	0.9375	0.9375	0.3194
10	4587723	69.68	0.9004	0.9005	0.3068
30	4141931	62.90	0.8128	0.8130	0.2769
60	3621867	54.99	0.7107	0.7109	0.2421

Table B.1.29 electrolysis: current 0.05 A, pH_i 3.0 with sulfuric acid, and Na_2SO_4 10 mM.

Time (min)	Area	TNT (ppm)	conc/conc	area/area	TNT (mM)
0	4965254	75.41	1.0000	1.0000	0.3320
1	4949986	75.18	0.9969	0.9969	0.3310
5	4536932	68.90	0.9137	0.9137	0.3034
10	4114342	62.48	0.8285	0.8286	0.2751
30	2694085	40.89	0.5422	0.5426	0.1800
60	1139824	17.27	0.2290	0.2296	0.0760

Table B.1.30 electrolysis: current 0.05 A, pH_i 3.0 with nitric acid, and Na_2SO_4 1 mM

Time (min)	Area	TNT (ppm)	conc/conc	area/area	TNT (mM)
0	4911722	74.60	1.0000	1.0000	0.3284
1	4901591	74.45	0.9979	0.9979	0.3278
5	4497631	68.31	0.9156	0.9157	0.3007
10	4290971	65.16	0.8735	0.8736	0.2869
30	2858712	43.39	0.5817	0.5820	0.1911
60	1494432	22.66	0.3037	0.3043	0.0998

Table B.1.31 electrolysis: current 0.05 A, pH_i 3.0 with nitric acid, and Na_2SO_4 100 mM

Time (min)	Area	TNT (ppm)	conc/conc	area/area	TNT (mM)
0	4959229	75.32	1.0000	1.0000	0.3316
1	4908077	74.54	0.9897	0.9897	0.3282
5	4624013	70.23	0.9324	0.9324	0.3092
10	4314473	65.52	0.8699	0.8700	0.2885
30	2890977	43.88	0.5826	0.5829	0.1932
60	1593014	24.16	0.3207	0.3212	0.1063

Table B.1.32 electrolysis: current 0.05 A, pH_i 3.0 with sulfuric acid, and Na_2SO_4 1 mM

Time (min)	Area	TNT (ppm)	conc/conc	area/area	TNT (mM)
0	4906965	74.53	1.0000	1.0000	0.3281
1	4746808	72.09	0.9673	0.9674	0.3174
5	4345372	65.99	0.8855	0.8856	0.2905
10	3827996	58.13	0.7799	0.7801	0.2559
30	2224548	33.75	0.4529	0.4533	0.1486
60	791349	11.97	0.1606	0.1613	0.0527

Table B.1.33 electrolysis: current 0.05 A, pH_i 3.0 with sulfuric acid, and Na_2SO_4 100 mM

Time (min)	Area	TNT (ppm)	conc/conc	area/area	TNT (mM)
0	4854398	73.73	1.0000	1.0000	0.3246
1	4837437	73.47	0.9965	0.9965	0.3235
5	4508990	68.48	0.9288	0.9288	0.3015
10	4145115	62.95	0.8538	0.8539	0.2771
30	2538078	38.52	0.5225	0.5228	0.1696
60	823617	12.46	0.1690	0.1697	0.0549

Table B.1.34 pH effect for electrolysis: current 0.20 A, pH_i 4.0, and Na_2SO_4 10 mM

Time (min)	Area	TNT (ppm)	conc/conc	area/area	TNT (mM)
0	4977440	75.60	1.0000	1.0000	0.3328
1	4692907	71.27	0.9428	0.9428	0.3138
5	4316304	65.55	0.8671	0.8672	0.2886
10	3608452	54.79	0.7247	0.7250	0.2412
30	2139618	32.46	0.4294	0.4299	0.1429
60	812598	12.29	0.1626	0.1633	0.0541

Table B.1.35 pH effect for electrolysis: current 0.20 A, pH_i 2.0, and Na_2SO_4 10 mM

Time (min)	Area	TNT (ppm)	conc/conc	area/area	TNT (mM)
0	5125416	77.85	1.0000	1.0000	0.3427
1	5035450	76.48	0.9824	0.9824	0.3367
5	4562704	69.29	0.8901	0.8902	0.3051
10	4032504	61.24	0.7866	0.7868	0.2696
30	2479683	37.63	0.4834	0.4838	0.1657
60	1000798	15.15	0.1947	0.1953	0.0667

Table B.1.36 temperature effect for electrolysis: current 0.20 A, pH_i 3.0, Na_2SO_4 10 mM and 50 ˚C

Time (min)	Area	TNT (ppm)	conc/conc	area/area	TNT (mM)
0	4815187	73.13	1.0000	1.0000	0.3220
1	4696950	71.34	0.9754	0.9754	0.3141
5	4802531	72.94	0.9974	0.9974	0.3211
10	4758451	72.27	0.9882	0.9882	0.3182
30	4736654	71.94	0.9837	0.9837	0.3167
60	4719834	71.68	0.9802	0.9802	0.3156

Table B.1.37 temperature effect for electrolysis: current 0.20 A, pH_i 3.0, Na_2SO_4 10 mM and 75 ˚C

Time (min)	Area	TNT (ppm)	conc/conc	area/area	TNT (mM)
0	4790465	72.76	1.0000	1.0000	0.3203
1	4846058	73.60	1.0116	1.0116	0.3241
5	4596630	69.81	0.9595	0.9595	0.3074
10	4969239	75.47	1.0373	1.0373	0.3323
30	4961244	75.35	1.0357	1.0356	0.3318
60	5039596	76.54	1.0520	1.0520	0.3370

B.2 Experimental data of RDX and HMX treatment experiments

Table B.2.1 RDX and HMX removal by electro-Fenton process.

No.	Actual and coded levels of variables				Experimental data					
	X_1, H_2O_2:Fe^{2+} (mM/mM)	X_2, Fe^{2+} (mM)	X_3, current (A)	X_4, pH	R_1, RDX remov. effi.	R_2, 1st-order kinetics (min^{-1})	R_3, H_2O_2 effi.	H_1, HMX remov. effi.	H_2, 1st-order kinetics (min^{-1})	H_3, H_2O_2 effi.
1	30(1)	0.55(0)	0.12(0)	4(1)	19.53	0.0011	0.252	29.4	0.0026	0.01
2	16.5(0)	0.55(0)	0.12(0)	3(0)	98.90	0.0416	1.418	98.0	0.0356	0.09
3	16.5(0)	0.10(-1)	0.12(0)	2(-1)	86.73	0.0166	8.882	82.5	0.0153	0.38
4	3(-1)	0.55(0)	0.04(-1)	3(0)	89.97	0.0173	9.463	86.2	0.0147	0.42
5	16.5(0)	1.00(1)	0.04(-1)	3(0)	99.13	0.0442	1.007	98.5	0.0401	0.03
6	16.5(0)	0.55(0)	0.04(-1)	2(-1)	98.72	0.0326	1.915	92.7	0.0236	0.09
7	16.5(0)	0.10(-1)	0.20(1)	3(0)	95.30	0.0248	10.124	96.0	0.0279	0.38
8	3(-1)	0.10(-1)	0.12(0)	3(0)	87.46	0.0169	55.177	93.4	0.0221	2.36
9	30(1)	0.55(0)	0.04(-1)	3(0)	99.44	0.0410	1.036	98.1	0.0373	0.04
10	16.5(0)	0.55(0)	0.04(-1)	4(1)	14.17	0.0006	0.526	85.4	0.0147	0.07
11	16.5(0)	1.00(1)	0.12(0)	4(1)	16.76	0.0008	0.273	19.3	0.0011	0.01
12	16.5(0)	0.55(0)	0.12(0)	3(0)	98.75	0.0403	1.888	97.0	0.0326	0.08
13	30(1)	0.55(0)	0.20(1)	3(0)	99.26	0.0385	1.045	97.3	0.0332	0.05
14	30(1)	1.00(1)	0.12(0)	3(0)	99.76	0.0560	0.578	98.5	0.0373	0.03
15	16.5(0)	0.55(0)	0.12(0)	3(0)	98.76	0.0399	2.038	97.4	0.0336	0.10
16	16.5(0)	1.00(1)	0.12(0)	2(-1)	99.74	0.0494	1.033	98.8	0.0396	0.04
17	30(1)	0.55(0)	0.12(0)	2(-1)	98.57	0.0328	1.082	97.8	0.0288	0.04
18	16.5(0)	0.55(0)	0.12(0)	3(0)	99.50	0.0482	1.899	97.0	0.0329	0.07
19	30(1)	0.10(-1)	0.12(0)	3(0)	87.41	0.0169	4.945	94.4	0.0253	0.25
20	3(-1)	0.55(0)	0.20(1)	3(0)	97.47	0.0288	9.965	97.4	0.0280	0.55
21	16.5(0)	1.00(1)	0.20(1)	3(0)	99.36	0.0468	1.007	96.3	0.0295	0.04
22	16.5(0)	0.10(-1)	0.04(-1)	3(0)	87.58	0.0171	9.219	94.3	0.0260	0.31
23	16.5(0)	0.55(0)	0.20(1)	4(1)	20.62	0.0010	0.411	94.8	0.0211	0.07
24	16.5(0)	0.55(0)	0.20(1)	2(-1)	99.30	0.0431	1.881	96.7	0.0316	0.04
25	3(-1)	0.55(0)	0.12(0)	4(1)	43.14	0.0032	4.738	98.7	0.0374	0.32
26	3(-1)	1.00(1)	0.12(0)	3(0)	96.77	0.0265	5.521	92.1	0.0191	0.27
27	3(-1)	0.55(0)	0.12(0)	2(-1)	94.75	0.0238	9.815	91.4	0.0193	0.43
28	16.5(0)	0.10(-1)	0.12(0)	4(1)	24.79	0.0017	2.530	6.19	0.0003	0.03

Table B.2.2 ANOVA test for RDX removal by Box-Behnken

Source	**Sum of squares**	**df**	**Mean square**	**F-value**	**p-value Prob > F**	
Model	25575.11	7	3653.59	154.94	<0.0001	significant
X_1-H_2O_2:Fe(II)	2.60	1	2.60	0.11	0.7431	
X_2-Fe(II)	148.76	1	148.76	6.31	0.0207	
X_4-pH	16045.45	1	16045.45	680.43	<0.0001	
X_1X_4	188.10	1	188.10	7.98	0.0105	
X_2X_4	110.67	1	110.67	4.69	0.0425	
X_2^2	98.00	1	98.00	4.16	0.0549	
X_4^2	9043.12	1	9043.12	383.49	<0.0001	
Residual	471.63	20	23.58			
Lack of Fit	471.25	17	27.72	219.96	0.0004	significant
Pure Error	0.38	3	0.13			
Cor Total	26046.74	27				
Std. Dev.	4.86		**R^2**	0.9819		
Mean	80.42		**Adj R^2**	0.9756		
C.V.%	6.04		**Pred R^2**	0.9505		
PRESS	1289.28		**Adeq Precis.**	33.459		

Table B.2.3 ANOVA test for HMX removal by Box-Behnken

Source	**Sum of squares**	**df**	**Mean square**	**F-value**	**p-value Prob > F**	
Model	10379.61	6	1729.93	6.01	0.0009	significant
X_1-H_2O_2:Fe(II)	159.14	1	159.14	0.55	0.4654	
X_2-Fe(II)	112.30	1	112.30	0.39	0.5389	
X_4-pH	4260.48	1	4260.48	14.80	0.0009	
X_1X_4	1432.62	1	1432.62	4.98	0.0367	
X_2^2	1312.93	1	1312.93	4.56	0.0446	
X_4^2	3715.74	1	3715.74	12.91	0.0017	
Residual	6044.46	21	287.83			
Lack of Fit	6043.79	18	335.77	1503.43	<0.0001	significant
Pure Error	0.67	3	0.22			
Cor Total	16424.07	27				
Std. Dev.	16.97		**R^2**	0.6320		
Mean	86.63		**Adj R^2**	0.5268		
C.V.%	19.58		**Pred R^2**	0.2418		
PRESS	12452.30		**Adeq Precis.**	8.904		

Table B.2.4 ANOVA test for 1st order kinetics of RDX by Box-Behnken

Source	**Sum of squares**	**df**	**Mean square**	**F-value**	**p-value Prob > F**	
Model	7.781E-3	10	7.781E-4	36.03	<0.0001	significant
X_1-H_2O_2:Fe(II)	4.060E-4	1	4.060E-4	18.80	0.0004	
X_2-Fe(II)	1.402E-3	1	1.402E-3	64.91	<0.0001	
X_3-current	7.600E-5	1	7.600E-5	3.52	0.0779	
X_4-pH	3.005E-3	1	3.005E-3	139.15	<0.0001	
X_1X_2	2.176E-4	1	2.176E-4	10.07	0.0056	
X_2X_4	2.839E-4	1	2.839E-4	13.15	0.0021	
X_1^2	3.492E-4	1	3.492E-4	16.17	0.0009	
X_2^2	1.995E-4	1	1.995E-4	9.24	0.0074	
X_3^2	7.368E-5	1	7.368E-5	3.41	0.0822	
X_4^2	2.315E-3	1	2.315E-3	107.18	<0.0001	
Residual	3.672E-4	17	2.160E-5			
Lack of Fit	3.223E-4	14	2.302E-5	1.54	0.4042	not signi
Pure Error	4.490E-5	3	1.497E-5			
Cor Total	8.148E-3	27				
Std. Dev.	4.647E-3		**R^2**	0.9549		
Mean	0.027		**Adj R^2**	0.9284		
C.V.%	17.32		**Pred R^2**	0.8800		
PRESS	9.780E-4		**Adeq Precis.**	20.433		

Table B.2.5 ANOVA test for 1st order kinetics of HMX by Box-Behnken

Source	**Sum of squares**	**df**	**Mean square**	**F-value**	**p-value Prob > F**	
Model	1.989E-3	5	3.978E-4	6.00	0.0012	significant
X_1-H_2O_2:Fe(II)	4.760E-5	1	4.760E-5	0.72	0.4057	
X_2-Fe(II)	2.067E-4	1	2.067E-4	3.12	0.0912	
X_4-pH	5.467E-4	1	5.467E-4	8.25	0.0088	
X_1X_4	4.906E-4	1	4.906E-4	7.41	0.0125	
X_4^2	6.972E-4	1	6.972E-4	10.52	0.0037	
Residual	1.452E-3	22	6.624E-5			
Lack of Fit	5.468E-6	19	7.642E-5	41.93	0.0052	significant
Pure Error	3.446E-3	3	1.823E-6			
Cor Total	8.148E-3	27				
Std. Dev.	8.139E-3		**R^2**	0.5771		
Mean	0.025		**Adj R^2**	0.4810		
C.V.%	32.07		**Pred R^2**	0.0567		
PRESS	3.251E-3		**Adeq Precis.**	9.462		

Table B.2.6 ANOVA test for H_2O_2 efficiency of RDX removal by Box-Behnken

Source	**Sum of squares**	**df**	**Mean square**	**F-value**	**p-value Prob > F**	
Model	2774.89	9	308.32	41.78	<0.0001	significant
X_1-H_2O_2:Fe(II)	116.79	1	116.79	15.83	0.0009	
X_2-Fe(II)	94.08	1	94.08	12.75	0.0022	
X_4-pH	21.01	1	21.01	2.85	0.1088	
X_1X_2	512.77	1	512.77	69.49	<0.0001	
X_1^2	256.83	1	256.83	34.81	<0.0001	
X_2^2	224.28	1	224.28	30.39	<0.0001	
X_4^2	38.42	1	38.42	5.21	0.0349	
$X_1^2X_2$	270.76	1	270.76	36.69	<0.0001	
$X_1X_2^2$	265.23	1	265.23	35.94	<0.0001	
Residual	132.83	18	7.38			
Lack of Fit	132.61	15	8.84	120.74	0.0011	significant
Pure Error	0.22	3	0.073			
Cor Total	2907.72	27				
Std. Dev.	2.72		**R^2**	0.9543		
Mean	5.35		**Adj R^2**	0.9315		
C.V.%	50.82		**Pred R^2**	-0.6225		
PRESS	4717.78		**Adeq Precis.**	33.664		

Table B.2.7 ANOVA test for H_2O_2 efficiency of HMX removal by Box-Behnken

Source	**Sum of squares**	**df**	**Mean square**	**F-value**	**p-value Prob > F**	
Model	5.06	9	0.56	32.82	<0.0001	significant
X_1-H_2O_2:Fe(II)	0.31	1	0.31	18.02	0.0005	
X_2-Fe(II)	0.12	1	0.12	6.79	0.0179	
X_4-pH	0.023	1	0.023	1.32	0.2659	
X_1X_2	0.88	1	0.88	51.44	<0.0001	
X_1^2	0.58	1	0.58	34.03	<0.0001	
X_2^2	0.31	1	0.31	18.37	0.0004	
X_4^2	0.067	1	0.067	3.92	0.0631	
$X_1^2X_2$	0.56	1	0.56	32.68	<0.0001	
$X_1X_2^2$	0.41	1	0.41	24.00	0.0001	
Residual	0.31	18	0.017			
Lack of Fit	0.31	15	0.021	146.93	0.0008	significant
Pure Error	4.191E-4	3	1.397E-4			
Cor Total	5.37	27				
Std. Dev.	0.13		**R^2**	0.9426		
Mean	0.24		**Adj R^2**	0.9138		
C.V.%	55.34		**Pred R^2**	-0.9270		
PRESS	10.34		**Adeq Precis.**	29.861		

Table B.2.8 Box-Behnken RDX run no.1 (6 May)

Time (min)	Area	RDX (ppm)	conc / $conc_0$	area / $area_0$	RDX (mM)	2nd order	H_2O_2 (mg/L)	H_2O_2 (mM)
0	729884	27.59	1.0000	1.0000	0.124191	8.05	561.17	16.50
1	659496	24.93	0.9037	0.9036	0.112233	8.91	525.82	15.46
5	653121	24.69	0.8950	0.8948	0.111150	9.00	520.36	15.30
10	652622	24.67	0.8943	0.8941	0.111066	9.00	508.55	14.95
30	638739	24.15	0.8753	0.8751	0.108707	9.20	454.91	13.38
60	629978	23.82	0.8633	0.8631	0.107219	9.33	376.73	11.08
90	619527	23.42	0.8490	0.8488	0.105443	9.48	303.09	8.91
120	587129	22.20	0.8047	0.8044	0.099939	10.01	233.09	6.85

Table B.2.9 Box-Behnken RDX run no.2 (6 May)

Time (min)	Area	RDX (ppm)	conc / $conc_0$	area / $area_0$	RDX (mM)	2nd order	H_2O_2 (mg/L)	H_2O_2 (mM)
0	738982	27.93	1.0000	1.0000	0.125737	7.95	308.64	9.08
1	618691	23.39	0.8375	0.8372	0.105301	9.50	283.09	8.32
5	537872	20.34	0.7283	0.7279	0.091571	10.92	242.18	7.12
10	421208	15.94	0.5706	0.5700	0.071751	13.94	194.91	5.73
30	136733	5.20	0.1863	0.1850	0.023422	42.69	65.82	1.94
60	13513	0.55	0.0198	0.0183	0.002488	401.85	14.00	0.41
90	9048	0.38	0.0138	0.0122	0.001730	578.06	11.27	0.33
120	7043	0.31	0.0110	0.0095	0.001389	719.79	10.36	0.30

Table B.2.10 Box-Behnken RDX run no.3 (13 May)

Time (min)	Area	RDX (ppm)	conc / $conc_0$	area / $area_0$	RDX (mM)	2nd order	H_2O_2 (mg/L)	H_2O_2 (mM)
0	990857	37.43	1.0000	1.0000	0.168528	5.93	56.12	1.65
1	929561	35.12	0.9382	0.9381	0.158114	6.32	51.05	1.50
5	883513	33.38	0.8918	0.8917	0.150291	6.65	45.24	1.33
10	838704	31.69	0.8466	0.8464	0.142679	7.01	39.42	1.16
30	596806	22.56	0.6028	0.6023	0.101583	9.84	20.51	0.60
60	367667	13.92	0.3718	0.3711	0.062655	15.96	4.51	0.13
90	219230	8.32	0.2221	0.2213	0.037437	26.71	0.87	0.03
120	130487	4.97	0.1327	0.1317	0.022361	44.72	0.15	0.00

Table B.2.11 Box-Behnken RDX run no.4 (10 May)

Time (min)	Area	RDX (ppm)	conc / $conc_0$	area / $area_0$	RDX (mM)	2nd order	H_2O_2 (mg/L)	H_2O_2 (mM)
0	984701	37.20	1.0000	1.0000	0.167482	5.97	56.12	1.65
1	740907	28.00	0.7527	0.7524	0.126064	7.93	34.69	1.02
5	597468	22.59	0.6072	0.6068	0.101695	9.83	28.51	0.84
10	472732	17.88	0.4807	0.4801	0.080504	12.42	18.69	0.55
30	248669	9.43	0.2534	0.2525	0.042439	23.56	4.51	0.13
60	200201	7.60	0.2042	0.2033	0.034205	29.24	1.60	0.05
90	139494	5.31	0.1426	0.1417	0.023891	41.86	1.24	0.04
120	97744	3.73	0.1003	0.0993	0.016798	59.53	1.96	0.06

Table B.2.12 Box-Behnken RDX run no.5 (10 May)

Time (min)	Area	RDX (ppm)	conc/conc$_0$	area/area$_0$	RDX (mM)	2nd order	H_2O_2 (mg/L)	H_2O_2 (mM)
0	979349	37.00	1.0000	1.0000	0.166573	6.00	561.17	16.50
1	846271	31.98	0.8643	0.8641	0.143964	6.95	500.36	14.71
5	768866	29.06	0.7853	0.7851	0.130814	7.64	454.91	13.38
10	663002	25.06	0.6774	0.6770	0.112829	8.86	407.64	11.99
30	349979	13.25	0.3581	0.3574	0.059650	16.76	229.45	6.75
60	48985	1.89	0.0511	0.0500	0.008515	117.44	36.73	1.08
90	7482	0.33	0.0088	0.0076	0.001464	683.12	6.73	0.20
120	7364	0.32	0.0087	0.0075	0.001444	692.60	3.09	0.09

Table B.2.13 Box-Behnken RDX run no.6 (13 May)

Time (min)	Area	RDX (ppm)	conc/conc$_0$	area/area$_0$	RDX (mM)	2nd order	H_2O_2 (mg/L)	H_2O_2 (mM)
0	1018705	38.48	1.0000	1.0000	0.173259	5.77	308.64	9.08
1	903953	34.15	0.8875	0.8874	0.153764	6.50	290.36	8.54
5	852168	32.20	0.8367	0.8365	0.144966	6.90	273.09	8.03
10	775747	29.32	0.7618	0.7615	0.131983	7.58	254.91	7.50
30	536202	20.28	0.5269	0.5264	0.091287	10.95	186.73	5.49
60	255551	9.69	0.2517	0.2509	0.043608	22.93	99.45	2.92
90	87341	3.34	0.0868	0.0857	0.015031	66.53	35.82	1.05
120	11955	0.49	0.0128	0.0117	0.002224	449.68	4.91	0.14

Table B.2.14 Box-Behnken RDX run no.7 (16 May)

Time (min)	Area	RDX (ppm)	conc/conc$_0$	area/area$_0$	RDX (mM)	2nd order	H_2O_2 (mg/L)	H_2O_2 (mM)
0	1021314	38.58	1.0000	1.0000	0.173702	5.76	56.12	1.65
1	923208	34.88	0.9040	0.9039	0.157035	6.37	48.51	1.43
5	848621	32.07	0.8311	0.8309	0.144363	6.93	44.15	1.30
10	731065	27.63	0.7161	0.7158	0.124392	8.04	39.05	1.15
30	448582	16.97	0.4398	0.4392	0.076402	13.09	19.42	0.57
60	224891	8.53	0.2211	0.2202	0.038399	26.04	5.60	0.16
90	104195	3.97	0.1030	0.1020	0.017894	55.88	0.51	0.01
120	46967	1.82	0.0470	0.0460	0.008172	122.37	0.51	0.01

Table B.2.15 Box-Behnken RDX run no.8 (16 May)

Time (min)	Area	RDX (ppm)	conc/conc$_0$	area/area$_0$	RDX (mM)	2nd order	H_2O_2 (mg/L)	H_2O_2 (mM)
0	1005739	37.99	1.0000	1.0000	0.171056	5.85	10.20	0.30
1	881165	33.29	0.8763	0.8761	0.149892	6.67	8.07	0.24
5	868530	32.82	0.8637	0.8636	0.147746	6.77	6.80	0.20
10	774397	29.26	0.7702	0.7700	0.131754	7.59	5.53	0.16
30	533013	20.16	0.5305	0.5300	0.090745	11.02	2.25	0.07
60	323932	12.27	0.3228	0.3221	0.055225	18.11	0.80	0.02
90	203205	7.71	0.2029	0.2020	0.034715	28.81	0.98	0.03
120	125148	4.77	0.1254	0.1244	0.021454	46.61	0.98	0.03

Table B.2.16 Box-Behnken RDX run no.9 (20 May)

Time (min)	Area	RDX (ppm)	conc / $conc_0$	area / $area_0$	RDX (mM)	2nd order	H_2O_2 (mg/L)	H_2O_2 (mM)
0	1007982	38.08	1.0000	1.0000	0.171437	5.83	561.17	16.50
1	933463	35.27	0.9262	0.9261	0.158777	6.30	532.18	15.65
5	872675	32.97	0.8659	0.8658	0.148450	6.74	505.82	14.87
10	801475	30.29	0.7954	0.7951	0.136354	7.33	474.00	13.94
30	559707	21.16	0.5558	0.5553	0.095280	10.50	337.64	9.93
60	223558	8.48	0.2227	0.2218	0.038173	26.20	154.91	4.55
90	32381	1.26	0.0332	0.0321	0.005694	175.63	24.91	0.73
120	4471	0.21	0.0056	0.0044	0.000952	1049.98	1.27	0.04

Table B.2.17 Box-Behnken RDX run no.10 (23 May)

Time (min)	Area	RDX (ppm)	conc / $conc_0$	area / $area_0$	RDX (mM)	2nd order	H_2O_2 (mg/L)	H_2O_2 (mM)
0	980508	37.04	1.0000	1.0000	0.166769	6.00	308.64	9.08
1	875001	33.06	0.8925	0.8924	0.148845	6.72	272.18	8.00
5	879108	33.22	0.8967	0.8966	0.149543	6.69	268.55	7.90
10	880768	33.28	0.8984	0.8983	0.149825	6.67	265.82	7.82
30	870094	32.88	0.8875	0.8874	0.148011	6.76	240.36	7.07
60	857394	32.40	0.8746	0.8744	0.145854	6.86	214.00	6.29
90	856491	32.36	0.8737	0.8735	0.145700	6.86	185.82	5.46
120	841406	31.79	0.8583	0.8581	0.143138	6.99	155.82	4.58

Table B.2.18 Box-Behnken RDX run no.11 (23 May)

Time (min)	Area	RDX (ppm)	conc / $conc_0$	area / $area_0$	RDX (mM)	2nd order	H_2O_2 (mg/L)	H_2O_2 (mM)
0	990379	37.41	1.0000	1.0000	0.168446	5.94	561.17	16.50
1	871798	32.94	0.8804	0.8803	0.148301	6.74	494.00	14.53
5	872096	32.95	0.8807	0.8806	0.148352	6.74	485.82	14.28
10	857486	32.40	0.8660	0.8658	0.145869	6.86	471.27	13.86
30	854009	32.27	0.8625	0.8623	0.145279	6.88	427.64	12.57
60	850078	32.12	0.8585	0.8583	0.144611	6.92	354.91	10.44
90	840917	31.77	0.8493	0.8491	0.143055	6.99	279.45	8.22
120	824220	31.14	0.8324	0.8322	0.140218	7.13	209.45	6.16

Table B.2.19 Box-Behnken RDX run no.12 (20 May)

Time (min)	Area	RDX (ppm)	conc / $conc_0$	area / $area_0$	RDX (mM)	2nd order	Fe^{2+} (mg/L)	Fe^{2+} (mM)
0	1019812	38.53	1.0000	1.0000	0.173447	5.77	31.50	0.56
1	891529	33.68	0.8743	0.8742	0.151653	6.59	1.25	0.02
5	782416	29.57	0.7675	0.7672	0.133116	7.51	1.75	0.03
10	642267	24.28	0.6302	0.6298	0.109306	9.15	2.25	0.04
30	262495	9.95	0.2582	0.2574	0.044788	22.33	2.25	0.04
60	29324	1.15	0.0298	0.0288	0.005175	193.25	3.25	0.06
90	15908	0.64	0.0167	0.0156	0.002895	345.38	19.25	0.34
120	11618	0.48	0.0125	0.0114	0.002167	461.57	25.50	0.46

Table B.2.20 Box-Behnken RDX run no.13 (28 May)

Time (min)	Area	RDX (ppm)	conc / $conc_0$	area / $area_0$	RDX (mM)	2nd order	H_2O_2 (mg/L)	H_2O_2 (mM)
0	1017142	38.42	1.0000	1.0000	0.172993	5.78	561.17	16.50
1	918358	34.70	0.9030	0.9029	0.156211	6.40	515.82	15.17
5	816338	30.85	0.8028	0.8026	0.138879	7.20	468.55	13.78
10	716803	27.09	0.7051	0.7047	0.121969	8.20	411.27	12.09
30	437328	16.55	0.4306	0.4300	0.074490	13.42	229.45	6.75
60	177461	6.74	0.1754	0.1745	0.030341	32.96	68.55	2.02
90	39506	1.53	0.0399	0.0388	0.006904	144.84	14.00	0.41
120	6440	0.29	0.0074	0.0063	0.001287	777.09	2.18	0.06

Table B.2.21 Box-Behnken RDX run no.14 (28 May)

Time (min)	Area	RDX (ppm)	conc / $conc_0$	area / $area_0$	RDX (mM)	2nd order	H_2O_2 (mg/L)	H_2O_2 (mM)
0	1019805	38.53	1.0000	1.0000	0.173446	5.77	1,020.30	30.00
1	923710	34.90	0.9059	0.9058	0.157120	6.36	933.09	27.44
5	845439	31.95	0.8292	0.8290	0.143823	6.95	857.64	25.22
10	714683	27.01	0.7011	0.7008	0.121609	8.22	760.36	22.36
30	334651	12.67	0.3289	0.3282	0.057046	17.53	393.09	11.56
60	28266	1.11	0.0288	0.0277	0.004995	200.21	46.73	1.37
90	1903	0.11	0.0030	0.0019	0.000516	1,937.97	4.91	0.14
120	1360	0.09	0.0024	0.0013	0.000424	2,359.15	2.18	0.06

Table B.2.22 Box-Behnken RDX run no.15 (28 May)

Time (min)	Area	RDX (ppm)	conc / $conc_0$	area / $area_0$	RDX (mM)	2nd order	H_2O_2 (mg/L)	H_2O_2 (mM)
0	1144697	43.24	1.0000	1.0000	0.194663	5.14	308.64	9.08
1	983306	37.15	0.8591	0.8590	0.167245	5.98		
5	853010	32.23	0.7454	0.7452	0.145109	6.89		
10	702516	26.55	0.6141	0.6137	0.119542	8.37		
30	258490	9.80	0.2266	0.2258	0.044107	22.67		
60	28976	1.14	0.0263	0.0253	0.005115	195.49		
90	20492	0.82	0.0189	0.0179	0.003674	272.17		
120	13100	0.54	0.0124	0.0114	0.002418	413.51	0.36	0.01

Table B.2.23 Box-Behnken RDX run no.16 (30 May)

Time (min)	Area	RDX (ppm)	conc / $conc_0$	area / $area_0$	RDX (mM)	2nd order	H_2O_2 (mg/L)	H_2O_2 (mM)
0	999978	37.78	1.0000	1.0000	0.170077	5.88	561.17	16.50
1	890753	33.66	0.8909	0.8908	0.151521	6.60	519.45	15.27
5	822934	31.10	0.8232	0.8230	0.139999	7.14	489.45	14.39
10	722390	27.30	0.7227	0.7224	0.122918	8.14	450.36	13.24
30	433400	16.40	0.4341	0.4334	0.073822	13.55	302.18	8.89
60	114193	4.35	0.1152	0.1142	0.019593	51.04	110.36	3.25
90	9428	0.40	0.0106	0.0094	0.001794	557.26	12.18	0.36
120	1502	0.10	0.0026	0.0015	0.000448	2,232.58	3.09	0.09

Table B.2.24 Box-Behnken RDX run no.17 (30 May)

Time (min)	Area	RDX (ppm)	conc/conc$_0$	area/area$_0$	RDX (mM)	2nd order	H_2O_2 (mg/L)	H_2O_2 (mM)
0	998240	37.71	1.0000	1.0000	0.169782	5.89	561.17	16.50
1	928878	35.09	0.9306	0.9305	0.157998	6.33	536.73	15.78
5	843655	31.88	0.8453	0.8451	0.143520	6.97	517.64	15.22
10	798749	30.18	0.8004	0.8002	0.135891	7.36	485.82	14.28
30	515623	19.50	0.5171	0.5165	0.087791	11.39	384.00	11.29
60	222779	8.45	0.2241	0.2232	0.038040	26.29	240.36	7.07
90	76530	2.93	0.0777	0.0767	0.013194	75.79	120.36	3.54
120	13144	0.54	0.0143	0.0132	0.002426	412.24	34.91	1.03

Table B.2.25 Box-Behnken RDX run no.18 (19 Jun)

Time (min)	Area	RDX (ppm)	conc/conc$_0$	area/area$_0$	RDX (mM)	2nd order	H_2O_2 (mg/L)	H_2O_2 (mM)
0	1018554	38.48	1.0000	1.0000	0.173233	5.77	308.64	9.08
1	889037	33.59	0.8730	0.8728	0.151230	6.61	278.55	8.19
5	773732	29.24	0.7599	0.7596	0.131641	7.60	240.36	7.07
10	640707	24.22	0.6294	0.6290	0.109041	9.17	203.09	5.97
30	262805	9.96	0.2588	0.2580	0.044840	22.30	84.91	2.50
60	26356	1.04	0.0270	0.0259	0.004670	214.12	4.91	0.14
90	6524	0.29	0.0075	0.0064	0.001301	768.57	1.27	0.04
120	3988	0.19	0.0050	0.0039	0.000870	1,149.04	0.02	0.00

Table B.2.26 Box-Behnken RDX run no.19 (3 Jun)

Time (min)	Area	RDX (ppm)	conc/conc$_0$	area/area$_0$	RDX (mM)	2nd order	H_2O_2 (mg/L)	H_2O_2 (mM)
0	971472	36.70	1.0000	1.0000	0.165234	6.05	102.03	3.00
1	850830	32.15	0.8760	0.8758	0.144739	6.91	92.51	2.72
5	875293	33.07	0.9011	0.9010	0.148895	6.72	87.05	2.56
10	829739	31.35	0.8543	0.8541	0.141156	7.08	81.24	2.39
30	573714	21.69	0.5910	0.5906	0.097660	10.24	55.05	1.62
60	351492	13.31	0.3626	0.3618	0.059907	16.69	21.24	0.62
90	205771	7.81	0.2127	0.2118	0.035151	28.45	4.51	0.13
120	121291	4.62	0.1259	0.1249	0.020799	48.08	2.69	0.08

Table B.2.27 Box-Behnken RDX run no.20 (4 Jun)

Time (min)	Area	RDX (ppm)	conc/conc$_0$	area/area$_0$	RDX (mM)	2nd order	H_2O_2 (mg/L)	H_2O_2 (mM)
0	976438	36.89	1.0000	1.0000	0.166078	6.02	56.12	1.65
1	719461	27.19	0.7371	0.7368	0.122421	8.17	37.60	1.11
5	588948	22.27	0.6036	0.6032	0.100248	9.98	27.42	0.81
10	445267	16.84	0.4566	0.4560	0.075838	13.19	18.69	0.55
30	188293	7.15	0.1938	0.1928	0.032182	31.07	4.51	0.13
60	102167	3.90	0.1057	0.1046	0.017550	56.98	1.60	0.05
90	51221	1.98	0.0536	0.0525	0.008895	112.43	0.87	0.03
120	23633	0.93	0.0253	0.0242	0.004208	237.66	0.87	0.03

Table B.2.28 Box-Behnken RDX run no.21 (4 Jun)

Time (min)	Area	RDX (ppm)	conc / $conc_0$	area / $area_0$	RDX (mM)	2nd order	H_2O_2 (mg/L)	H_2O_2 (mM)
0	977879	36.94	1.0000	1.0000	0.166323	6.01	561.17	16.50
1	827291	31.26	0.8462	0.8460	0.140740	7.11	480.36	14.12
5	687799	26.00	0.7037	0.7034	0.117042	8.54	408.55	12.01
10	530246	20.05	0.5428	0.5422	0.090275	11.08	318.55	9.37
30	122889	4.68	0.1267	0.1257	0.021070	47.46	75.82	2.23
60	9310	0.39	0.0107	0.0095	0.001774	563.56	5.82	0.17
90	6951	0.31	0.0083	0.0071	0.001374	727.98	3.09	0.09
120	5177	0.24	0.0064	0.0053	0.001072	932.59	3.09	0.09

Table B.2.29 Box-Behnken RDX run no.22 (15 Jun)

Time (min)	Area	RDX (ppm)	conc / $conc_0$	area / $area_0$	RDX (mM)	2nd order	H_2O_2 (mg/L)	H_2O_2 (mM)
0	1005365	37.98	1.0000	1.0000	0.170992	5.85	56.12	1.65
1	934854	35.32	0.9299	0.9299	0.159013	6.29	49.24	1.45
5	896135	33.86	0.8915	0.8914	0.152435	6.56	45.24	1.33
10	798766	30.18	0.7947	0.7945	0.135894	7.36	40.51	1.19
30	586227	22.16	0.5836	0.5831	0.099786	10.02	26.33	0.77
60	351784	13.32	0.3506	0.3499	0.059957	16.68	10.69	0.31
90	209701	7.96	0.2095	0.2086	0.035818	27.92	3.42	0.10
120	123873	4.72	0.1242	0.1232	0.021237	47.09	0.87	0.03

Table B.2.30 Box-Behnken RDX run no.23 (19 Jun)

Time (min)	Area	RDX (ppm)	conc / $conc_0$	area / $area_0$	RDX (mM)	2nd order	H_2O_2 (mg/L)	H_2O_2 (mM)
0	1043760	39.43	1.0000	1.0000	0.177515	5.63	308.64	9.08
1	899202	33.97	0.8617	0.8615	0.152957	6.54	267.64	7.87
5	887957	33.55	0.8509	0.8507	0.151046	6.62	259.45	7.63
10	884367	33.41	0.8475	0.8473	0.150436	6.65	244.00	7.17
30	897329	33.90	0.8599	0.8597	0.152638	6.55	183.09	5.38
60	877012	33.14	0.8404	0.8402	0.149187	6.70	105.82	3.11
90	863815	32.64	0.8278	0.8276	0.146945	6.81	33.09	0.97
120	828321	31.30	0.7938	0.7936	0.140915	7.10	5.82	0.17

Table B.2.31 Box-Behnken RDX run no.24 (12 Jun)

Time (min)	Area	RDX (ppm)	conc / $conc_0$	area / $area_0$	RDX (mM)	2nd order	H_2O_2 (mg/L)	H_2O_2 (mM)
0	1010764	38.18	1.0000	1.0000	0.171910	5.82	308.64	9.08
1	897489	33.91	0.8881	0.8879	0.152666	6.55	282.18	8.30
5	792720	29.96	0.7845	0.7843	0.134866	7.41	261.27	7.68
10	702082	26.54	0.6949	0.6946	0.119468	8.37	233.09	6.85
30	388655	14.71	0.3852	0.3845	0.066221	15.10	136.73	4.02
60	106142	4.05	0.1060	0.1050	0.018225	54.87	33.09	0.97
90	12248	0.50	0.0132	0.0121	0.002274	439.84	2.18	0.06
120	5988	0.27	0.0070	0.0059	0.001210	826.40	0.02	0.00

Table B.2.32 Box-Behnken RDX run no.25 (17 Jun)

Time (min)	Area	RDX (ppm)	conc/conc$_0$	area/area$_0$	RDX (mM)	2nd order	H_2O_2 (mg/L)	H_2O_2 (mM)
0	986685	37.28	1.0000	1.0000	0.167819	5.96	56.12	1.65
1	761419	28.77	0.7720	0.7717	0.129549	7.72	36.87	1.08
5	767983	29.02	0.7786	0.7783	0.130664	7.65	32.51	0.96
10	766568	28.97	0.7772	0.7769	0.130424	7.67	25.96	0.76
30	740037	27.97	0.7503	0.7500	0.125916	7.94	9.96	0.29
60	706432	26.70	0.7163	0.7160	0.120207	8.32	4.87	0.14
90	624433	23.61	0.6333	0.6329	0.106277	9.41	4.15	0.12
120	560560	21.20	0.5686	0.5681	0.095425	10.48	4.15	0.12

Table B.2.33 Box-Behnken RDX run no.26 (15 Jun)

Time (min)	Area	RDX (ppm)	conc/conc$_0$	area/area$_0$	RDX (mM)	2nd order	H_2O_2 (mg/L)	H_2O_2 (mM)
0	994128	37.56	1.0000	1.0000	0.169083	5.91	102.03	3.00
1	696805	26.34	0.7013	0.7009	0.118572	8.43	67.05	1.97
5	488170	18.46	0.4916	0.4911	0.083127	12.03	46.33	1.36
10	317835	12.04	0.3205	0.3197	0.054189	18.45	28.87	0.85
30	112040	4.27	0.1137	0.1127	0.019227	52.01	6.69	0.20
60	76964	2.95	0.0785	0.0774	0.013268	75.37	2.33	0.07
90	47691	1.84	0.0491	0.0480	0.008295	120.56	1.24	0.04
120	30997	1.21	0.0323	0.0312	0.005459	183.19	1.24	0.04

Table B.2.34 Box-Behnken RDX run no.27 (15 Jun)

Time (min)	Area	RDX (ppm)	conc/conc$_0$	area/area$_0$	RDX (mM)	2nd order	H_2O_2 (mg/L)	H_2O_2 (mM)
0	989362	37.38	1.0000	1.0000	0.168274	5.94	56.12	1.65
1	762131	28.80	0.7706	0.7703	0.129670	7.71	37.60	1.11
5	640998	24.23	0.6483	0.6479	0.109091	9.17	31.42	0.92
10	503463	19.04	0.5094	0.5089	0.085725	11.67	23.42	0.69
30	204902	7.77	0.2080	0.2071	0.035003	28.57	5.24	0.15
60	116725	4.45	0.1190	0.1180	0.020023	49.94	1.96	0.06
90	78695	3.01	0.0806	0.0795	0.013562	73.73	1.24	0.04
120	50899	1.96	0.0525	0.0514	0.008840	113.12	0.87	0.03

Table B.2.35 Box-Behnken RDX run no.28 (17 Jun)

Time (min)	Area	RDX (ppm)	conc/conc$_0$	area/area$_0$	RDX (mM)	2nd order	H_2O_2 (mg/L)	H_2O_2 (mM)
0	981133	37.07	1.0000	1.0000	0.166876	5.99	56.12	1.65
1	904774	34.18	0.9223	0.9222	0.153903	6.50	44.87	1.32
5	890554	33.65	0.9078	0.9077	0.151487	6.60	37.96	1.12
10	896525	33.87	0.9139	0.9138	0.152502	6.56	31.05	0.91
30	887658	33.54	0.9048	0.9047	0.150995	6.62	6.69	0.20
60	882836	33.36	0.8999	0.8998	0.150176	6.66	1.24	0.04
90	801538	30.29	0.8172	0.8170	0.136365	7.33	0.87	0.03
120	737669	27.88	0.7521	0.7519	0.125514	7.97	0.51	0.01

Table B.2.36 Box-Behnken HMX run no.1 (13 Mar)

Time (min)	Area	HMX (mg/L)	conc/conc	area/area	HMX (mM)	2nd order	H_2O_2 (mg/L)	H_2O_2 (mM)
0	50222	1.52	1	1.0000	0.0051	194.97	561.17	16.50
1	47081	1.42	0.937942	0.9375	0.0048	207.87	529.45	15.57
5	47339	1.43	0.943040	0.9426	0.0048	206.75	514.00	15.11
10	46273	1.40	0.921978	0.9214	0.0047	211.47	492.18	14.47
30	42734	1.29	0.852057	0.8509	0.0044	228.83	422.18	12.41
60	40309	1.22	0.804146	0.8026	0.0041	242.46	328.55	9.66
90	37785	1.15	0.754278	0.7524	0.0039	258.49	246.73	7.25
120	35354	1.07	0.706248	0.7040	0.0036	276.07	164.91	4.85

Table B.2.37 Box-Behnken HMX run no.2 (20 Feb)

Time (min)	Area	HMX (mg/L)	conc/conc	area/area	HMX (mM)	2nd order	H_2O_2 (mg/L)	H_2O_2 (mM)
0	85897	2.59	1.0000	1.0000	0.0087	114.36	308.64	9.08
1	77134	2.33	0.8984	0.8980	0.0079	127.29	264.00	7.76
5	65987	1.99	0.7693	0.7682	0.0067	148.67	214.91	6.32
10	52606	1.59	0.6142	0.6124	0.0054	186.20	154.91	4.55
30	15211	0.47	0.1808	0.1771	0.0016	632.46	25.82	0.76
60	2656	0.09	0.0353	0.0309	0.0003	3,238.00	1.27	0.04
90	1914	0.07	0.0267	0.0223	0.0002	4,279.65	0.06	0.00
120	1346	0.05	0.0201	0.0157	0.0002	5,677.23	0.05	0.00

Table B.2.38 Box-Behnken HMX run no.3 (29 Mar)

Time (min)	Area	HMX (mg/L)	conc/conc	area/area	HMX (mM)	2nd order	H_2O_2 (mg/L)	H_2O_2 (mM)
0	73871	2.23	1	1.0000	0.0075	132.88	56.12	1.65
1	67304	2.03	0.911571	0.9111	0.0069	145.78	49.96	1.47
5	63085	1.90	0.854760	0.8540	0.0064	155.46	45.24	1.33
10	59796	1.81	0.810471	0.8095	0.0061	163.96	38.33	1.13
30	42850	1.30	0.582283	0.5801	0.0044	228.21	16.51	0.49
60	21654	0.66	0.296866	0.2931	0.0022	447.63	2.69	0.08
90	15114	0.47	0.208801	0.2046	0.0016	636.42	0.51	0.01
120	12578	0.39	0.174652	0.1703	0.0013	760.85	0.01	0.00

Table B.2.39 Box-Behnken HMX run no.4 (26 Mar)

Time (min)	Area	HMX (mg/L)	conc/conc	area/area	HMX (mM)	2nd order	H_2O_2 (mg/L)	H_2O_2 (mM)
0	79392	2.39	1	1.0000	0.0081	123.69	56.12	1.65
1	60359	1.82	0.761444	0.7603	0.0062	162.44	33.60	0.99
5	44075	1.33	0.557343	0.5552	0.0045	221.93	20.15	0.59
10	30477	0.93	0.386909	0.3839	0.0031	319.69	11.42	0.34
30	12837	0.40	0.165812	0.1617	0.0013	745.96	1.60	0.05
60	12158	0.38	0.157302	0.1531	0.0013	786.32	0.15	0.00
90	11876	0.37	0.153765	0.1496	0.0012	804.40	0.51	0.01
120	10657	0.33	0.138489	0.1342	0.0011	893.14	0.00	0.00

Table B.2.40 Box-Behnken HMX run no.5 (6 Mar)

Time (min)	Area	HMX (mg/L)	conc/conc	area/area	HMX (mM)	2nd order	H_2O_2 (mg/L)	H_2O_2 (mM)
0	53454	1.62	1	1.0000	0.0055	183.27	561.17	16.50
1	48238	1.46	0.903132	0.9024	0.0049	202.93	491.27	14.44
5	42855	1.30	0.803162	0.8017	0.0044	228.19	416.73	12.25
10	36661	1.11	0.688130	0.6858	0.0038	266.33	345.82	10.17
30	12730	0.39	0.243698	0.2381	0.0013	752.04	99.45	2.92
60	868	0.04	0.023394	0.0162	0.0001	7,833.97	0.00	0.00
90	487	0.03	0.016333	0.0091	0.0001	11,221.18	0.00	0.00
120	408	0.02	0.014853	0.0076	0.0001	12,338.67	0.00	0.00

Table B.2.41 Box-Behnken HMX run no.6 (20 Feb)

Time (min)	Area	HMX (mg/L)	conc/conc	area/area	HMX (mM)	2nd order	H_2O_2 (mg/L)	H_2O_2 (mM)
0	88351	2.66	1.0000	1.0000	0.0090	111.20	308.64	9.08
1	79054	2.38	0.8952	0.8948	0.0081	124.22	287.64	8.46
5	76357	2.30	0.8648	0.8642	0.0078	128.58	268.55	7.90
10	72675	2.19	0.8234	0.8226	0.0074	135.06	244.00	7.17
30	72871	2.20	0.8256	0.8248	0.0074	134.70	154.00	4.53
60	21589	0.66	0.2477	0.2444	0.0022	448.95	46.73	1.37
90	7294	0.23	0.0866	0.0826	0.0008	1,283.92	4.00	0.12
120	6108	0.20	0.0732	0.0691	0.0007	1,518.17	0.36	0.01

Table B.2.42 Box-Behnken HMX run no.7 (18 Mar)

Time (min)	Area	HMX (mg/L)	conc/conc	area/area	HMX (mM)	2nd order	H_2O_2 (mg/L)	H_2O_2 (mM)
0	64534	1.95	1	1.0000	0.0066	151.99	56.12	1.65
1	58088	1.76	0.900718	0.9001	0.0059	168.75	46.33	1.36
5	52158	1.58	0.809384	0.8082	0.0053	187.79	35.78	1.05
10	45126	1.37	0.701076	0.6993	0.0046	216.80	25.96	0.76
30	22170	0.68	0.347505	0.3435	0.0023	437.39	3.78	0.11
60	8325	0.26	0.134263	0.1290	0.0009	1,132.07	1.24	0.04
90	3619	0.12	0.061779	0.0561	0.0004	2,460.31	0.51	0.01
120	2224	0.08	0.040289	0.0345	0.0003	3,772.63	0.01	0.00

Table B.2.43 Box-Behnken HMX run no.8 (27 Feb)

Time (min)	Area	HMX (mg/L)	conc/conc	area/area	HMX (mM)	2nd order	H_2O_2 (mg/L)	H_2O_2 (mM)
0	74529	2.25	1	1.0000	0.0076	131.72	10.20	0.30
1	65389	1.97	0.878005	0.8774	0.0067	150.02	5.96	0.18
5	54187	1.64	0.728488	0.7271	0.0055	180.81	4.87	0.14
10	44984	1.36	0.605652	0.6036	0.0046	217.48	3.42	0.10
30	25992	0.79	0.352159	0.3488	0.0027	374.03	0.87	0.03
60	13630	0.42	0.187159	0.1829	0.0014	703.77	0.51	0.01
90	7857	0.25	0.110105	0.1054	0.0008	1,196.29	0.15	0.00
120	4548	0.15	0.065938	0.0610	0.0005	1,997.60	0.00	0.00

Table B.2.44 Box-Behnken HMX run no.9 (25 Mar)

Time (min)	Area	HMX (mg/L)	conc/conc	area/area	HMX (mM)	2nd order	H_2O_2 (mg/L)	H_2O_2 (mM)
0	68185	2.06	1	1.0000	0.0069	143.90	561.17	16.50
1	65679	1.98	0.963457	0.9632	0.0067	149.36	508.55	14.95
5	58440	1.77	0.857897	0.8571	0.0060	167.74	474.00	13.94
10	53024	1.60	0.778921	0.7776	0.0054	184.75	417.64	12.28
30	29247	0.89	0.432202	0.4289	0.0030	332.95	191.27	5.62
60	3371	0.11	0.054869	0.0494	0.0004	2,622.67	14.91	0.44
90	1209	0.05	0.023354	0.0177	0.0002	6,161.81	1.27	0.04
120	900	0.04	0.018845	0.0132	0.0001	7,636.05	0.02	0.00

Table B.2.45 Box-Behnken HMX run no.10 (26 Feb)

Time (min)	Area	HMX (mg/L)	conc/conc	area/area	HMX (mM)	2nd order	H_2O_2 (mg/L)	H_2O_2 (mM)
0	69005	2.08	1	1.0000	0.0070	142.20	308.64	9.08
1	63279	1.91	0.917489	0.9170	0.0065	154.99	277.64	8.16
5	60403	1.82	0.876047	0.8753	0.0062	162.32	257.64	7.58
10	59211	1.79	0.858870	0.8581	0.0060	165.57	240.36	7.07
30	46461	1.41	0.675145	0.6733	0.0047	210.62	174.91	5.14
60	32613	0.99	0.475598	0.4726	0.0033	299.00	99.45	2.92
90	20152	0.62	0.296038	0.2920	0.0021	480.35	48.55	1.43
120	9731	0.30	0.145873	0.1410	0.0010	974.83	19.45	0.57

Table B.2.46 Box-Behnken HMX run no.11 (28 Mar)

Time (min)	Area	HMX (mg/L)	conc/conc	area/area	HMX (mM)	2nd order	H_2O_2 (mg/L)	H_2O_2 (mM)
0	66924	2.02	1	1.0000	0.0068	146.60	561.17	16.50
1	59721	1.80	0.892998	0.8924	0.0061	164.16	481.27	14.15
5	60260	1.82	0.901005	0.9004	0.0061	162.71	470.36	13.83
10	59284	1.79	0.886506	0.8858	0.0060	165.37	456.73	13.43
30	59388	1.79	0.888051	0.8874	0.0061	165.08	397.64	11.69
60	58043	1.75	0.868070	0.8673	0.0059	168.88	330.36	9.71
90	56834	1.72	0.850110	0.8492	0.0058	172.45	100.87	2.97
120	53965	1.63	0.807491	0.8064	0.0055	181.55	70.33	2.07

Table B.2.47 Box-Behnken HMX run no.12 (21 Mar)

Time (min)	Area	HMX (mg/L)	conc/conc	area/area	HMX (mM)	2nd order	H_2O_2 (mg/L)	H_2O_2 (mM)
0	77110	2.33	1	1.0000	0.0079	127.33	308.64	9.08
1	68476	2.07	0.888597	0.8880	0.0070	143.29	268.87	7.91
5	58254	1.76	0.756704	0.7555	0.0059	168.27	219.78	6.46
10	45288	1.37	0.589405	0.5873	0.0046	216.03	159.42	4.69
30	10675	0.33	0.142798	0.1384	0.0011	891.68	22.69	0.67
60	2415	0.08	0.036214	0.0313	0.0003	3,516.03	2.33	0.07
90	1947	0.07	0.030176	0.0252	0.0002	4,219.63	0.87	0.03
120	1955	0.07	0.030280	0.0253	0.0002	4,205.06	0.51	0.01

Table B.2.48 Box-Behnken HMX run no.13 (26 Mar)

Time (min)	Area	HMX (mg/L)	conc/conc	area/area	HMX (mM)	2nd order	H_2O_2 (mg/L)	H_2O_2 (mM)
0	78191	2.36	1	1.0000	0.0080	125.58	561.17	16.50
1	72419	2.19	0.926549	0.9262	0.0074	135.53	664.00	19.52
5	66866	2.02	0.855885	0.8552	0.0068	146.72	588.55	17.31
10	59566	1.80	0.762990	0.7618	0.0061	164.59	499.45	14.69
30	33475	1.02	0.430973	0.4281	0.0034	291.39	206.73	6.08
60	6299	0.20	0.085148	0.0806	0.0007	1,474.84	14.00	0.41
90	2144	0.08	0.032279	0.0274	0.0003	3,890.42	1.60	0.05
120	1859	0.07	0.028650	0.0238	0.0002	4,383.25	1.60	0.05

Table B.2.49 Box-Behnken HMX run no.14 (18 Feb)

Time (min)	Area	HMX (mg/L)	conc/conc	area/area	HMX (mM)	2nd order	H_2O_2 (mg/L)	H_2O_2 (mM)
0	86419	2.61	1.0000	1.0000	0.0088	113.68	1,020.30	30.00
1	78789	2.38	0.9121	0.9117	0.0080	124.63	931.27	27.38
5	73579	2.22	0.8521	0.8514	0.0075	133.41	849.45	24.98
10	68602	2.07	0.7948	0.7938	0.0070	143.03	753.09	22.14
30	47172	1.43	0.5479	0.5459	0.0048	207.48	449.45	13.22
60	19478	0.60	0.2289	0.2254	0.0020	496.65	129.45	3.81
90	1268	0.05	0.0191	0.0147	0.0002	5,945.21	1.27	0.04
120	921	0.04	0.0151	0.0107	0.0001	7,513.96	0.09	0.00

Table B.2.50 Box-Behnken HMX run no.15 (23 Mar)

Time (min)	Area	HMX (mg/L)	conc/conc	area/area	HMX (mM)	2nd order	Fe^{2+} (mg/L)	Fe^{2+} (mM)
0	92470	2.79	1	1.0000	0.0094	106.27	31.30	0.56
1	83279	2.51	0.901025	0.9006	0.0085	117.94	0.70	0.01
5	69671	2.10	0.754486	0.7534	0.0071	140.85	0.70	0.01
10	55106	1.67	0.59764	0.5959	0.0056	177.82	0.80	0.01
30	14894	0.46	0.164612	0.1611	0.0015	645.58	1.20	0.02
60	2865	0.10	0.035073	0.0310	0.0003	3,029.92	10.00	0.18
90	2499	0.09	0.031129	0.0270	0.0003	3,413.80	20.50	0.37
120	2010	0.07	0.025872	0.0217	0.0002	4,107.49	23.40	0.42

Table B.2.51 Box-Behnken HMX run no.16 (29 Mar)

Time (min)	Area	HMX (mg/L)	conc/conc	area/area	HMX (mM)	2nd order	H_2O_2 (mg/L)	H_2O_2 (mM)
0	72585	2.19	1	1.0000	0.0074	135.23	561.17	16.50
1	66321	2.00	0.914165	0.9137	0.0068	147.92	509.45	14.98
5	60563	1.83	0.835264	0.8344	0.0062	161.90	463.09	13.62
10	53966	1.63	0.744866	0.7435	0.0055	181.54	404.91	11.91
30	27813	0.85	0.386493	0.3832	0.0029	349.88	186.73	5.49
60	2779	0.10	0.043449	0.0383	0.0003	3,112.29	17.64	0.52
90	1370	0.05	0.024153	0.0189	0.0002	5,598.80	3.78	0.11
120	493	0.03	0.012127	0.0068	0.0001	11,150.81	1.24	0.04

Table B.2.52 Box-Behnken HMX run no.17 (11 Mar)

Time (min)	Area	HMX (mg/L)	conc/conc	area/area	HMX (mM)	2nd order	H_2O_2 (mg/L)	H_2O_2 (mM)
0	72794	2.20	1	1.0000	0.0074	134.84	561.17	16.50
1	65077	1.96	0.894557	0.8940	0.0066	150.73	542.18	15.94
5	59988	1.81	0.825022	0.8241	0.0061	163.44	521.27	15.33
10	58295	1.76	0.801889	0.8008	0.0059	168.15	476.73	14.02
30	38344	1.16	0.529283	0.5267	0.0039	254.76	332.18	9.77
60	22420	0.68	0.311701	0.3080	0.0023	432.59	142.18	4.18
90	7180	0.23	0.103465	0.0986	0.0008	1,303.25	33.09	0.97
120	1231	0.05	0.022181	0.0169	0.0002	6,079.07	3.09	0.09

Table B.2.53 Box-Behnken HMX run no.18 (25 Mar)

Time (min)	Area	HMX (mg/L)	conc/conc	area/area	HMX (mM)	2nd order	H_2O_2 (mg/L)	H_2O_2 (mM)
0	68499	2.07	1	1.0000	0.0070	143.25	308.64	9.08
1	61221	1.85	0.894355	0.8938	0.0062	160.17	272.15	8.00
5	51382	1.55	0.751536	0.7501	0.0052	190.61	217.96	6.41
10	38932	1.18	0.570816	0.5684	0.0040	250.95	156.87	4.61
30	8949	0.28	0.135593	0.1306	0.0009	1,056.44	22.69	0.67
60	1929	0.07	0.033698	0.0282	0.0002	4,250.89	1.60	0.05
90	1607	0.06	0.029017	0.0235	0.0002	4,936.69	0.15	0.00
120	1641	0.06	0.029518	0.0240	0.0002	4,852.82	0.00	0.00

Table B.2.54 Box-Behnken HMX run no.19 (27 Feb)

Time (min)	Area	HMX (mg/L)	conc/conc	area/area	HMX (mM)	2nd order	H_2O_2 (mg/L)	H_2O_2 (mM)
0	77172	2.33	1	1.0000	0.0079	127.23	102.03	3.00
1	71866	2.17	0.931592	0.9312	0.0073	136.57	92.18	2.71
5	67554	2.04	0.875999	0.8754	0.0069	145.24	81.27	2.39
10	61008	1.84	0.791605	0.7905	0.0062	160.72	68.55	2.02
30	39072	1.18	0.508794	0.5063	0.0040	250.06	31.27	0.92
60	16201	0.50	0.213929	0.2099	0.0017	594.73	5.82	0.17
90	5864	0.19	0.080658	0.0760	0.0006	1,577.39	0.36	0.01
120	3939	0.13	0.055844	0.0510	0.0004	2,278.30	0.09	0.00

Table B.2.55 Box-Behnken HMX run no.20 (23 Mar)

Time (min)	Area	HMX (mg/L)	conc/conc	area/area	HMX (mM)	2nd order	H_2O_2 (mg/L)	H_2O_2 (mM)
0	90119	2.72	1	1.0000	0.0092	109.03	56.12	1.65
1	69956	2.11	0.777232	0.7763	0.0071	140.28	29.60	0.87
5	47172	1.43	0.525506	0.5234	0.0048	207.48	15.78	0.46
10	28919	0.88	0.323841	0.3209	0.0030	336.68	7.42	0.22
30	11133	0.35	0.127334	0.1235	0.0012	856.25	3.05	0.09
60	7143	0.23	0.083252	0.0793	0.0008	1,309.65	1.24	0.04
90	4371	0.14	0.052622	0.0485	0.0005	2,071.94	0.87	0.03
120	1944	0.07	0.025807	0.0216	0.0002	4,224.87	0.51	0.01

Table B.2.56 Box-Behnken HMX run no.21 (11 Mar)

Time (min)	Area	HMX (mg/L)	conc/conc	area/area	HMX (mM)	2nd order	H_2O_2 (mg/L)	H_2O_2 (mM)
0	71778	2.17	1	1.0000	0.0073	136.74	561.17	16.50
1	63827	1.93	0.88983	0.8892	0.0065	153.67	501.27	14.74
5	52174	1.58	0.728364	0.7269	0.0053	187.73	394.91	11.61
10	38767	1.18	0.542595	0.5401	0.0040	252.01	275.82	8.11
30	5916	0.19	0.087407	0.0824	0.0006	1,564.38	25.82	0.76
60	2473	0.09	0.039703	0.0345	0.0003	3,444.00	4.91	0.14
90	2889	0.10	0.045462	0.0402	0.0003	3,007.75	0.36	0.01
120	2259	0.08	0.036737	0.0315	0.0003	3,722.12	0.01	0.00

Table B.2.57 Box-Behnken HMX run no.22 (6 Mar)

Time (min)	Area	HMX (mg/L)	conc/conc	area/area	HMX (mM)	2nd order	H_2O_2 (mg/L)	H_2O_2 (mM)
0	52422	1.58	1	1.0000	0.0054	186.85	56.12	1.65
1	47750	1.44	0.911539	0.9109	0.0049	204.99	50.33	1.48
5	46530	1.41	0.888439	0.8876	0.0048	210.31	44.15	1.30
10	39563	1.20	0.756524	0.7547	0.0040	246.99	36.51	1.07
30	22846	0.70	0.439999	0.4358	0.0024	424.66	16.15	0.47
60	7710	0.24	0.153409	0.1471	0.0008	1,217.99	3.05	0.09
90	3285	0.11	0.069616	0.0627	0.0004	2,684.05	0.51	0.01
120	2599	0.09	0.056632	0.0496	0.0003	3,299.43	0.51	0.01

Table B.2.58 Box-Behnken HMX run no.23 (26 Feb)

Time (min)	Area	HMX (mg/L)	conc/conc	area/area	HMX (mM)	2nd order	H_2O_2 (mg/L)	H_2O_2 (mM)
0	68047	2.05	1.000000	1.0000	0.0069	144.19	308.64	9.08
1	61844	1.87	0.909365	0.9088	0.0063	158.56	269.45	7.92
5	57145	1.73	0.840705	0.8398	0.0058	171.51	245.82	7.23
10	56034	1.69	0.824472	0.8235	0.0057	174.89	179.45	5.28
30	45347	1.37	0.668319	0.6664	0.0046	215.75	91.27	2.68
60	29888	0.91	0.442439	0.4392	0.0031	325.90	38.55	1.13
90	13101	0.40	0.197156	0.1925	0.0014	731.36	9.45	0.28
120	3566	0.12	0.057832	0.0524	0.0004	2,493.29	2.18	0.06

Table B.2.59 Box-Behnken HMX run no.24 (3 Mar)

Time (min)	Area	HMX (mg/L)	conc/conc	area/area	HMX (mM)	2nd order	H_2O_2 (mg/L)	H_2O_2 (mM)
0	36891	1.12	1	1.0000	0.0038	264.69	308.64	9.08
1	33451	1.02	0.907733	0.9068	0.0034	291.59	286.73	8.43
5	30585	0.93	0.830862	0.8291	0.0031	318.57	257.64	7.58
10	25769	0.79	0.701689	0.6985	0.0027	377.22	218.55	6.43
30	14015	0.43	0.386426	0.3799	0.0015	684.97	93.09	2.74
60	2298	0.08	0.072154	0.0623	0.0003	3,668.36	6.73	0.20
90	1077	0.04	0.039401	0.0292	0.0001	6,717.80	0.36	0.01
120	837	0.04	0.032967	0.0227	0.0001	8,029.01	0.04	0.00

Table B.2.60 Box-Behnken HMX run no.25 (13 Mar)

Time (min)	Area	HMX (mg/L)	conc/conc	area/area	HMX (mM)	2nd order	H_2O_2 (mg/L)	H_2O_2 (mM)
0	48370	1.46	1	1.0000	0.0049	202.38	56.12	1.65
1	37434	1.14	0.775728	0.7739	0.0038	260.89	31.27	0.92
5	31292	0.95	0.649770	0.6469	0.0032	311.46	22.18	0.65
10	25471	0.78	0.530394	0.5266	0.0026	381.56	15.82	0.47
30	10014	0.31	0.213407	0.2070	0.0011	948.32	6.69	0.20
60	2761	0.09	0.064663	0.0571	0.0003	3,129.76	6.69	0.20
90	577	0.03	0.019874	0.0119	0.0001	10,183.12	3.78	0.11
120	226	0.02	0.012676	0.0047	0.0001	15,965.82	3.78	0.11

Table B.2.61 Box-Behnken HMX run no.26 (18 Feb)

Time (min)	Area	HMX (mg/L)	conc/conc	area/area	HMX (mM)	2nd order	H_2O_2 (mg/L)	H_2O_2 (mM)
0	85700	2.58	1.0000	1.0000	0.0087	114.63	102.03	3.00
1	62914	1.90	0.7353	0.7341	0.0064	155.88	55.82	1.64
5	43196	1.31	0.5063	0.5040	0.0044	226.40	32.18	0.95
10	27429	0.83	0.3232	0.3201	0.0028	354.71	14.91	0.44
30	9360	0.29	0.1133	0.1092	0.0010	1,011.92	0.36	0.01
60	8927	0.28	0.1082	0.1042	0.0009	1,058.94	0.36	0.01
90	7713	0.24	0.0941	0.0900	0.0008	1,217.54	0.09	0.00
120	6400	0.20	0.0789	0.0747	.0007	1,452.91	0.09	0.00

Table B.2.62 Box-Behnken HMX run no.27 (21 Mar)

Time (min)	Area	HMX (mg/L)	conc/conc	area/area	HMX (mM)	2nd order	H_2O_2 (mg/L)	H_2O_2 (mM)
0	75424	2.28	1	1.0000	0.0077	130.16	56.12	1.65
1	65018	1.96	0.862747	0.8620	0.0066	150.87	33.60	0.99
5	41501	1.26	0.552563	0.5502	0.0042	235.56	24.51	0.72
10	29460	0.90	0.393744	0.3906	0.0030	330.58	14.69	0.43
30	9438	0.30	0.129658	0.1251	0.0010	1,003.89	3.78	0.11
60	8644	0.27	0.119186	0.1146	0.0009	1,092.10	1.60	0.05
90	7326	0.23	0.101801	0.0971	0.0008	1,278.59	1.24	0.04
120	6156	0.20	0.086369	0.0816	0.0007	1,507.05	0.87	0.03

Table B.2.63 Box-Behnken HMX run no.28 (28 Mar)

Time (min)	Area	HMX (mg/L)	conc/conc	area/area	HMX (mM)	2nd order	H_2O_2 (mg/L)	H_2O_2 (mM)
0	66924	2.02	1	1.0000	0.0068	146.60	56.12	1.65
1	62886	1.90	0.940014	0.9397	0.0064	155.95	48.87	1.44
5	64021	1.93	0.956875	0.9566	0.0065	153.21	41.60	1.22
10	66080	1.99	0.987462	0.9874	0.0067	148.46	33.24	0.98
30	65334	1.97	0.976380	0.9762	0.0067	150.14	7.05	0.21
60	64621	1.95	0.965788	0.9656	0.0066	151.79	0.15	0.00
90	63519	1.92	0.949418	0.9491	0.0065	154.41	0.01	0.00
120	62760	1.90	0.938143	0.9378	0.0064	156.26	0.00	0.00

B.3 Experimental data of real wastewater treatment experiments

Table B.3.1 RDX (C/C_0) treatment by various processes.

Time (min)	electrolysis	Fenton	H_2O_2/UVA	photo-Fenton	electro-Fenton
0	1	1	1	1	1
10	0.53453	0.66636	1.02109	0.88228	0.59799
30	0.37625	0.29379	0.9656	0.40882	0.23283
60	0.11341	0.05757	0.82034	0.02254	0.01016
90	0.03965	0.00722	0.74208	0.00108	8.47643E-4
120	0.01253	8.11377E-4	0.64529	0.00108	8.47643E-4

Table B.3.2 HMX (C/C_0) treatment by various processes.

Time (min)	electrolysis	Fenton	H_2O_2/UVA	photo-Fenton	electro-Fenton
0	1	1	1	1	1
10	0.67234	0.92019	0.9847	1.04468	0.85889
30	0.60019	0.78031	1.01384	0.80272	0.59746
60	0.25556	0.40069	0.95572	0.46409	0.29315
90	0.06873	0.15828	0.94995	0.18625	0.11065
120	0.02687	0.04423	0.93212	0.04385	0.02938

Table B.3.3 COD (C/C_0) treatment by various processes.

Time (min)	electrolysis	Fenton	H_2O_2/UVA	photo-Fenton	electro-Fenton
0	1	1	1	1	1
10	1.00943	1.04462	0.98044	0.99541	0.95294
30	0.98821	0.84777	0.92176	0.8211	0.81882
60	1.00236	0.65879	0.92176	0.40826	0.63765
90	0.92217	0.47244	0.89242	0.29587	0.40706
120	0.98349	0.26772	0.76528	0.10092	0.30824

Table B.3.4 TOC (C/C_0) treatment by various processes.

Time (min)	electrolysis	Fenton	H_2O_2/UVA	photo-Fenton	electro-Fenton
0	1	1	1	1	1
10	1.00044	0.94529	0.95985	0.96006	1.01475
30	1.00307	0.75434	0.97638	0.79145	0.87414
60	0.98379	0.61519	0.93041	0.59336	0.65883
90	0.97635	0.45114	0.87136	0.43966	0.46681
120	0.98817	0.30601	0.85761	0.32048	0.3697

Table B.3.5 BOD (C/C_0) treatment by various processes.

Time (min)	electrolysis	Fenton	H_2O_2/UVA	photo-Fenton	electro-Fenton
0	1	1	1	1	1
30	1.0339	0.825	0.99	0.73171	0.83051
60	1.01695	0.75	0.875	0.63415	0.44068
90	1.01695	1	0.98	0.34146	0.38983
120	1.0339	0.95	0.975	0.04878	0.18644

Table B.3.6 RDX (mM) treatment by various processes.

Time (min)	electrolysis	Fenton	H_2O_2/UVA	photo-Fenton	electro-Fenton
0	0.3182	0.3600	0.2753	0.2703	0.3446
10	0.1701	0.2399	0.2811	0.2385	0.2061
30	0.1197	0.1058	0.2659	0.1105	0.0802
60	0.0361	0.0207	0.2259	0.0061	0.0035
90	0.0126	0.0026	0.2043	0.0003	0.0003
120	0.0040	0.0003	0.1777	0.0003	0.0003

Table B.3.7 HMX (mM) treatment by various processes.

Time (min)	electrolysis	Fenton	H_2O_2/UVA	photo-Fenton	electro-Fenton
0	0.0514	0.0514	0.0267	0.0321	0.0514
10	0.0346	0.0473	0.0263	0.0335	0.0442
30	0.0309	0.0401	0.0271	0.0258	0.0307
60	0.0131	0.0206	0.0255	0.0149	0.0151
90	0.0035	0.0081	0.0254	0.0060	0.0057
120	0.0014	0.0023	0.0249	0.0014	0.0015

Table B.3.8 possible intermediates peak for HPLC.

Name	60ACN:40DI (min)
Acetone	3.2
Hydroquinone	4.0
Benzoic acid	4.1
Phenol	4.9
Aniline	5.0
o-toluidine	5.6
Nitrobenzene	7.4
Benzene	8.6
Toluene	10.4

Table B.3.8 COD (mg/L) treatment by various processes.

Time (min)	electrolysis	Fenton	H_2O_2/UVA	photo-Fenton	electro-Fenton
0	33,807	27,134	30,532	32,271	31,481
10	34,126	28,344	29,935	32,123	30,000
30	33,409	23,003	28,143	26,498	25,778
60	33,887	17,875	28,143	13,175	20,074
90	31,176	12,819	27,247	9,548	12,815
120	33,249	7,264	23,365	3,257	9,704

Table B.3.9 TOC (mg/L)treatment by various processes.

Time (min)	electrolysis	Fenton	H_2O_2/UVA	photo-Fenton	electro-Fenton
0	11,415	7,381	10,585	10,890	10,505
10	11,420	6,977	10,160	10,455	10,660
30	11,450	5,568	10,335	8,619	9,183
60	11,230	4,541	9,848	6,462	6,921
90	11,145	3,330	9,223	4,788	4,904
120	11,280	2,259	9,078	3,490	3,884

Table B.3.10 BOD (mg/L) treatment by various processes.

Time (min)	electrolysis	Fenton	H_2O_2/UVA	photo-Fenton	electro-Fenton
0	17,700	12,000	12,000	12,300	17,700
30	18,300	9,900	11,880	9,000	14,700
60	18,000	9,000	10,500	7,800	7,800
90	18,000	12,000	11,760	4,200	6,900
120	18,300	11,400	11,700	600	3,300

Table B.3.11 First order kinetics (min^{-1}) of HMX-RDX wastewater treatment.

	electrolysis	Fenton	H_2O_2/UVA	photo-Fenton	electro-Fenton
RDX	0.036	0.059	0.004	0.066	0.066
R^2	0.9947	0.9894	0.9768	0.9455	0.9483
HMX	0.030	0.025	0.0006	0.025	0.029
R^2	0.9748	0.9480	0.7722	0.9247	0.9713
COD	0.0004	0.011	0.002	0.019	0.010
R^2	0.3126	0.9565	0.8589	0.9505	0.9846
TOC	0.0002	0.010	0.001	0.010	0.009
R^2	0.5762	0.9900	0.9296	0.9973	0.9856

Table B.3.12 Intermediates peak and area by electrolysis of HMX-RDX wastewater.

Time (min)	Intermediate1 4.0min	HMX 4.2min	Intermediate2 4.5min	RDX 4.8min
0		378,461	7,492,215	4,958,029
30		1,000,600	6,746,654	3,023,107
60		2,115,296	5,828,107	1,688,218
120	350,950	3,101,992	3,830,598	499,769
240	1,514,875	2,893,555	900,551	500
480	4,450,472	351,468	500	5

Table B.3.13 H_2O_2 efficiency for HMX-RDX wastewater treatment.

Time (min)	Fenton	H_2O_2/UVA	photo-Fenton	electro-Fenton
0	0%	0%	0%	0%
10	-41%	2%	-10%	24%
30	23%	8%	37%	37%
60	29%	-2%	74%	39%
90	32%	-2%	59%	46%
120	40%	6%	61%	43%

BIOGRAPHY

Mr. Piyawat Tanvanit was born on April 3rd, 1975 in Bangkok, Thailand. He received his Bachelor Degree in Environmental Engineering from Department of Environmental Engineering, Faculty of Engineering, Chulalongkorn University, Bangkok, Thailand in 1997. He has carried out this research as a part of his study, Doctoral Degree of Philosophy Program in Environmental Management at the graduate school, Chulalongkorn University under National Center of Excellence for Environmental and Hazardous Waste Management (NCE-EHWM).

Publications from this thesis as of May 2011, 4 papers have been produced from these studies as follows;

1 Piyawat Tanvanit, Jin Anotai, and Ming Chun Lu. 2008. "Effect of pH and current on the electro deposition of Nickel" Proceeding of 2008 International Conference on Environmental Quality Concern, Control and Conservation, Tainan, Taiwan, May 23rd, 2008.

2 Piyawat Tanvanit, Ming Jer Liou, Jin Anotai, and Ming Chun Lu. 2008. "Treatment of wastewater containing HMX by UV-Fenton process and electro-Fenton process" Proceeding of 2008 Asian-Pacific Regional Conference on Practical Environmental Technologies at Quezon City, Philippines June 30th-July 1st, 2008.

3 Piyawat Tanvanit, Ming Jer Liou, Jin Anotai, and Ming Chun Lu. 2008. "Treatment of explosive production wastewater by Fenton's reagent" at the 12th International Conference on Integrated Diffuse Pollution Management, Khon Kaen, Thailand, August 25-29, 2008.

4 Piyawat Tanvanit, Ming Jer Liou, Jin Anotai, and Ming Chun Lu. 2009. "Response surface methodology for optimization HMX treatment with electro-Fenton method" Proceeding of 2009 International Conference on Environmental Quality Concern, Control and Conservation, Kaohsiung, Taiwan, May 22, 2009.